The impacts of demographic stochasticity on populations and communities

by

Geoffrey B. Legault

B.Sc., University of Toronto, 2009

M.Sc., University of Toronto, 2011

A thesis submitted to the

Faculty of the Graduate School of the

University of Colorado in partial fulfillment

of the requirements for the degree of

Doctor of Philosophy

Department of Ecology and Evolutionary Biology

2017

This thesis entitled:
The impacts of demographic stochasticity on populations and communities
written by Geoffrey B. Legault
has been approved for the Department of Ecology and Evolutionary Biology

_____
Associate Professor Brett A. Melbourne

_____
Associate Professor Kendi Davies

_____
Associate Professor Sam Flaxman

_____
Professor Katharine Suding

Date _____

The final copy of this thesis has been examined by the signatories, and we find that both the content and the form meet acceptable presentation standards of scholarly work in the above mentioned discipline.

Legault, Geoffrey B. (Ph.D., Ecology and Evolutionary Biology)

The impacts of demographic stochasticity on populations and communities

Thesis directed by Associate Professor Brett A. Melbourne

Accurate descriptions of ecological processes often require accounting for demographic stochasticity, the variation that arises in populations and communities as a result of probabilistic demography (e.g., birth, death, migration). Much theory has been developed for understanding the population-level effects of demographic stochasticity, but ecology largely lacks rigorous community-level descriptions of its consequences. Furthermore, how demographic stochasticity affects other complex biological systems, such as populations responding to continuously-changing environments or populations undergoing range expansion, is not well understood. Here I address some of these gaps using theoretical and experimental approaches. First, I examine how demographic stochasticity affects competitive dynamics in two-species communities and find, both experimentally and using simulations, that demographic stochasticity can produce outcomes not predicted by traditional deterministic models. In the next section, I consider the effects of continuously-changing environments and describe a continuous-time simulation approach that combines environment-dependent demography and demographic stochasticity. I simulate the approach for multiple ecological models and environmental change scenarios and find that accounting for environment-dependent demography in stochastic systems is often necessary for avoiding bias. In the last two sections, I examine the applied issue of geographic range shifts, a multi-faceted phemonemon affecting many species globally and one with substantial economic and social costs. Recognizing the significant variation in range shifts arising from, in part, probabilistic demography, I use highly-replicated experimental approaches to understand the effects of two different processes thought to affect range shifts: spatial selection, and interspecific competition. In the first of these sections, I find that the effects of spatial selection

depend on both the intrinsic dispersal ability of expanding organisms as well as the environment into which they expand. In the second section, I show, for the first time empirically, that interspecific competition can effectively halt range expansion for multiple generations. Throughout this work, I illustrate both the role of demographic stochasticity as an emergent driver of ecological dynamics and the importance of using controlled, replicated experiments for understanding highly stochastic biological processes.

Dedication

To my family.

Acknowledgements

I wish to thank my advisor, Dr. Brett Melbourne, who provided excellent support over the past three years and taught me what it means to think about biology quantitatively. Thanks also to Dr. Jeremy Fox, with whom I began studying theoretical ecology at the University of Calgary. I have been fortunate to work with many excellent students during my graduate training; for Chapter 2, G. Osgoode assisted with the experimental work; and for Chapters 4 and 5, I was assisted by the Melbourne Lab beetle team, whose members are too numerous to list here. Special thanks to E. Angell, R. Beeler, M. Bullock, K. Phan, and M. Riley for their contributions.

Members of my dissertation committee, Drs. Kendi Davies, Dan Doak, Sam Flaxman, and Katharine Suding, have been more than generous with their time during my tenure and their advice has much improved the quality and applicability of my work. I have also benefitted from thoughtful discussions with M. Bitters, T. Dallas, A. Hastings, J. McClenahan, J. Resasco, L. Shoemaker, J. Tuff, T. Tuff, and C. Weiss-Lehman.

Funding was provided in part by a National Science Foundation grant to Brett Melbourne (DEB 13007494) and a department research grant to me. I am grateful for a Dissertation Completion Fellowship from CU and to the ESA Theoretical Ecology Section for a poster award on an early version of Chapter 3.

My partner Caroline has been a constant source of inspiration and encouragement. Her contributions to this work, both personal and academic, could fill a tome of the same length.

Finally, not a single page of this dissertation would have been possible without the love and support of my family, Susan, Gary, and Tim. **Thank you**.

Contents

Chapter

1 Introduction **1**

1.1 Overview of Chapters 6

2 Demographic stochasticity alters expected outcomes in experimental and simulated communities **9**

2.1 Introduction 9

2.2 Methods 12

2.2.1 Part 1: Experimental microcosms 12

2.2.2 Part 2: Stochastic simulations of consumer-resource dynamics 15

2.3 Results 19

2.3.1 Competitive exclusion in the experimental microcosms 19

2.3.2 Competitive exclusion in the stochastic simulations 20

2.3.3 Conditional mean densities in the experimental microcosms 22

2.3.4 Conditional mean densities in the stochastic simulations 22

2.3.5 Effective fitness inequalities 25

2.4 Discussion 25

3 Accounting for environmental change in continuous-time stochastic population models **32**

3.1 Introduction 32

3.2 Methods . . . 35
3.2.1 Non-stationary demography in non-SSA models . . . 35
3.2.2 Gillespie's stochastic simulation algorithm (SSA) . . . 35
3.2.3 Changing environments: non-stationary Poisson processes . . . 38
3.2.4 Stochastic population models . . . 40
3.2.5 Comparing CDFs of inter-arrival times . . . 44
3.2.6 Diagnostics and analysis . . . 46
3.3 Results . . . 47
3.4 Discussion . . . 48

4 Intrinsic dispersal ability and environment affect trait evolution during range expansion **55**
4.1 Introduction . . . 55
4.2 Methods . . . 57
4.2.1 Details on model system and range expansion phase . . . 58
4.2.2 Expansion of CORE and EDGE populations . . . 60
4.2.3 Comparing population growth and dispersal . . . 61
4.3 Results . . . 63
4.3.1 Range expansion phase . . . 63
4.3.2 Population growth in CORE and EDGE populations . . . 66
4.3.3 Dispersal in CORE and EDGE populations . . . 66
4.4 Discussion . . . 69

5 Interspecific competition halts range expansions in an experimental system **73**
5.1 Introduction . . . 73
5.2 Methods . . . 74
5.2.1 Design of range expansion experiment . . . 75
5.3 Results . . . 76

5.4 Discussion 78

6 Conclusions **87**

Bibliography **91**

Appendix

A Supplemental information for Chapter 2 **106**

A.1 Monocultures 106

A.1.1 Experimental procedures 106

A.1.2 Consumer-resource models 106

A.1.3 Model-fitting 109

A.1.4 Results 110

A.2 Stochastic consumer-resource model 110

A.3 R code for Gillespie's stochastic simulation algorithm 114

A.4 R code for model-fitting 117

A.5 Model fits to simulated data 120

A.6 Coefficients of variation 120

B Supplemental information for Chapter 3 **125**

B.1 Diagnostic tests of SSA+ method 125

B.2 R code for SSA+ method 129

B.3 Comparison of SSAn and SSA+ for slower environment functions 140

C Supplemental information for Chapter 4 **142**

C.1 Comparison of F1 and F2 populations 142

C.1.1 Background 142

C.1.2 Results 143
C.2 R code for dispersal kernel and likelihood function 146
C.3 Fitted dispersal kernels 148
C.4 Correlation of dispersal and growth rate 148

Tables

Table

2.1 Parameter values in consumer-resource simulations 17

3.1 Ecological models considered in SSA and SSA+ comparison 41

3.2 Environment functions used in the stochastic simulations 42

A.1 Consumption and death functions 108

A.2 Model fits to monoculture data 112

Figures

Figure

1.1 Random timing in birth and death of *Daphnia magna* 4

2.1 Survivorship in experimental jars 21
2.2 Survivorship of weaker consumer in stochastic simulations 23
2.3 Mean densities over time in experimental jars 24
2.4 Mean densities over time in stochastic simulations 26
2.5 Actual versus estimated niche differences in the stochastic simulations 27

3.1 Visualizations of the environment functions 43
3.2 Distribution of inter-arrival times for models and environment functions . . . 45
3.3 Comparison of SSAn and SSA+ predictions for each model and environment function 49
3.4 Expected values of exponential growth model simulations 50

4.1 Design of experiment on trait evolution during range expansion 59
4.2 Mean abundances in the landscapes over five generations 64
4.3 Abundances in the single-patch controls over five generations 65
4.4 Population growth rates of F2 beetles 67
4.5 Estimated diffusion coefficients of F2 beetles 68

5.1 Design of experiment on interspecific competition during range expansion . . 77

5.2 Mean abundances of *T. castaneum* in one-patch controls 79
5.3 Mean abundances of *T. confusum* in one-patch controls 80
5.4 Mean abundances and spread of *T. castaneum* in WET environment 81
5.5 Mean abundances and spread of *T. castaneum* in DRY environment 82
5.6 Mean abundances and spread of *T. confusum* in WET and DRY environments 83
5.7 Furthest patches occupied by *T. castaneum* across six generations 84

A.1 Density over time of monocultures with model fits 111
A.2 Model fits for consumer 1 121
A.3 Model fits of consumer 2 122
A.4 Variation over time in experimental jars 123
A.5 Variation over time in stochastic simulations 124

B.1 Arrival times generated with Weibull method versus SSA+ method 126
B.2 Predicted population sizes for SSA and SSA+ under a constant environment 127
B.3 Change in expected values of exponential growth models with increasing simulations 128
B.4 Comparison of SSAn and SSA+ predictions when environmental change is slower 141

C.1 Comparison of F1 and F2 growth rates 144
C.2 Comparison of F1 and F2 dispersal 145
C.3 Proportion of *T. castaneum* found in WET patches and their fitted dispersal kernels 149
C.4 Proportion of *T. castaneum* found in DRY patches and their fitted dispersal kernels 150
C.5 Proportion of *T. confusum* found in WET patches and their fitted dispersal kernels 151

C.6 Proportion of *T. confusum* found in DRY patches and their fitted dispersal kernels 152

C.7 Correlations between dispersal and growth in F2 beetles 153

Chapter 1

Introduction

A central goal in ecology is to describe species responses to biotic and abiotic factors using mathematical models. Commonly, ecologists apply models that are deterministic, meaning that for a given set of model parameters and initial conditions, they always predict the same outcome. Many of the foundational models or approaches in ecology are deterministic in this way, including the Lotka-Volterra equations (Lotka, 1925; Volterra, 1926), the Levins metapopulation model (Levins, 1969), consumer-resource models (MacArthur, 1970), biological chaos theory (Schaffer, 1984), S-I-R disease models (Kermack and McKendrick, 1927), and coexistence theory (Tilman, 1982; Chesson, 2000). While such equations are and will continue to be useful to ecologists, they represent an intentionally simplified view of biology ("mathematical hope rather than biological reality", according to Renshaw (1991), p. xiii) insofar as natural populations and communities rarely exhibit dynamics exactly in line with classic deterministic models (e.g., Taylor et al., 1980; Bjrnstad et al., 1998; Rohani et al., 2002). Moreover - and especially problematic for a purely deterministic conception of biology - even under highly controlled laboratory conditions, replicated systems frequently exhibit dissimilar dynamics and outcomes (e.g., Park, 1954; Dickerson and Robinson, 1985; Fox and Smith, 1997; Desharnais et al., 2006; Melbourne and Hastings, 2009).

When population dynamics differ from deterministic expectations, the unexplained variation is often referred to as "noise" or "stochastic". In ecology, these terms are applied to variation arising from at least three distinct phenomena: (1) misspecificed models (e.g.,

models missing relevant parameters); (2) error, in either observations or the precision of measurements; and (3) intrinsic variation in the responses of individuals (or cells, or DNA, etc.) to biotic or abiotic conditions. Both (1) and (2) represent significant problems for ecology and other disciplines, but do not conflict with a deterministic conception of biology, and will not be discussed further. Instead, I will focus on the intrinsic variation arising from (3), which at the population-level is called demographic stochasticity.

Demographic stochasticity arises when demographic processes (e.g., birth, death, migration) occur probabilistically (May, 1973; Renshaw, 1991; Melbourne, 2012). In other words, it is a consequence of demographic processes having multiple possible outcomes (instead of only one possible outcome) for the same initial conditions (i.e., the same environment, the same genetic variation, etc.). In mathematics, any such process is known formally as a stochastic process (van Kampen, 1992; Renshaw, 1991; Ross, 2014) and can be described using probability mass/density functions. For instance, a (theoretical) coin flip is a classic example of a stochastic process, and it is straightforward to determine the probability of obtaining exactly k heads for, say, 10 coin flips using the probability mass function of a binomial distribution (in this case: $\binom{10}{k}0.5^k(1-0.5)^{10-k}$). In biology, where we might instead be interested in modelling the probability distribution of population sizes over time, more complicated methods for obtaining the relevant distributions are usually necessary (e.g., Kolmogorov forward equations; Kolmogorov (1931)). Nevertheless, the general notion of dealing with probabilities rather than deterministic certainties is the same for random coin flips as it is for more complex biological outcomes.

In addition to allowing for variable demographic outcomes, a probabilistic treatment of demography means that population size can directly affect population-level variability. This results from the fact that populations are a collection of a finite number of individuals and thus are influenced by a finite number of realizations (or samples) of underlying demographic processes. When populations are large and well-mixed, there will generally be little difference between the expected population size (i.e., the most likely outcome of all

demographic processes considered together) and what is observed. However, in the same way that a small number of fair coin flips may not produce the expected 50:50 ratio of heads to tails, a small number of stochastic demographic processes may not produce the expected population size. Thus, not only does probabilistic demography mean that identical individuals in a population can vary in their demography, it means that the collective demography of entire populations (i.e., population trajectories) can change according to population size and, in some cases, vary significantly from expectations.

While there is some debate about whether demographic processes are inherently probabilistic (some argue they merely seem probabilistic because we lack the information necessary for describing them deterministically; sensu Clark (2009)), there is good evidence that biological processes at the microscopic scale behave non-deterministically. Examples include observations from highly controlled experiments showing significant variation in the traits of genetically identical (single-celled) organisms experiencing identical environmental conditions (e.g., Spudich and Kosland, 1976; Avery, 2006; Norman et al., 2013; Adiciptaningrum et al., 2015), as well as evidence of probabilistic gene (e.g., Kærn et al., 2005) and protein expression (e.g., Novick and Weiner, 1957; Bar-Even et al., 2006). How intrinsic variability in these microscopic processes scales up for larger organisms composed of thousands or millions of cells is unclear, but it seems reasonable to suppose that microscopic variability could lead to macroscopic variability in demographic processes such as birth or death. The only study to date that has come close to characterizing such macroscopic variability is Stroustrup et al. (2016), which documented variation in individual death rates for tens of thousands of (non-clonal) *Caenorhabditis elegans* (approximately 1000 cells) and found broad adherence in the data to the well-known stochastic Poisson process. My own unpublished work on the demographic rates of *Daphnia magna* clones (shown in Figure 1.1) is also suggestive (though not definitively) of non-deterministic demography at macroscopic scales.

Whether demographic processes are actually probabilistic, or merely seem that way to us (or other organisms) given the available information/scale of analysis, is not necessarily

Figure 1.1: The proportion of clonal *Daphnia magna* having their first brood (blue) or dieing (black) on a particular day. All individuals (65 total) were kept in separate containers under controlled conditions and were fed the same concentration of algae (*Chlamydomonas reinhardtii*, from a large, well-fixed stock culture) every day.

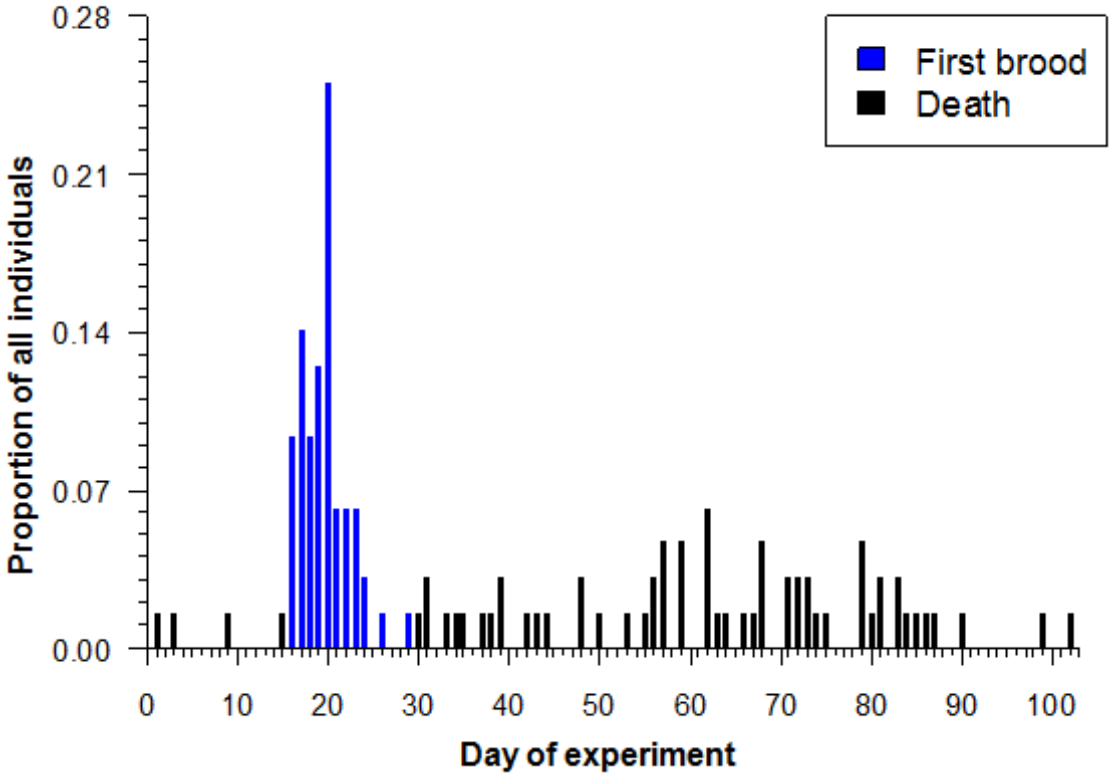

important so long as they can be described quantitatively. The earliest work on such descriptions for biology came with Feller (1939), who used Kolmogorov's foundational approaches for modelling stochastic processes (Kolmogorov, 1931) to examine probabilistic versions of the Lotka-Volterra equations. This was followed by Kendall (1949), who examined solutions to a closely-related stochastic birth-death process. Shortly thereafter came Bartlett's (1960) seminal book on continuous-time stochastic models in ecology and epidemiology, and since then, there has been considerable theory on the implications of demographic stochasticity for populations and communities (e.g., Kurtz, 1970; Nisbet and Gurney, 1982; Lande, 1993; Matis and Kiffe, 2000; Nsell, 2001; Kilpatrick and Ives, 2003; Orrock and Fletcher, 2005; Vindenes et al., 2008; Orrock and Watling, 2010; Gokhale et al., 2013; Fisher and Mehta, 2014). From this and other work, it has been shown that stochastic versions of some simple population-level (and rarely, community-level) models can have widely different outcomes and dynamics than their deterministic analogs, especially when demography is non-linear (e.g., density-dependent growth) or when population sizes are small. Predicted effects include increased extinction risk in populations (Shaffer, 1981; Lande, 1993), higher probabilities of coexistence between competitors (Orrock and Fletcher, 2005; Orrock and Watling, 2010), and increased persistence time of disease (Bartlett, 1957). Some of these effects have been supported by empirical work, most notably the influence of stochasticity on extinction rates (Burkey, 1997; Belovsky et al., 1999; Desharnais et al., 2006; Griffen and Drake, 2008; Ovaskainen and Meerson, 2010); however, most remain theoretical and have not been demonstrated or quantified in real populations. Moreover, the impacts of demographic stochasticity on populations with complex demography (e.g., multiple life-stages), or on multiple interacting populations (i.e., communities), are largely unexplored either theoretically or empirically.

Given that the effects of demographic stochasticity on *simple* populations and communities go beyond simply adding noise to their dynamics, it is worth considering the effects of demographic stochasticity for the more complex systems and scenarios that are of concern

to ecologists. **As such, my aim is to move beyond the "mathematical hope" of deterministic biology and help address important basic and applied questions by providing more realistic descriptions of stochastic biological phenomena**.

1.1 Overview of Chapters

In **Chapter 2**, I address the basic question of how demographic stochasticity affects a community of competitors. Prior theoretical work has suggested that when population sizes are small, demographic stochasticity alone can alter competitive outcomes in communities. In particular, the variability caused by demographic stochasticity has been predicted to effectively weaken competition in small patches, allowing weaker competitors to outcompete superior competitors (Orrock and Fletcher, 2005; Orrock and Watling, 2010; Pedruski et al., 2015; Okuyama, 2015). I test this theory in a laboratory system of protists and examine how absolute population size affects the likelihood of coexistence between competitors. Further, I use continuous-time stochastic models of competition to examine how demographic stochasticity affects other aspects of community dynamics, such as mean densities over time and the effective demographic rates of competitors.

Chapter 3 addresses how demographic stochasticity interacts with environmental change. Specifically, I consider how to account for environment-dependent demography (i.e., demographic rates that respond to environmental change) in a commonly-used algorithm for simulating stochastic continuous-time models, Gillespie's stochastic simulation algorithm [SSA] (Gillespie, 1977). The issue has relevance to both basic and applied researchers as the traits of many species are known to respond to the environment (e.g., Deutsch et al., 2008; Dell et al., 2011; Estay et al., 2014; Stroustrup et al., 2016), yet continuous-time stochastic ecological models rarely account for such environmental-dependency. I describe an extension to the SSA (SSA+) that allows demography to respond to environmental fluctuations and compare predictions SSA+, under a variety of environmental change scenarios, to the standard SSA for two fundamental ecological models (exponential growth, logistic growth).

Further, I outline a computationally inexpensive approach for estimating when and under what circumstances it can be important to fully account for environment-dependent demography for any class of model.

In **Chapters 4 and 5**, I shift away from examining the effects of demographic stochasticity specifically and focus on the applied issue of range shifts, a phenomenon that has been of great interest to biologists for decades (Andrewartha and Birch, 1954). Range shifts, particularly the spread or expansion of invasive species, impose significant economic and social costs. For example, the range expansion of invasive species into the United States has previously been estimated to cost $120 billion a year (Pimentel et al., 2005). It is a problem globally as well, with invasive species esimated to have contributed to as much as 50% of recent extinctions (Clavero and Garcia-Berthou, 2005). Moreover, the anticipated range shifts of native and endangered species due to factors such as climate change and habitat loss (Chen et al., 2011), is expected to impose significant costs due to losses of ecosystem services (e.g., forest products, tourism) and ecosystem functioning (e.g., water use efficiency). As a result, modelling the dynamics of range expansion is an important goal in applied ecology. However, ecologists have so far been unsuccessful in creating accurate models of range expansion for such applications (Kubisch et al., 2014; Louthan et al., 2015).

Part of the difficulty associated with modelling range expansion is that it represents the sum of many different stochastic demographic processes occurring over time and across space. As a result, the best predictive models have come from laboratory experiments, where there is sufficient data and - crucially - sufficient replication to characterize the probability distributions of the many underlying demographic processes (e.g., Fronhofer and Altermatt, 2015). Such laboratory efforts have so far been modestly successful for predicting single-species range expansion into unoccupied habitat (e.g., Melbourne and Hastings, 2009; Szücs et al., 2017; Hufbauer et al., 2015) and have even considered the added effects of evolutionary change during expansion (Fronhofer and Altermatt, 2015; Williams et al., 2016; Weiss-Lehman et al., 2017; Ochocki and Miller, 2017). However, to date these efforts have

not considered the additional complexities we would expect to occur during natural range shifts, such as the effects of heterogenous environments, different rates of local adaptation, and competition between species. In the interest of creating more realistic templates for modelling stochastic range expansions in nature, **Chapters 4** and **5** examine how evolution and competition between species affects range dynamics. Each chapter describes large, long-term experiments involving the flour beetle model system (*Tribolium* species) expanding across artificial landscapes. **Chapter 4** examines the role of evolutionary change during expansion for each of two species of beetles experiencing different environments, and **Chapter 5** examines the role of both competition between species in slowing, or halting altogether, the speed of expansion.

Finally, in **Chapter 6**, I summarize my results and briefly discuss the importance and tractability of accounting for demographic stochasticity in natural systems.

Chapter 2

Demographic stochasticity alters expected outcomes in experimental and simulated communities

Geoffrey B. Legault, Jeremy W. Fox, Brett A. Melbourne

2.1 Introduction

Studies of interspecific competition in communities often treat competition as a deterministic process, meaning that the same initial conditions (e.g., genes, traits, niches, environment, etc.) are expected to produce the same competitive outcomes (e.g., coexistence, exclusion). For example, it is common to model communities using deterministic equations representing species niches (e.g., Lotka-Volterra equations: Lotka, 1925; Volterra, 1926) and to use solutions of those equations to make predictions about whether and how coexistence occurs (Gause, 1934; Macarthur and Levins, 1967; Luckinbill, 1979; Hansen and Hubbell, 1980; Chesson, 2000; Levine and HilleRisLambers, 2009). However, deterministic equations are not always sufficient for predicting outcomes in real communities (e.g., Park, 1954; Dickerson and Robinson, 1985; Fox and Smith, 1997; Fukami, 2004).

One reason the deterministic framework may be inadequate for predicting competitive outcomes is that community dynamics are also affected by demographic stochasticity, the randomness in population demographic rates (e.g., birth, death) arising from the discrete and probabilistic nature of biological processes (May, 1973; Renshaw, 1991; Melbourne, 2012). The importance of demographic stochasticity is relatively well-established, with a large body

of theoretical and experimental work showing that it significantly increases extinction risk for small populations (Bartlett, 1960; Kurtz, 1970; Shaffer, 1981; Lande, 1993; Burkey, 1997; Belovsky et al., 1999; Matis and Kiffe, 2000; Griffen and Drake, 2008; Ovaskainen and Meerson, 2010). However, it has so far been difficult to generalize beyond effects on extinction risk as the impacts of demographic stochasticity appear to be context-specific, for instance depending on population structure (Engen et al., 2005), specific vital rates (Vindenes et al., 2008), and nonlinearities (Bolnick et al., 2011). Further, even though demographic stochasticity tends to be most important in small populations, large populations may also be strongly affected by demographic stochasticity if total abundance is divided across many different life stages or if particular life stages play major roles in demography (Melbourne and Hastings, 2008). Such context-specific effects at the population level are compounded at the community level, where these effects plus those related to interspecific interactions must also be taken into account. For instance, when a large population of one species interacts with small populations of other species, the demographic stochasticity exhibited by those small populations will affect the large population. It is perhaps not surprising then, that despite continued interest in how demographic stochasticity affects communities, it is a topic that remains largely unresolved (Bell, 2000; Hubbell, 2001; Volkov et al., 2003; David, 2004; Adler et al., 2007; Chase, 2007; Chase and Myers, 2011; Rosindell et al., 2012; Vellend et al., 2014; Wang et al., 2016).

The few theoretical and simulation studies on the effects of demographic stochasticity in communities show a range of impacts, including both higher and lower probabilities of coexistence (Orrock and Fletcher, 2005; Orrock and Watling, 2010; Fisher and Mehta, 2014; Pedruski et al., 2015), lower spatial synchrony (Simonis, 2012), and the disruption of coevolutionary dynamics (Gokhale et al., 2013). Most theoretical studies to date also restrict attention to discrete time population models rather than the continuous-time models appropriate for species with overlapping generations, or only approximate the added variation caused by demographic stochasticity (Simonis, 2012; Gokhale et al., 2013; Okuyama, 2015,

but see). Empirical work on demographic stochasticity has tended to proceed independent of such theory, focusing instead on the effects of stochasticity on long-term community-level outcomes such as local and regional species diversity (e.g., Spencer and Warren, 1996; Fukami, 2004; Wang et al., 2016). We are aware of only one study of demographic stochasticity that has linked mechanistic population-level models with real community-level patterns (Gilbert and Levine, 2017), a study of plant communities.

Here we use experimental microcosms and exact stochastic simulations in continuous-time to understand how demographic stochasticity affects population dynamics in simple communities of consumers competing for shared food resources. Specifically, we manipulated total abundance (and thus demographic stochasticity) and examined its effects both on exclusion rates and abundances over time of competitors. We also developed a stochastic continuous-time competition model to check whether our experimental results can be explained by demographic stochasticity alone, and to explore a wider range of ecological scenarios than could be explored experimentally. Our approach was as follows:

(1) Experimental microcosms: We created three types of two-species communities, consisting of protist and rotifer competitors with a range of competitive abilities between them (i.e., from small to large differences in fitness). We manipulated the strength of demographic stochasticity in these communities by varying absolute abundances over 2 orders of magnitude (500 to 40,000 individuals). We then observed how our manipulations affected competitive outcomes and species abundances over time.

(2) Stochastic simulations: We used Gillespie's stochastic simulation algorithm (SSA) to simulate a consumer-resource model for a range of absolute abundances and differences in competitive abilities, similar to those in our experiment. We then observed how demographic stochasticity in these simulations affected competitive outcomes and dynamics. Finally, we assessed how demographic stochasticity quantitatively changed fitness difference by comparing fitness differences in the deterministic model

to the effective fitness differences implied by the mean dynamics of the stochastic model. Any such changes to effective population processes would reflect real, practical effects that demographic stochasticity could have on the drivers of community dynamics.

2.2 Methods

2.2.1 Part 1: Experimental microcosms

We used laboratory microcosms to examine the impact of absolute abundance (a proxy for demographic stochasticity) on competitive outcomes and dynamics. Experimental units consisted of different sized jars containing liquid medium, bacteria, and one or two protist/rotifer species. The three species used were the ciliate protists *Paramecium aurelia* and *Paramecium caudatum*, and the bdelloid rotifer *Philodina americanum*. All three species are fast-growing bacterivores and came from large laboratory stock cultures ($>$ 1.5 years old) raised under constant conditions (described below). From prior work in our system and under the same experimental conditions, we knew that *P. americanum* was the strongest competitor of the three focal species, followed by *P. caudatum* and, lastly, *P. aurelia*.

Microcosm medium was spring water collected from Big Hill Springs Provincial Park, Alberta (Canada), mixed with 1.0 g/L of crushed protozoan pellets (Carolina Biological Supply, USA). Prior to the start of the experiment, the medium was autoclaved and allowed to cool for 1.5 hours before being vacuum filtered through autoclaved Whatman GF/A filters (2-3 for each L of fluid) to remove large particles. Each litre of filtrate was then inoculated with a long-running (more than 1.5 years) lab strain of unidentified bacteria originally isolated from a stock culture of Colpidium striatum. All filtrations and inoculations were done under sterile conditions in a laminar flow hood, but it is likely that small amounts of unknown bacteria were also introduced into the medium at this time. The inoculated medium was then loosely capped and stored in an incubator with constant light and a

constant temperature of 22 C (stirred every 10-12 hours) until day 0 of the experiment (66 hours total).

Three microcosm sizes were used to manipulate the maximum population size of the protist communities: 1 mL (small), 10 mL (medium), and 80 mL (large). Air-surface to volume ratios were constant between small and large jars, but were slightly lower in medium-sized jars. Except during sampling (see below), all jars were kept with loose caps in incubators with constant temperature (22 C) and 24 hours of light for the duration of the experiment.

On day 0 of the experiment (August 12th 2013), autoclaved jars were filled in a laminar flow hood with the inoculated/incubated medium and seeded with all possible two-species combinations of the three microzooplankton species: *P. aurelia* and *P. caudatum* (AC), *P. aurelia* and *P. americanum* (AP), and *P. americanum* and *P. caudatum* (PC).

In the small jars, 5 individuals of each relevant species were added directly to the jars to create initial densities of exactly 5 mL-1. For the medium and large jars, it was impractical to add a precise number of individuals to attain starting densities of 5 mL-1, so we subsampled individuals from stock cultures of known densities to create initial densities of approximately 5 individuals mL-1. Each combination of jar size and species pairing was replicated 12 times, for a total of 108 experimental microcosms. We also established 10 replicate monocultures of each species at the large jar size, but do not report those results here (but see Appendix A: Monocultures).

2.2.1.1 Sampling and census

On day 2 and every two days thereafter, jars were shaken to homogenize the distribution of microzooplankton) and a 0.3 mL subsample was removed. Subsamples were carefully scanned under a dissecting microscope to count the number of individuals of each species. Then, subsamples were returned to the jars (i.e., non-destructive sampling). In practice, a small amount of liquid (free of protists and/or rotifers) was left behind on the counting

plates, meaning that our sampling procedure gradually reduced the volume of liquid within jars over time. This effect was only noticeable in the small jars beginning after day 36.

On day 8 and every eight days thereafter, 9% of the fluid (including protists and/or rotifers) in each jar (0.09 mL for small jars, 0.9 mL for medium jars, 7.2 mL for large jars) was removed in a laminar flow hood and replaced with new sterile media (made as above, except without the addition of bacteria). We replaced the removed medium with a volume of fresh sterile medium equal to 10% of the nominal culture volume (0.1 mL for small jars, 1 mL for medium jars, 8 mL for large jars). We replaced a larger volume of medium than we removed to replace evaporation and medium lost during sampling.

Individual jars were removed from the experiment once competitive exclusion had been observed. Competitive exclusion was defined as the absence of one of the two competing species in the 0.3 mL subsample and, for the medium and large jars, from a subsequent 10% subsample (1 mL for medium jars, 8 mL for large jars). We ended the experiment on day 72 after observing the last exclusion in our competitive pairings.

2.2.1.2 Analysis of competitive outcomes and mean densities

To assess the effects of demographic stochasticity on competitive outcomes, we compared exclusion rates for the AC, AP, and PC pairings across jar sizes. We tested the effect of jar size on competitive outcome statistically using a logit model (family: binomial; exclusion by the superior competitor was scored as 1, 0 otherwise), with species pairing and jar size as categorical explanatory variables. All jars had the same initial and maximum densities, differing only in their initial and maximum absolute abundances. In addition, environmental conditions and initial resources were the same for jars of all sizes. Thus, jar size was treated as a proxy for the strength of demographic stochasticity.

We examined the effects of jar size on mean abundances by comparing the 95% confidence intervals of the abundances in different jar sizes over time. We focus on estimating and reporting experimental means and their uncertainties but note that if the confidence

intervals of two means do not overlap, there are highly significant differences between those means. Using confidence intervals of abundances over time allowed us to broadly (and conservatively) compare abundances over time in the different jar sizes.

2.2.2 Part 2: Stochastic simulations of consumer-resource dynamics

We used simulations of a simple stochastic consumer-resource model to understand how demographic stochasticity could alter competitive outcomes, mean abundances over time, and effective demographic rates in two-species competitive communities. The model describes two consumers (N_1 and N_2) competing for a shared resource (R), the deterministic version of which is as follows (MacArthur, 1970):

$$\begin{aligned} \frac{dR}{dt} &= rR(1-\frac{R}{K}) - a_1RN_1 - a_2RN_2 \\ \frac{dN_1}{dt} &= e_1a_1RN_1 - d_1N_1 \\ \frac{dN_2}{dt} &= e_2a_2RN_2 - d_2N_2 \end{aligned} \tag{2.1}$$

where r is the density-independent growth rate of the resource, K is the carrying capacity of the source, a_i is the area of attack of consumer i (proportional to the size of the system), e_i is the conversion efficiency of consumer i, and d_i is the density-independent per-capita mortality rate of consumer i.

When only a single consumer is present in model 2.1, the resource R has a stable equilibrium (R^*) equal to $\frac{d_i}{e_ia_i}$. This equilibrium is the lowest abundance of the resource at which consumer i has a non-negative growth rate. In the two-consumer case, the system will approach or oscillate towards the lowest of these R^*s, meaning that the consumer with the lowest R^* will ultimately exclude its competitor (Tilman, 1982). Thus, any difference between consumers in R^* values represent a fitness inequality (Chesson, 2000; Adler et al., 2007).

A comparable stochastic version of model 2.1 can be created by assigning probabilistic intensity functions (i.e., transition rates) to discrete demographic events (e.g. birth, death). This type of model, also known as a jump process, along with Gillespie's stochastic simulation algorithm (SSA), can then be used to accurately simulate demographic stochasticity in continuous-time (Gillespie, 1977; Black and McKane, 2012). The stochastic analogue of model 2.1 has the following 6 discrete events:

$$\begin{aligned}
\text{R birth: } R &\xrightarrow{r_1 R(1-\frac{R}{K})} R+1 \\
\text{R death: } R &\xrightarrow{(1-e_1)a_1 R N_1 + (1-e_2)a_2 R N_2} R-1 \\
\text{R death, N1 birth: } R,\, N_1 &\xrightarrow{e_1 a_1 R N_1} R-1,\, N_1+1 \\
\text{R death, N2 birth: } R,\, N_2 &\xrightarrow{e_2 a_2 R N_2} R-1,\, N_2+1 \\
\text{N1 death: } N_1 &\xrightarrow{d_1 N_1} N_1-1 \\
\text{N2 death: } N_2 &\xrightarrow{d_2 N_2} N_2-1
\end{aligned} \tag{2.2}$$

Each equation above an arrow represents the probability that a transition occurs. For example, the first line (*R birth*) represents the birth of a resource (i.e., the population size of R increases by 1) and occurs with probability $r_1 R(1-\frac{R}{K})$ (i.e., the resource grows logistically). The expected value of model 2.2 broadly matches model 2.1, except for differences arising from lattice effects (due to discrete individuals: Henson et al., 2001) and Jensen's inequality (Jensen, 1906; Ruel and Ayres, 1999; Inouye, 2005; Chesson et al., 2005). Further details on developing the stochastic model, as well as R code, are given in Appendix A.

We simulated model 2.2 using the SSA across 11 different sets of parameter values, beginning with the neutral case (i.e., both consumers had identical demographic parameters), then for fitness inequalities of 0.1%, 1%, and 5% and then for increasing fitness inequalities between consumers in 5% increments (by lowering the death rate of consumer 2) up to a difference of 50%. Two additional niche differences (0.1% and 1%) were simulated to aid in our interpretation of the exclusion results below, but these simulations were not used for subsequent model-fitting. Parameter values for these simulations (see Table 2.1) were chosen

such that: (1) they produced dynamics broadly similar to those observed in our experimental system; (2) quasi-equilibria for consumers were near what we observed in our experimental monocultures (densities between 100 and 300 per 1/3 mL); (3) the quasi-equilibrium for the resource was higher than consumer equilibria by at least one order of magnitude; and (4) consumer death rates were high. In preliminary testing, we found that stochastic simulations of consumer-resource models with a highly abundant resource such as bacteria (with densities as high as 10^8 cells per mL) were computationally impractical using our methods. Thus, point (3) is a compromise to speed computation by assuming that the bacterial resource grows and is consumed in multiples of individuals.

Table 2.1: Parameter values for the neutral simulations of the stochastic consumer-resource model. For the large population size, K and a_i were scaled so that density-dependence was identical across population sizes. Non-neutral simulations used these parameter values, lowering only the death rate of consumer 2 in increments of 0.01 (making consumer 2 an increasingly superior competitor).

Model parameters	Values
r_1	1
K (small)	1000
K (large)	10000
a_1, a_2 (small)	0.04
a_1, a_2 (large)	0.004
e_1, e_2	0.02
d_1, d_2	0.2

For each set of parameter values, we simulated model 2.2 20,000 times using the Gillespie algorithm (Gillespie, 1977; Black and McKane, 2012) for two different initial community sizes, which differed by an order of magnitude in terms of absolute abundance: small ($R(0) = 1000$, $N_1(0) = N_2(0) = 5$) and large ($R(0) = 10000$, $N_1(0) = N_2(0) = 50$). Simulations were run to $t = 1000$, at which point competitive exclusion had been observed in the majority of the neutral simulations, in which the two consumer species had identical R^* values (competitive exclusion happened earlier as fitness differences increased).

To ensure that small and large simulations differed only with respect to the strength of demographic stochasticity, we scaled all density-dependent parameters so that simulations began in the same area of state space and so that individuals experienced the same degree of density-dependence throughout (e.g., Nisbet et al., 2016). Specifically, the resource carrying capacity, K, was scaled in the same way as initial abundance ($K_{small} = 1000$, $K_{large} = 10000$) and the attack rates, a_i, which represent the proportion of the total habitat area subject to attack, were reduced by a factor of 10 for the large simulations.

2.2.2.1 Simulation analysis and quantifying effective fitness inequalities

As with the experimental data, we quantified the probability of competitive exclusion across the different fitness inequalities and simulation sizes. Further, we assessed how population size affected abundances over time. Finally, we quantified how demographic stochasticity altered effective demographic rates and hence the effective fitness inequality between the two consumers.

To quantify change in abundance over time, for each parameter combination of the stochastic model we calculated the mean density (and its 95% confidence interval, as in the experiment) across 20,000 replicate simulations, for each time point (t = 1-100), conditioning on both consumers being extant. Using the conditional means focuses our analysis on quantitative differences between multi-species simulations and avoids biases in estimates that could arise from fitting to simulations where a consumer had previously gone extinct (differences are more extreme if these are included).

One way to quantify how stochasticity alters dynamics of abundance over time is to ask how demographic rates in a deterministic model would need to change to compensate for the effect of demographic stochasticity. In other words, what are the effective new parameter values of the deterministic model that best capture the mean dynamics of the stochastic model? We estimated effective parameter values by fitting the deterministic model to the simulated data. To do so, we used a least square approach in which parameter estimates were

optimized by minimizing the difference in the sum of squares between the solution of the deterministic model (model 2.1) and the conditional means (above). This method produces the same mean parameter estimates as a maximum likelihood approach where model 2.1 is treated as the mean of a normal or Poisson distribution.

In separate simulations of model 2.1 where the resource grew in the absence of consumers, we found that the effect of stochasticity on the effective values of r_1 and K were negligible. Thus, we assumed that the resource parameters, r_1 and K, were fixed, leaving six free parameters to be estimates (a_1, a_2, e_1, e_2, d_1, d_2).

We expressed the fitted parameters as the relative fitness inequality between consumers, specifically:

$$1 - \frac{R^*_{N_2}}{R^*_{N_2}} \tag{2.3}$$

where $R^*_{N_i}$ is the stable equilibrium for the resource in model 2.1 when only N_i is present. We obtained 95% confidence intervals for the estimated fitness inequality using a non-parametric bootstrap (percentile method; Davidson and Hinkley (1997)). As described in Appendix A, such model-fitting was possible only for the simulated data.

We used the program R, version 3.4.0 (R Core Team, 2017), with package 'deSolve' (Soetaert et al., 2010). See Appendix A for example code for these steps.

2.3 Results

2.3.1 Competitive exclusion in the experimental microcosms

We knew from prior observations of the three species of zooplankton (G. Legault, unpublished data) that the competitive hierarchy in our system was as follows: *Philodina americanum* >> *P. caudatum* > *P. aurelia*. As a result, we expected the AP and PC pairings to be characterized by large fitness inequalities and the AC pairing to be characterized by small fitness inequalities between competitors. This assumption agreed with our experimental findings: *P. aurelia* was the weakest competitor in the AC pairing and was excluded

by *P. caudatum* in 10 of 12 replicates of the large jar size (Figure 2.1 a). The exclusion rate in the medium jars was similarly high; *P. aurelia* was outcompeted in 11 of 12 replicates. In the small jars, however, where the impact of demographic stochasticity was strongest, the exclusion rate was half that of the other sizes, with *P. aurelia* excluded in only 5 of 12 replicates. Consistent with these qualitative differences, there was a statistically significant difference between exclusion rates in small jars versus those in the large and medium jars (Estimate = -1.945, 95% confidence interval = $(-4.103, -0.168)$; Binomial model [logit scale]).

The weakest competitor in the AP pairing, *P. aurelia*, was excluded in all replicates across jar sizes (Figure 2.1 b). Similarly, for the PC pairing, *P. caudatum* was excluded in all replicates and population sizes (Figure 2.1 c). As there were no differences in the ultimate exclusion outcomes across jar sizes for the AP and PC pairings, statistical analysis was not necessary for we did not fit binomial models to these data.

Finally, we note that both the AC and AP pairings had earlier exclusions in the small jar size, consistent with the notion that demographic stochasticity increases the likelihood of early stochastic extinctions.

2.3.2 Competitive exclusion in the stochastic simulations

When there were no differences in fitness between competitors (the neutral scenario), competitive exclusion was similar between the small and large simulations. By $t = 1000$, each consumer type won competition (i.e., outlasted the other consumer) in approximately 50% of cases (Figure 2.2). However, when fitness inequalities were non-zero, competitive exclusion differed between small and large simulations. For example, when the relative fitness inequality was 0.01 (i.e., consumer 2 had an R^* 1% lower than consumer 1), the superior competitor excluded the weaker competitor in 75.0% of the large simulations, but only 51.6% of the small simulations. Similarly, when the relative fitness inequality was 0.05, the superior competitor won in 99.4% of large simulations versus 58.1% in the small

Figure 2.1: Proportion of experimental jars in which the weaker competitor persisted, as a function of time. *Paramecium aurelia* was the weakest competitor in the (a) AC and (b) AP pairing, while *Paramecium caudatum* was the weakest competitor in the (c) PC pairing. Different colored lines represent the proportion surviving (out of 12 replicates) in different jar sizes (red = 1 mL habitat; gray = 10 mL habitat; blue = 80 mL habitat).

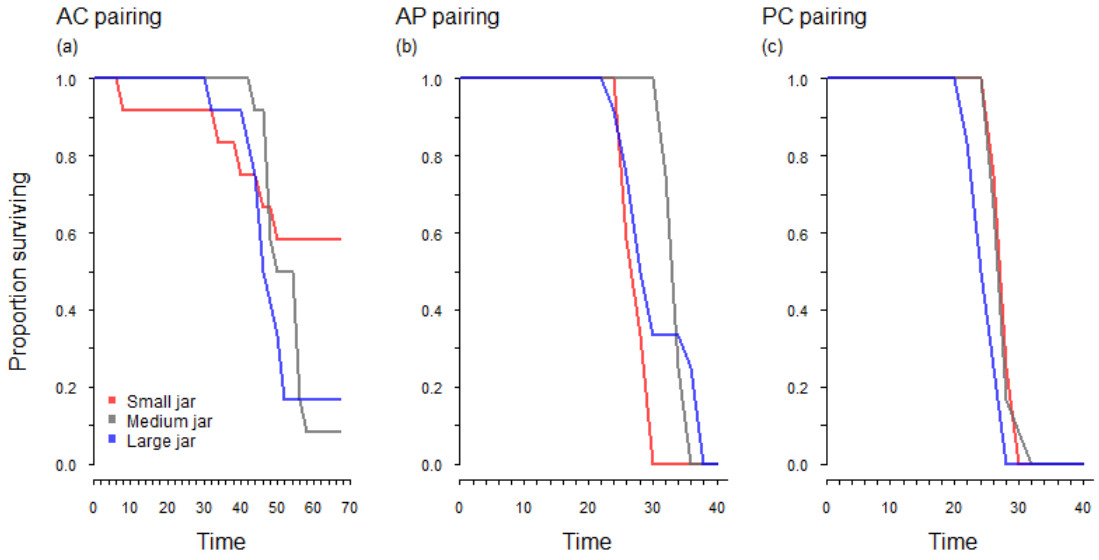

simulations (Figure 2.2).

In the deterministic version of the consumer-resource model, any non-zero fitness inequalities between consumers will always lead to the exclusion of the weaker competitor, thus the results of the large stochastic simulations were largely in line with deterministic expectations. In contrast, stochasticity in the small simulations led to many cases in which the weaker consumer excluded the stronger competitor (e.g., 41.9% of cases when the relative niche difference was 0.05). As fitness inequalities increased, the proportion of trials where the weaker consumer won in the small simulations decreased gradually (compared to a consistent win rate of 0-1% in the large simulations), but only when fitness differences were very large (e.g., consumer 2 had an R* 50% lower than consumer 1) were these proportions similar to those of the large simulations.

2.3.3 Conditional mean densities in the experimental microcosms

For the AC pairing, the pairing in which fitness inequality between competitors was small, both species had consistently lower densities in small jars relative to large jars (i.e., 95% confidence intervals did not overlap; Figure 2.3 a and b). In other words, when demographic stochasticity was strong, both consumers had lower mean densities. When fitness inequalities were larger, as in the AP and PC pairings, densities of the weaker competitors were also lower in small jars compared to large jars (Figure 2.3 c and e). However, jar size appeared to have less dramatic effects on the mean densities of the superior competitors in the AP and PC pairings (Figure 2.3 d and f).

2.3.4 Conditional mean densities in the stochastic simulations

Demographic stochasticity also affected the conditional mean densities of consumers in the simulations. In general, early in the time series the mean densities of both consumers were lower in the small simulations where demographic stochasticity was strongest compared to the large simulations (Figure 2.4). Over the long term, however, demographic stochasticity

Figure 2.2: Proportion of simulations in which the weaker consumer won as a function of relative fitness inequalities between consumers. Points represent the proportion (y-axis) of stochastic simulations where the weaker consumer (consumer 1) persisted longer than the superior consumer across a range of 13 relative fitness inequalities (one minus the ratio of consumers R^*s; x-axis; increasing fitness inequalities left to right) for the duration of the simulations ($t = 1000$). Squares represent proportions from the large simulations, where the effect of demographic stochasticity was weak, and circles represents proportions from the small simulations, where the effect of demographic stochasticity was strong. See Table 2.1 for the parameter values used in the neutral simulations (i.e., consumers had the same fitness).

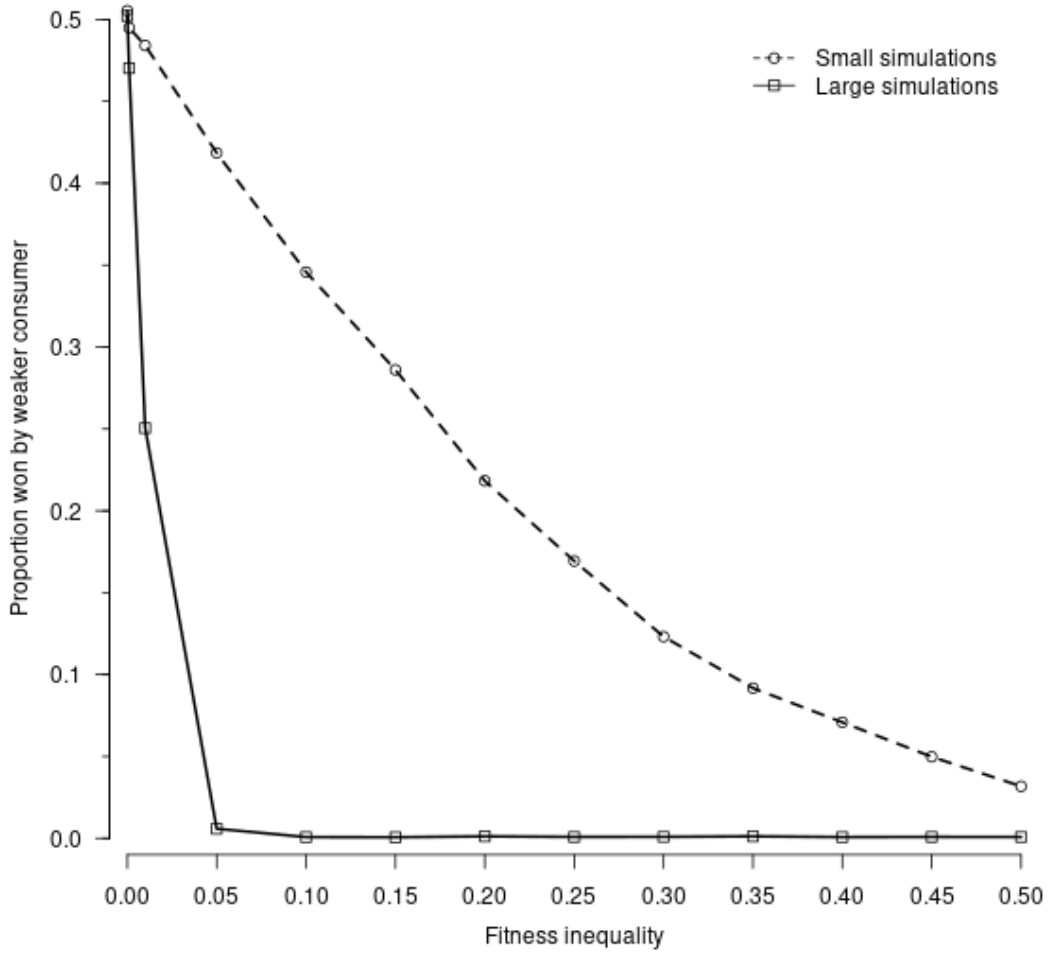

Figure 2.3: Densities over time in the experimental microcosms. Shown are means and 95% confidence intervals (from 12 replicates each) of the weaker competitors (top row) and stronger competitors (bottom row) in each of the three competitive pairings (AC, column 1; AP, column 2; PC, column 3). For clarity, only small (red) and large (blue) jars are shown here. Confidence intervals were conditioned on both competitors being extant and therefore some intervals are especially large or missing at different time points.

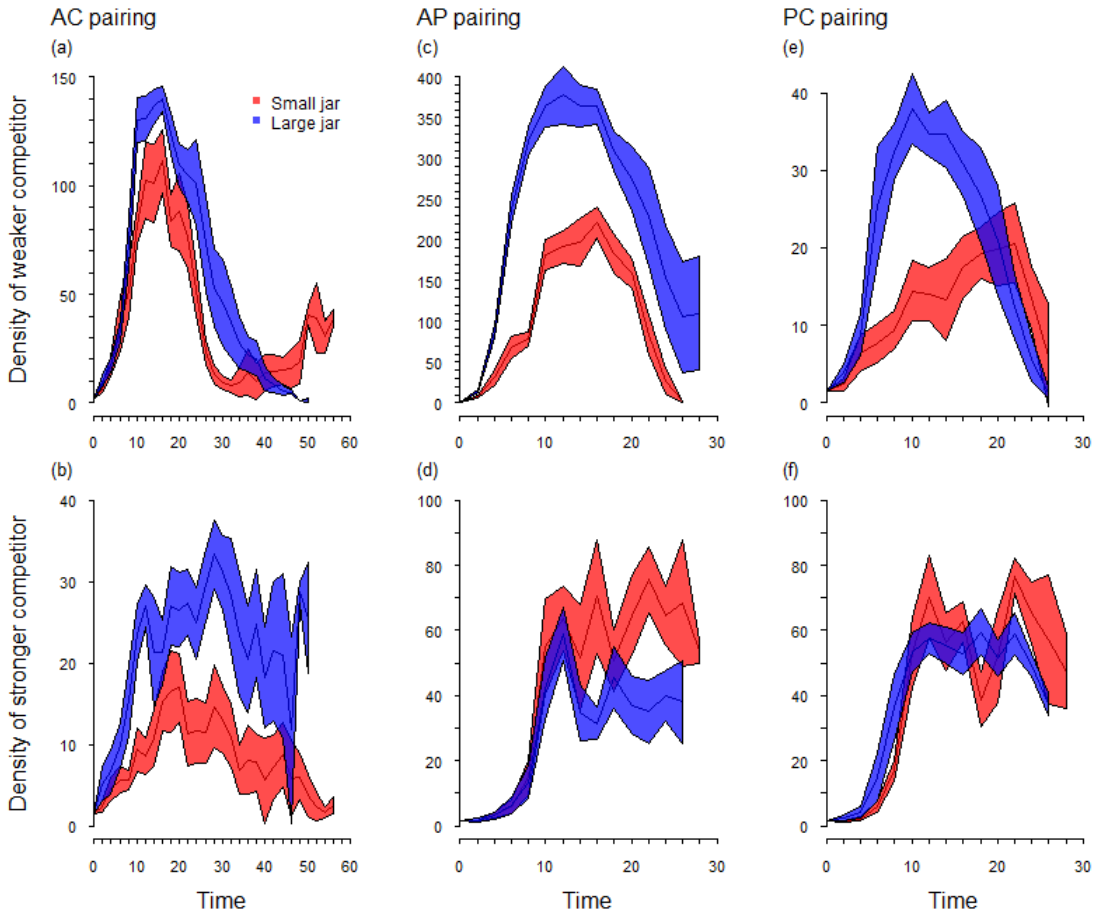

lead to higher mean densities of the weaker consumer and lower mean densities of the stronger consumer (see Appendix A for plots of all 11 fitness inequalities).

2.3.5 Effective fitness inequalities

There were minimal differences between small and large simulations in the effective fitness inequalities between consumers. In other words, when species had identical demographic rates, demographic stochasticity during the simulations did not alter the effective demographic rates of either consumer in a significant way. However, as the true fitness inequalities between consumers increased, demographic stochasticity altered the effective fitness inequalities of the consumers (Figure 2.5). In particular, the effective fitness inequalities in large simulations were generally in line with the true values, whereas the effective fitness inequalities in small simulations were consistently below both the true values and those of the large simulations. Visualizations of the deterministic model fitted to the expected values for the stochastic model for every parameter set are shown in Appendix A.

2.4 Discussion

We explored the effects of demographic stochasticity on competition using experimental communities of microzooplankton and simulations of continuous-time stochastic models, demonstrating that stochasticity (here driven by population size) can alter competitive outcomes and competitive dynamics. In particular, demographic stochasticity reduced the exclusion rates of weaker competitors, generally lowered mean densities over time of all species, and reduced effective fitness inequalities between species.

One of our key findings, that demographic stochasticity alters competitive outcomes, agrees with existing theory on the effects of demographic stochasticity in simple communities. Orrock and Fletcher (2005) and Pedruski et al. (2015) both used discrete-time models of consumer-resource dynamics and an approximation of demographic stochasticity to show that it can allow weaker competitors to out-compete stronger competitors when niche differ-

Figure 2.4: Conditional mean densities over time of consumers from the stochastic simulations. Shown are the 95% confidence intervals (from 20,000 initial replicates) of the weaker competitors (top row) and stronger competitors (bottom row) for increasing fitness inequalities from 5% to 35%.

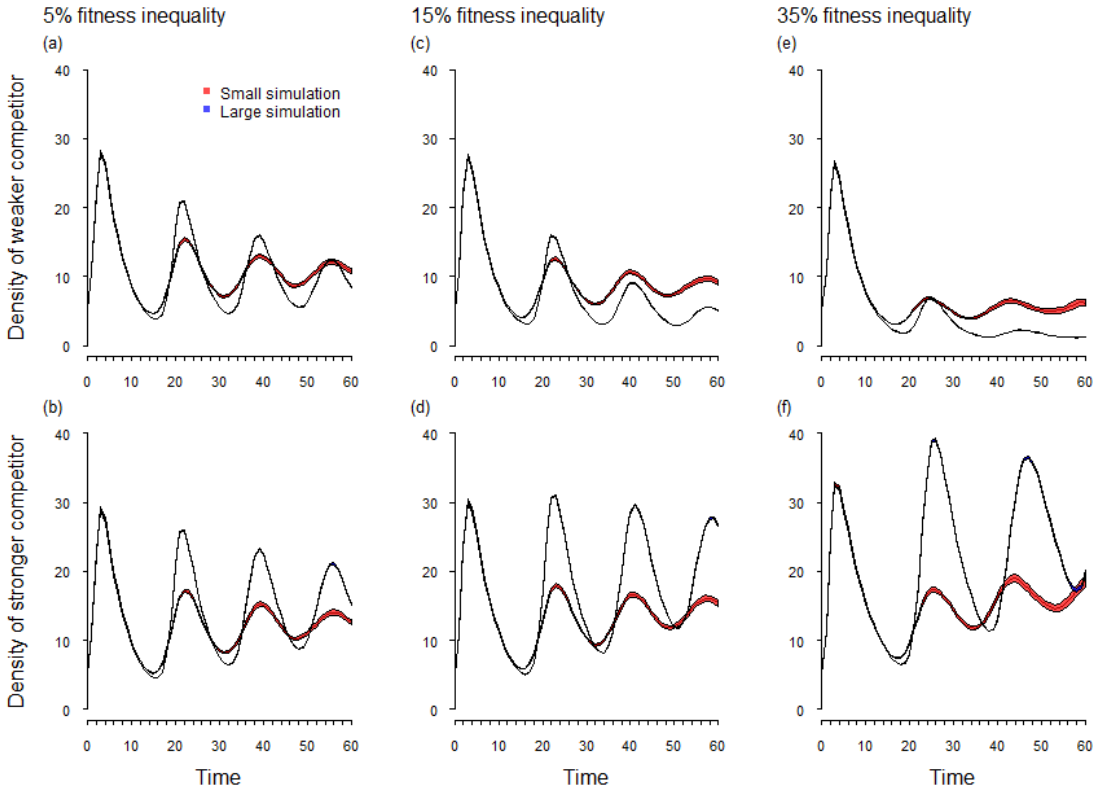

Figure 2.5: The impact of demographic stochasticity on the effective relative fitness inequalities of consumers in the simulations. Points represent the effective relative fitness inequality (one minus the ratio of consumers R*s; y-axis), calculated from parameter estimates based on fitting the deterministic model to the conditional means (conditioned on both consumers being extant) of the stochastic simulations, across the 11 relative niche differences calculated from the actual parameters used in the stochastic simulations. Squares represent niche differences for the large simulations and circles represent niche differences for the small simulations. Non-parametric bootstrap 95% confidence intervals are shown (small for most niche differences). The dotted line is the 1-to-1 line.

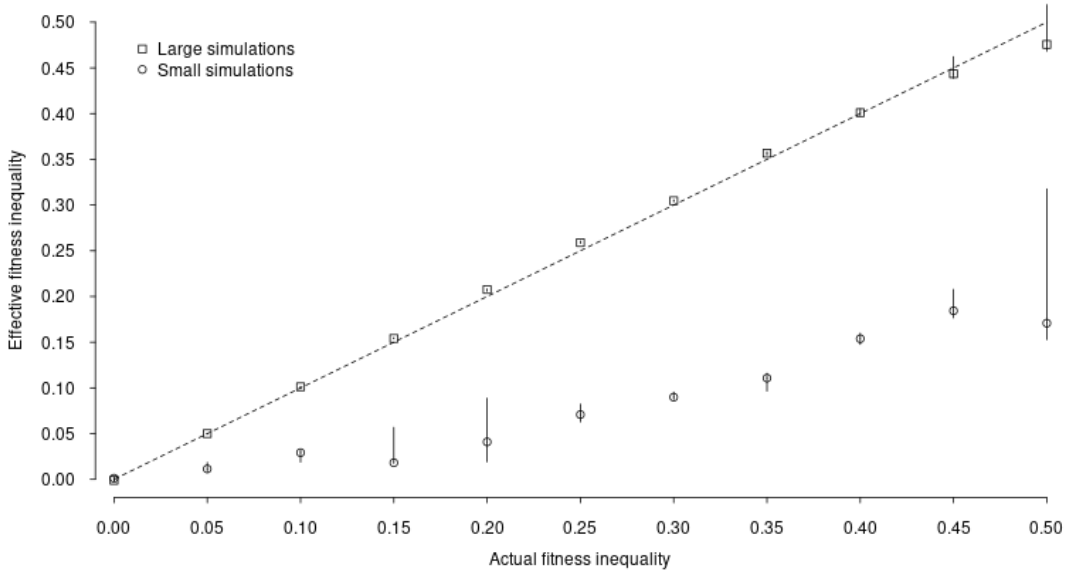

ences were small, but not when they were large. Similarly, Okuyama (2015) used continuous-time models of consumer-resource dynamics to show that demographic stochasticity can lead to competitive outcomes not predicted by the deterministic model. Our simulation results extend such work by examining the effects of demographic stochasticity on competitive outcomes across different absolute abundances and fitness differences. In particular, across 13 sets of stochastic simulations, we found that the identity of the winner was more variable in small simulations than in large simulations. Only when fitness differences were very large ($> 30\%$) was competitive exclusion not affected by simulation size. Furthermore, our experimental findings demonstrate how such effects of demographic stochasticity manifest in real populations. We found that when fitness differences were small, a weaker competitor (*P. aurelia*) was able to exclude its superior rival (*P. caudatum*) more frequently in small jars than in larger jars with otherwise comparable environmental conditions. However, when fitness differences were large, as they were in the other species pairings, jar size had no discernible effect on competitive outcomes. Thus our experiment results are consistent with theory on demographic stochasticity and provide support for the notion that absolute abundance is an important consideration when trying to assess the relative importance of niche versus stochastic processes in real communities (Adler et al., 2007; Gravel et al., 2011; Vellend et al., 2014).

In addition to altering competitive outcomes, demographic stochasticity affected the densities over time of consumers in both our experimental jars and in the simulations. In the AC pairing where fitness differences were small (*P. aurelia* and *P. caudatum*), each species had lower mean densities in small jars compared to large jars. When fitness differences were larger, as in the PC and AP pairings, only the densities of the weaker competitor were reduced in the presence of strong demographic stochasticity. In the simulations, initial densities in the small simulations were also generally lower than those in the large simulations for both consumers. However, over the long-term, densities of the weaker competitor were often highest, and densities of the stronger competitor often lowest, in the small simulations.

In other words, demographic stochasticity gradually led to higher than expected densities of the weaker consumer and lower than expected densities of the stronger consumer. Consistent with this, we found that the effective fitness inequalities between consumers were lower in the small simulations for all but the neutral case (Figure 2.5). To our knowledge, our study is the first such test of how demographic stochasticity affects mean densities over time as well as the effective demographic rates of populations.

We likely did not observe the long-term increases/decreases in the densities of weaker/stronger consumers in our experimental system for two reasons: (1) our experiment did not persist long enough; and (2) our species did not experience the same degree of demographic stochasticity as in our simulations. Regarding (2), this can be seen by comparing Figures 2.3 and 2.4, which highlights the often large differences in abundance between the two competing species, compared to the mostly similar consumer abundances in the simulations. For instance, in the AP pairing, *P. aurelia* had approximately 4-fold higher absolute abundances over time than its competitor *P. caudatum*. We intentionally chose to simulate consumers with similar absolute abundances as it meant that both consumers could be expected to experience a similar degree of demographic stochasticity at each simulation size. However, this choice also ignored the very real possibility that some consumers may naturally have lower densities than their competitors, and therefore experience demographic stochasticity differently across habitat sizes. This was likely the case for some of our experimental jars.

Founder effects could have played a role in explaining the differences we observed in competitive outcomes across population sizes in our experiment; however, this is unlikely. If founder effects were important, we would expect to see large differences over time between replicates of the small jars compared to replicates of larger jars due to the stronger influence of genetic drift in the small jars over and above the effects of demographic stochasticity (e.g., Dobzhansky and Pavlovsky, 1957). However, the coefficients of variation across replicates were not consistently higher for the small jars (see Appendix A). Moreover, the stock cultures

used for our experiment had spent more than 1.5 years at conditions similar to those used in the experiment, representing thousands of protist generations in a constant environment. As a result, the standing genetic diversity of the protists used in our competitive trials was likely to be low, meaning that different jar sizes likely had similar starting diversities.

Our findings regarding the effects of demographic stochasticity on competitive outcomes are analogous to the effects of genetic drift (i.e., random sampling of alleles) on evolutionary dynamics. As far back as Wright (1931), it has been recognized that evolving populations are subject to the effects of both selection and genetic drift, and that at small population sizes, genetic drift may be strong enough to interfere with selection. Since then, there has been strong experimental support for the notion that small population size may lead to evolutionary outcomes not predicted by fitness differences alone (e.g., Dobzhansky and Pavlovsky, 1957; Weber, 1990; Lynch and Conery, 2003; Paland and Schmid, 2003; Petit and Barbadilla, 2009). Insofar as selection for adaptive traits may be considered analogous to competition for shared resources (sensu Vellend, 2010), we found similar results: that small population size can lead to competitive outcomes not predicted by differences in competitive abilities alone.

Demographic stochasticity is ubiquitous in natural systems and represents a significant source of intraspecific variation in populations and communities. Recognizing the potential role for such stochasticity is important (Vellend et al., 2014) as it can produce outcomes not predicted by common, deterministic models of competition and other processes. Future work should focus on how to better characterize and quantify the impacts of demographic stochasticity in natural communities and in more realistic continuous-time descriptions of such systems. Even in a controlled microcosm system such as ours, this may not always be straightforward, and will likely need to be preceded by initial development and testing of appropriate population models (e.g., Melbourne and Hastings, 2008). However, given the potential for demographic stochasticity to erode our expectations of community dynamics and outcomes, such work may be necessary if we are to better predict how communities

assemble and change with time.

Chapter 3

Accounting for environmental change in continuous-time stochastic population models

Geoffrey B. Legault, Brett A. Melbourne

3.1 Introduction

Ecologists use stochastic population models to account for intrinsic sources of population variability, particularly the variability arising from probabilistic demographic events at the individual level (e.g., random births and deaths), also known as demographic stochasticity. The importance of accounting for demographic stochasticity in populations is well established in the theoretical literature, where it has been shown to increase extinction risk (Shaffer, 1981; Lande, 1993; Ovaskainen and Meerson, 2010), alter coexistence patterns (Orrock and Fletcher, 2005; Orrock and Watling, 2010; Okuyama, 2015; Pedruski et al., 2015; Hart et al., 2016), increase the persistence time of disease (Bartlett, 1957), and reduce spatial synchrony in metacommunities (Simonis, 2012).

For continuous-time population models, the effects of demographic stochasticity can be approximated by adding white noise terms to differential equations (turning them from deterministic differential equations into stochastic differential equations [SDEs]) or by embedding such equations into standard probability distributions with an appropriate scaling term for the variance (e.g., the system-size expansion; van Kampen, 1992). However, these approximations are generally accurate only for predicting small deviations from the expected

value of the stochastic process (e.g., near stable equilibria; van Kampen, 1992; Ovaskainen and Meerson, 2010; Black and McKane, 2012), and can fail to predict large deviations, such as those leading to population extinction (e.g., Wilcox and Possingham, 2002; Doering et al., 2005; Kessler and Shnerb, 2007). When predicting large deviations is important (e.g., for predicting extinction risk or modelling populations not at equilibrium), population models can be reformulated in terms of a set of partial differential equations that exactly describes the time-evolving probability density of the system (also known as Kolmogorov forward equations (Kolmogorov, 1931), or the master equation). In practice, solving Kolmogorov forward equations is often infeasible (even numerically) for ecological systems (Keeling and Ross, 2008), particularly those that are large (population size > 1000) and/or multi-dimensional (i.e., contain many species). A convenient alternative, which effectively samples from the probability density one would obtain by solving the forward equation, is Gillespie's stochastic simulation algorithm [SSA] (Gillespie, 1977). Due to its tractability and the relative ease and speed of implementing the algorithm, the SSA is now commonly used in ecology to account for and explore the effects of demographic stochasticity in populations and communities (e.g., Kolpas and Nisbet, 2010; Kramer and Drake, 2010; Simonis, 2012; Yaari et al., 2012; Gokhale et al., 2013; Huang et al., 2015; Vestergaard and Gnois, 2015; Nisbet et al., 2016).

An important limitation of the SSA, as it is currently used in ecology, is that it treats demographic processes, such as birth or death, as time-independent (i.e., as stationary [or homogenous] Poisson processes). In other words, the SSA assumes that the demographic rates of individuals do not change over time. Such an assumption may be adequate over short time scales or under highly controlled conditions, but is unrealistic for modelling stochasticity in many natural systems. One reason is that demographic traits often depend on factors that are not included in typical population models and which themselves change over time. A key example of this kind of non-stationary demography is the fact that the demographic traits (e.g., birth, death, dispersal rates) of many species are temperature-dependent (Parme-

san, 2006; Deutsch et al., 2008; Angilletta, 2009; Dell et al., 2011) and may change within individual lifetimes as a result of short- or long-term temperature variability (e.g., Miquel et al., 1976; Kingsolver et al., 2013, 2015; Paaijmans et al., 2013; Estay et al., 2014; Stroustrup et al., 2016). Similarly, plant growth is strongly associated with precipitation (e.g., Novoplansky and Goldberg, 2001; Fay et al., 2003; Angert et al., 2007; Heisler-White et al., 2008), which, like temperature, may vary considerably over the lifespan of an individual. The strong link between the external environment and demographic traits is why ecologists routinely incorporate environmental variability into determinstic or approximately-stochastic populations models. However, to our knowledge, environmental variability (and the resulting non-stationary demography) has not been considered in more exact continuous-time stochastic models such as those simulated by the SSA. This is problematic because stochastic models that do not account for environment-dependent (i.e., non-stationary) demography may be insufficient for forecasting the combined effects of environmental variability and probabilistic demography in populations and communities.

We describe an extension of the SSA that allows for non-stationary demography and explore how, under a variety of realistic environmental-change scenarios, its predictions differ from the traditional, stationary SSA for continuous-time models of exponential and logistic growth (Verhulst, 1845; Pearl and Reed, 1920). We show that using a stationary SSA when demography is non-stationary can lead to biased predictions about the effects of stochasticity on populations and communities. Furthermore, we outline a straightforward and computationally inexpensive approach for estimating when it may be appropriate to use the non-stationary extension of the SSA.

3.2 Methods

3.2.1 Non-stationary demography in non-SSA models

Non-stationary demography can be easily incorporated into standard deterministic models, either by converting one or more demographic parameters (e.g., birth rate) into time-dependent functions or, if demography is non-stationary because of some extrinsic factor like temperature, by adding that factor as a new state variable and linking it to the relevant parameter(s) with an appropriate parameter or function (also known as a coupling factor; van Kampen, 1992). This approach can also be used for stochastic differential equations (SDEs), since they are essentially deterministic equations either embedded in standard distributions or with added white noise terms that are independent of demographic rates or environmental variability. However, as previously discussed, these approximations commonly fail, particularly when there are large deviations from an equilibrium, as might be expected during rapid environmental change. As an exact approach to modelling stochasticity, the SSA has the potential to avoid such failings. However, as we describe below, additional challenges arise when trying to use the SSA approach when demography is non-stationary.

3.2.2 Gillespie's stochastic simulation algorithm (SSA)

We begin by describing the traditional (stationary) SSA (Gillespie, 1977), also known as the direct method, and use a simple exponential growth model to illustrate the issue of non-stationary demography. Other implementations of the algorithm have been proposed, such as the tau-leap method (Gillespie, 2001), all of which sacrifice accuracy for simulation speed. As a result, we will not address these less accurate implementations here.

The basic SSA can be conceived of as iteratively answering two questions: (1) When does the next demographic process (e.g., birth, death) occur? and (2) Which demographic process occurs? It has four steps (Gillespie, 1977):

(1) Initialization of the system, which includes setting the rates (i.e., the probability

an event occurs per unit time) of all demographic processes, the effects of those processes (e.g., birth = +1 individual), the starting population size(s), and the end time of the simulation.

(2) Determine the inter-arrival time (i.e., waiting time), τ, until the next demographic event by sampling from an exponential distribution with mean equal to the sum of all demographic process rates.

(3) Determine which demographic event occurs by sampling from the list of possible processes, the probability of each process conditioned on the fact that an event (of any kind) has occurred at $t + \tau$.

(4) Update the time based on (2) and update population size(s) based on (3) [this may also change future demographic rates if they depend on population size], then return to step 2 until all demographic rates are zero or the end time has been reached.

Implementing the above algorithm is straightforward for most ecological models, the most difficult aspect often being the creation of the rate function(s) in step (1). For example, beginning with an exponential growth model with deterministic equation $\frac{dN}{dt} = rN$, a choice has to be made about whether the parameter r represents only a birth rate (i.e., we are modelling a *pure birth* process) or whether it represents the net effect of a birth rate minus a death rate (i.e., $r = b - d$). For the purpose of illustrating the SSA, we will keep things simple and model a pure birth process only, in which case r can be interpreted as the expected number of births per unit time. The stochastic formulation for a pure birth model (also known as Yule process; Yule, 1925) can be represented as follows:

$$N \xrightarrow{rN} N + 1 \tag{3.1}$$

Here, equation 3.1 means that births occur at rate rN and that each birth has the effect of increasing the population by 1. A single iteration through the SSA using this model,

beginning at time t and population size N, would proceed in this manner: calculate the birth rate (rN), obtain a sample (τ) from an exponential distribution with mean equal to the birth rate, update the time from t to $t + \tau$ and update the population from N to $N + 1$.

The decision to sample from an exponential distribution to determine the timing of the next demographic event in the stationary SSA is based on assumptions about what it means for a demographic process to be random. These assumptions are: (a) the process happens at some average rate within a given time interval, although when in the interval it happens is completely random (i.e., the occurrence times within an interval are uniformly distributed); (b) occurrence times of the process are independent of each other. Taken together, these assumptions describe what is known as a Poisson point process, which is used to represent random processes in continuous time across many disciplines. One useful feature of these processes in the context of ecological models is that the occurrence time of a set of multiple, independent Poisson processes (e.g., a population experiencing both birth and death) can itself be described by a single Poisson point process with rate, λ, equal to the sum of the rates of the individual processes.

When the rate, λ, of a Poisson point process is constant through time, it is called a stationary (or homogeneous) Poisson process and has inter-arrival times (i.e., times between event occurrences) that follow a cumulative distribution function (CDF) of the form:

$$1 - exp(-\lambda t) \tag{3.2}$$

Equation 3.2 is also the CDF of an exponential distribution, so it is possible to generate the inter-arrival times of a stationary Poisson process by sampling from an exponential distribution with rate λ. However, because it is generally faster computationally to sample from a uniform distribution than it is from an exponential distribution, it is common to obtain inter-arrival times of stationary processes by generating sample U from a uniform distribution on the interval [0, 1) and then converting it to the appropriate exponential random variable, X, using the inverse transform method, with equation $X = \frac{-1}{\lambda} ln(\frac{1}{U})$.

3.2.3 Changing environments: non-stationary Poisson processes

When the rate of a Poisson point process is not constant over time, say when it depends on changing temperatures, it is called a non-stationary (or non-homogeneous) Poisson process. In such cases, the rate of the process is described by a time-dependent function, $F(t)$, and the CDF for inter-arrival time τ, following the last occurrence of the process at time T, is:

$$1 - exp(-\int_0^t F(T+\tau)d\tau) \tag{3.3}$$

In some cases, analytical solutions to the integral in equation 3.3 are possible. For example, if the model contains only one non-stationary Poisson process with a rate function of the form $F(t) = \alpha t^{-\beta}$ (i.e., a power law function), equation 3.3 reduces to:

$$1 - exp(-\alpha(T+t)^{\beta} - T^{\beta}) \tag{3.4}$$

which is also the CDF of a Weibull distribution. Thus, for extremely simple non-stationary processes, the traditional SSA can be modified to obtain τ via sampling from a Weibull distribution with scale parameter α and shape parameter β. However, many non-stationary demographic processes will not follow a power law function. For example, if the birth rate r in our pure birth model were time- or environment-dependent, the model would become:

$$N \xrightarrow{r(t)N} N+1 \tag{3.5}$$

Here, unless the time-dependent birth rate $r(t)$ can be expressed as $t^{-\beta}$, the Weibull method discussed above is not appropriate. Further, even if a single demographic process could be described by a power law function, most population models will involve many different demographic processes. Since multiple demographic processes could depend on environmental conditions in different ways (some processes may also be stationary), it is unlikely that the combination of all such processes can be expressed in a power law form.

For most population- or community-level models with any kind of complexity, analytical solutions to the CDF in equation 3.3 are unavailable. Various methods have been

proposed to simulate such non-stationary models (e.g., Boguñá et al., 2014; Vestergaard and Gnois, 2015; Duan and Liu, 2015), most of which involve thinning or rejection sampling (Buffon, 1774; Von Neumann, 1951). We will not describe these methods here, other than to say that while they are often computationally efficient, they require bounded rate functions $\lambda(t)$ and do not perform well for high-dimensional (e.g., models of many species) systems (Ross, 2014). In any case, our goal is not to propose the most efficient method for simulating non-stationary biological processes, but rather to explore the conditions in which fully accounting for non-stationary demography may be important. Thus, we employ an exact, direct approach to simulating non-stationary stochastic models.

The direct approach, which we will refer to as SSA+, replaces step (2) of Gillespie's SSA by generating τ using the inverse transform method, which can be implemented as follows:

(1) Generate random number U from a uniform distribution on the interval [0, 1).

(2) Find the value of X which solves $F(X) = U$, where $F(t)$ is the CDF in 3.3.

(3) Set inter-arrival time τ to X.

Because both the direct method above and the rejection-based methods mentioned previously are computationally expensive compared to a stationary SSA, many ecologists might be willing to sacrifice some accuracy for a faster approach. One way to do so, which we will call the naive SSA (SSAn), would be to convert a non-stationary process to a stationary one for each inter-arrival period by fixing $\lambda(t)$ to the value at the current time of the simulation. This algorithm would continue to sample inter-arrival times from an exponential distribution and would be naive to changes in the environment only for the duration of an inter-arrival period.

Supposing $\lambda(t)$ was an increasing function (i.e., the rates of demographic events increased through time), one would expect the SSAn to, on average, produce inter-arrival

times that were smaller than the inter-arrival times that would be produced by the exact SSA+ method. Since inter-arrival times determine when events occur in the simulations, for an exponential growth model, this would lead to smaller population sizes over time than those predicted by the SSA+. However, for other kinds of models and or patterns of environmental change, it is difficult to know *a priori* how the SSAn and SSA+ methods might differ. Therefore, to help generate some intuition about when such scenarios might arise, we explore how predictions of the SSAn and SSA+ differ for two different ecological models in a variety of environmental change scenarios.

3.2.4 Stochastic population models

To assess the importance of fully accounting for non-stationary demography, we consider two population models: exponential and logistic growth. The deterministic forms of these models and their stochastic analogs are presented in Table 3.1.

Each model includes a density-independent birth rate, $b(t)$, which we set as the non-stationary demographic process in all our simulations. Specifically, we assume a fixed density-independent birth term, b_1, which is multiplied by a time-dependent environment function, env(t), to produce a birth rate that changes through time. We modelled 6 different non-stationary functions representing environmental change (herein environment functions; equations in Table 3.2): (1) constant, slow increase (increasing 1); (2) constant, fast increase (increasing 2); (3) slow, regular fluctuations around a mean (fluctuating 1); (4) fast, regular fluctuations around a mean (fluctuating 2); (5) slow, random fluctuations around a mean (random 1); (6) fast, random fluctuations around a mean (random 2). The two increasing scenarios are analogous to a demographic process that depends on external temperature increases, as might occur over a growing season or in an environment where temperatures are gradually increasing over time. The two fluctuating scenarios are analogous to a demographic process that responds to fluctuating temperatures, as might occur in an environment with strong diurnal or seasonal temperature changes. Finally, the two random scenarios are

Table 3.1: The ecological models considered in the study, specified as deterministic equations with their stochastic analogs. Parameters b_1 and d_1 are density-independent birth and death rates. Density-dependent growth in species N is incorporated with a density-dependent death rate, d_2. For the stochastic intensity functions, the functions above the arrows have the same parameter values as their deterministic counterparts. The environment functions, env(t), are defined in Table 3.2

Model	Deterministic equations	Stochastic intensity functions
Exponential growth	$\frac{dN}{dt} = b(t)N - d(t)N$ where $b(t) = b_1 \cdot \text{env(t)}$ $d(t) = d_1$	N birth: $N \xrightarrow{b(t)N} N+1$ N death: $N \xrightarrow{d(t)N} N-1$
Logistic growth	$\frac{dN}{dt} = b(t)N - d(t)N$ where $b(t) = b_1 \cdot \text{env(t)}$ $d(t) = d_1 + d_2 N$	N birth: $N \xrightarrow{b(t)N} N+1$ N death: $N \xrightarrow{d(t)N} N-1$

analogous to a demographic process that responds to stochastic temperature fluctuations (i.e., environmental stochasticity), which occur, to some degree, in nearly all natural environments. Figure 3.1 illustrates how the value of each environment function changes over time.

Table 3.2: The environment functions or distributions considered in our simulations. To create time-dependent equations for the random simulations, we first sampled from a normal distribution (n samples = number of integer time steps in the simulation interval) then created splines using those samples so that we had a continuous-time function over which to integrate. Values outside the simulation interval were set as the mean of the distribution (1.5).

Description	Environment function, env(t)
Increasing 1	$0.04t + 1$
Increasing 2	$0.08t + 1$
Fluctuating 1	$\frac{sin(t)+1}{1.5}$
Fluctuating 2	$\frac{sin(2t)+1}{1.5}$
Random 1	env(t) = spline($\{1, 2, ..., 100\}$, $\{Y_1, Y_2, ..., Y_{100}\}$) where $Y_i \sim \mathcal{N}(\mu = 1.5, \sigma^2 = 0.25)$
Random 2	env(t) = spline($\{1, 2, ..., 100\}$, $\{Y_1, Y_2, ..., Y_{100}\}$) where $Y_i \sim \mathcal{N}(\mu = 1.5, \sigma^2 = 0.50)$

For implementing the SSAn method, we treated demography as non-stationary, but allowed rates to be updated after each step through the algorithm. In particular, we calculated the inter-arrival time of the next event, τ, by sampling from an exponential distribution with rate $\lambda = \lambda(Y)$, where Y is the current time of the simulation. As mentioned previously, this implementation is naive to changes in the environment for the duration of an inter-arrival period and, in this way, does not fully account for non-stationary demography. In general, if the frequency of inter-arrival periods in a system far exceed the rate of environmental

Figure 3.1: Values of the time-dependent environment functions used in the simulations of non-stationary demography. In all cases, the value on the y-axis corresponds to the numerical solution of env(t) at time t (x-axis). Equations for these functions are in Table 3.2

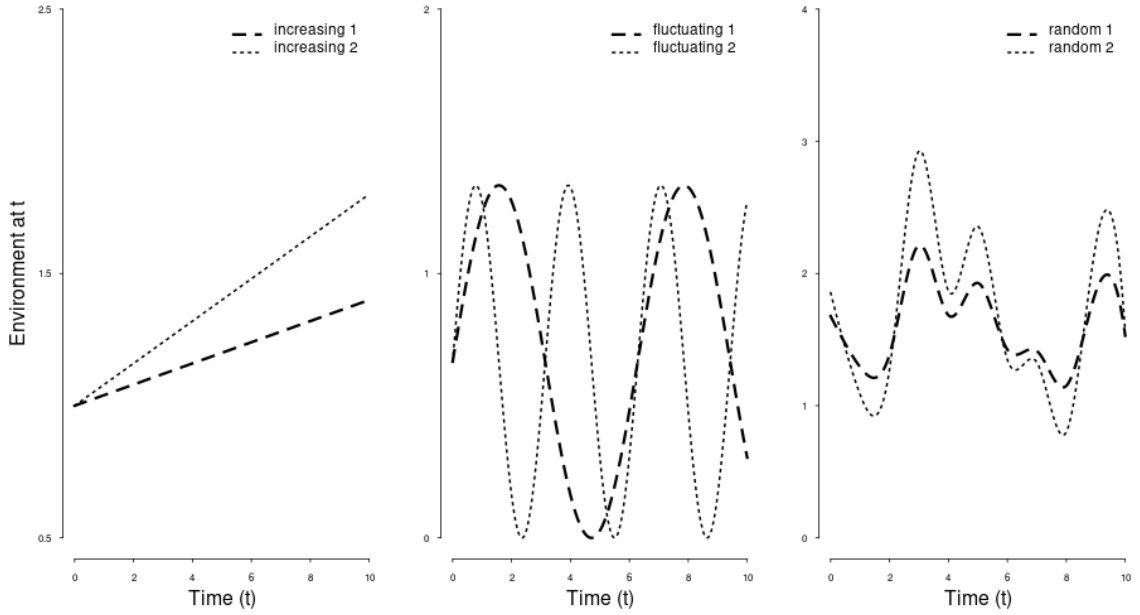

change, we would expect this approximation to produce population estimates fairly close to those of the SSA+.

For each model and environment function, we ran 10,000 simulations of both the SSAn and SSA+ methods with a starting population size of $N = 100$, using the following parameter values: $b_1 = 0.003$ and $d_1 = 0.0027$; and for the logistic growth model, $d_2 = 0.000003$ (with this parameterization, carrying capacity $K = \frac{b_1 - d_1}{d_2}$). The above values were chosen such that individual demographic processes occurred somewhat slowly in comparison to the rate of environmental change (e.g., in the increasing 1 scenario, the environment changes by 0.04 per unit time while the density-independent birth rate was 0.003 per individual [0.3 for the population of 100] over the same time period). We ran both models to $t = 100$.

3.2.5 Comparing CDFs of inter-arrival times

Prior to examining the results of the simulations, we can derive some intuition about which models and which environment functions may lead to significant differences in the predictions of the SSAn and SSA+. One way to do so is to examine the CDFs of the waiting times, τ, at $t = 0$ based on both stationary and non-stationary treatments. Figure 2 shows these CDFs for each model and environment function. We can see from Figure 3.2a, for example, that the CDFs of the SSA+ method are consistently higher than those of the SSAn. This suggests that demographic events will occur earlier in the SSA+ simulations, translating to higher population sizes over time. For fluctuating environment functions, as in Figure 3.2b, differences between the CDFs of the SSAn and SSA+ are even more pronounced, as we might expect simply from looking at how quickly the environment changes in Figure 3.1b compared to Figure 3.1a. In Figure 3.2c, the SSA+ CDFs appear to be somewhat lower than those of the SSAn, which we would expect to lead to lower projected population sizes for these early time points. Differences between the inter-arrival times appear smaller for the logistic growth model (Figure 3.2d-f), thus we expect to see smaller differences between SSAn and SSA+ results.

Figure 3.2: Cumulative probabilities over time (from $t = 0$) that the next demographic event will occur, for all models and environment functions. The top row highlights the probabilities for the exponential growth model for the (a) increasing; (b) fluctuating; and (c) random environment functions, while the bottom row shows the probabilities for the logistic growth model (d-f). The solid line represents the probabilities for the SSAn method, which assumes that demographic processes occur at constant rates over time (in this case, the rate at $t = 0$). Dashed and dotted lines represent the probabilities for the SSA+ method which accurately accounts for non-stationary demographic rates (compare to Figure 3.1). Curves are similar for both models.

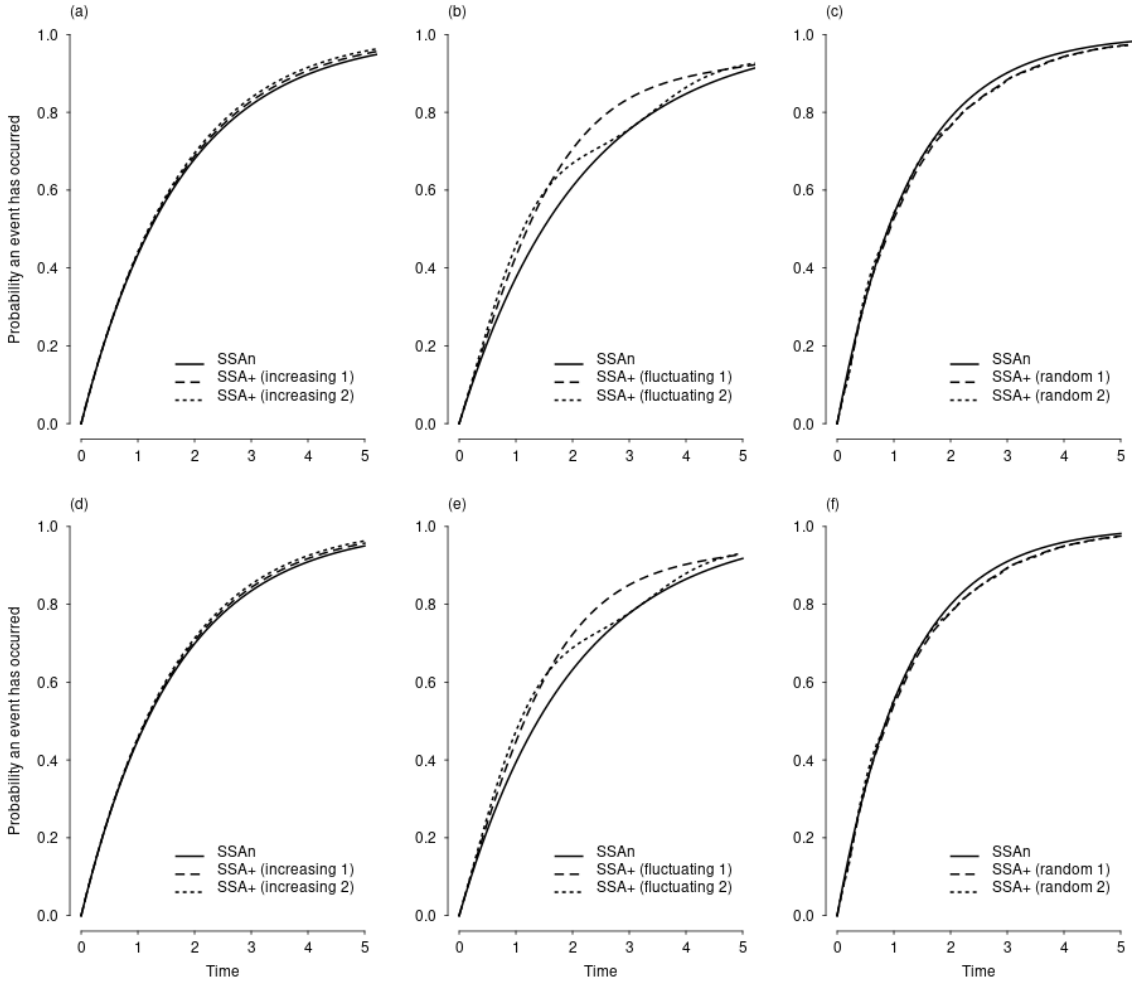

3.2.6 Diagnostics and analysis

We performed three independent diagnostic tests of our simulation algorithms. First, we tested our implementation of sampling inter-arrival times for non-stationary processes. To do so, we simulated a non-stationary process with a rate function of the form $F(t) = \alpha t^{-\beta}$, a power law function. As discussed above, when a non-stationary process has such a rate function, it is possible to obtain inter-arrival times by sampling from a Weibull distribution with parameters α and β. After sampling 1,000,000 inter-arrival times using each method, we found nearly identical distributions of waiting times (Appendix B).

Second, we compared the results of SSAn and SSA+ simulations when the environment function was constant through time. As discussed above, the SSAn method treats demography as being non-stationary by obtaining waiting times from an exponential distribution, whereas the SSA+ method uses the inverse transform method. When demographic processes are stationary, both methods should produce the same distribution of waiting times and, subsequently, the same distribution of population sizes over time. As expected, for both exponential growth and logistic growth with a constant environment function, both the SSAn and SSA+ algorithms produced strongly overlapping population size distributions (Appendix B).

To analyze the final simulation results (presented below), for each model and environment function, we compared the 95% confidence intervals for the mean across 10,000 replicate simulations of the SSAn and SSA+ methods at each interval time step, obtained using non-parametric bootstraps (percentile method; Davidson and Hinkley, 1997). Prior to this, we tested whether 10,000 simulations were enough to accurately characterize the probability density of the stochastic processes. Specifically, we examined how the variation in population projections changed as more simulations were added. For all models and environment functions, there were minimal changes in the mean and standard deviation across simulations for resulting population sizes beyond 1,000 simulations (Appendix B). Thus,

running 10,000 simulations was more than sufficient to minimize Monte Carlo errors in the estimated means, and confidence intervals were very small.

Since the exponential growth model is linear with respect to density, the only differences that should arise between the expected (mean) values of deterministic and stochastic versions of the exponential model will be due to lattice effects (Henson et al., 2001), the impacts of which should be minimal at population sizes larger than 100 (as in our case). Thus, in addition to examining the confidence intervals, it is possible to directly compare the results of the SSAn and SSA+ simulations to numerical solutions of the deterministic equation for exponential growth in 3.1. In the absence of Monte Carlo error or lattice effects, if the SSA+ is properly accounting for non-stationary demography, the mean value of the simulations at particular times should be equal to the solutions of the deterministic equations at those times. Since the logistic growth model is non-linear with respect to density, both lattice effects and non-linear averaging will lead to differences between the expected values of deterministic and stochastic versions of the model. As such, we compare SSAn and SSA+ results to the deterministic results only for the exponential growth model. For all the simulations and analyses above, we used R, version 3.4.0 (R Core Team, 2017), and for solving the deterministic equations, the R package 'deSolve' (Soetaert et al., 2010). R code necessary for running SSAn and SSA+ simulations is provided in Appendix B.

3.3 Results

When the environment was changing, there were often differences in the predicted distributions of population sizes between the SSAn and SSA+ methods (Figure 3.3, the [similar] results for the *slower* environment functions are in Appendix B). Generally, the magnitude of these differences corresponded with what could be predicted qualitatively from the CDFs in Figure 3.2. For example, the distributions of population size predicted by the SSAn and SSA+ algorithms for exponential growth overlapped the least when the environment fluctuated rapidly (Figure 3.3b,c), the scenarios which also had the largest differences in the CDFs

between SSAn and SSA+ (Figure 3.2b,c). Similarly, the predictions of SSAn and SSA+ logistic growth were fairly similar (i.e., distributions and expected values were similar) when there was an increasing environment function (Figure 3.3d), a function for which there were minimal differences between SSA and SSA+ inter-arrival times according to Figure 3.2d.

Differences between exactly accounting for (SSA+) or not fully accounting for (SSAn) environmental change can also be seen in Figure 3.4, which shows the expected values and their 95% confidence intervals over time of the SSAn and SSA+ methods for exponential growth. Furthermore, as expected from theory, the expected values from the SSA+ method closely match that of the deterministic version of the exponential growth model with a changing environment.

Differences in the expected values, $\bar{N}$, of the SSAn and SSA+ simulations were qualitatively consistent with the CDFs, in that their direction (higher or lower) could be predicted from Figure 3.2. For example, for exponential growth the SSA+ CDF curves for increasing and fluctuating environment functions were generally above those of the SSAn curves, suggesting births (the only possible demographic events) would happen more frequently in the SSA+ simulations. Consistent with this, the mean population size $\bar{N}$ of the SSA+ simulations for increasing and fluctuating conditions were higher at $t = 100$ than their SSAn equivalents. The CDFs for the random environments (Figure 3.2c,f) were a notable exception to this: The initial SSA+ CDF curves were below their equivalent SSAn curves at $t = 0$, but at $t = 100$, $\bar{N}$ for SSA+ was higher than that of SSAn. This can be attributed to the fact that the random environment function gradually declined at early time points (shown in Figure 3.2) but ultimately increased at later time points (not shown).

3.4 Discussion

Recent uses of SSAs in ecology explore cases where demography is constant through time (Kolpas and Nisbet, 2010; Kramer and Drake, 2010; Simonis, 2012; Yaari et al., 2012; Gokhale et al., 2013; Huang et al., 2015; Nisbet et al., 2016), even though by now it is well-

Figure 3.3: The frequency distribution of population sizes (N) at $t = 100$ for the exponential growth (a-c) and logistic growth (d-f) models, simulated using either the SSAn (red) or SSA+ (blue) method. Displayed are the population size distributions for environment functions: increasing 2 (a, d), fluctuating 2 (b, e), and random 2 (c, f). Colors are transparent, so purple indicates overlap between the SSAn and SSA+ methods. Also displayed are the expected values, $\bar{N}$, for each simulation method (same coloration as above). Note the different scales on both axes for each panel.

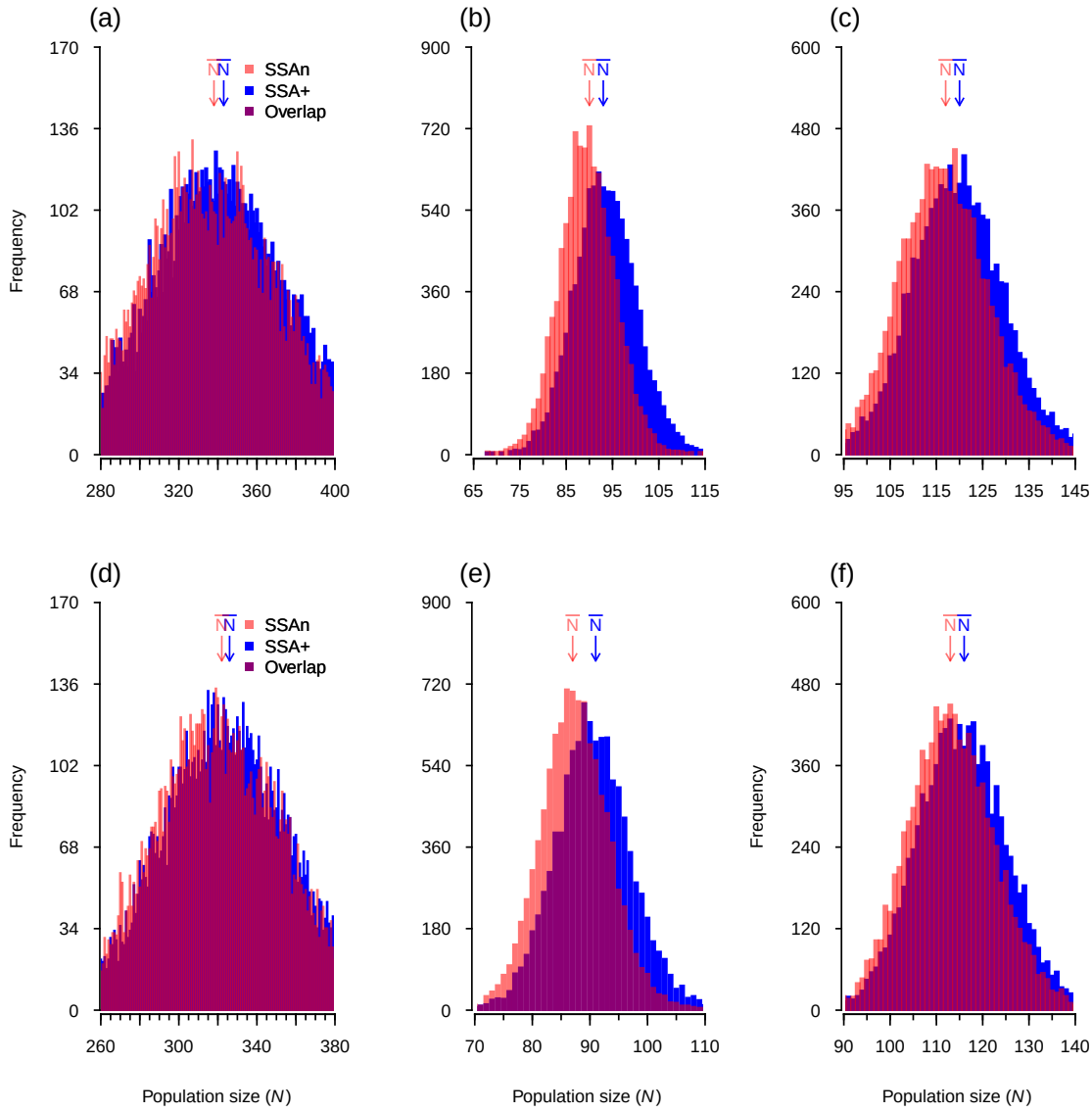

Figure 3.4: The 95% confidence intervals over time for the expected (mean) population size (N) of the SSAn (red) and SSA+ (blue) simulations of the exponential growth model. Displayed are the expected values (y-axis) for increasing 2 (a), fluctuating 2 (b), and random 2 (c) environment functions. Also displayed are the numerical solutions to the ordinary differential equation describing the deterministic versions of exponential growth with the same changing-environment functions. In general, confidence intervals were tiny and may be hard to distinguish.

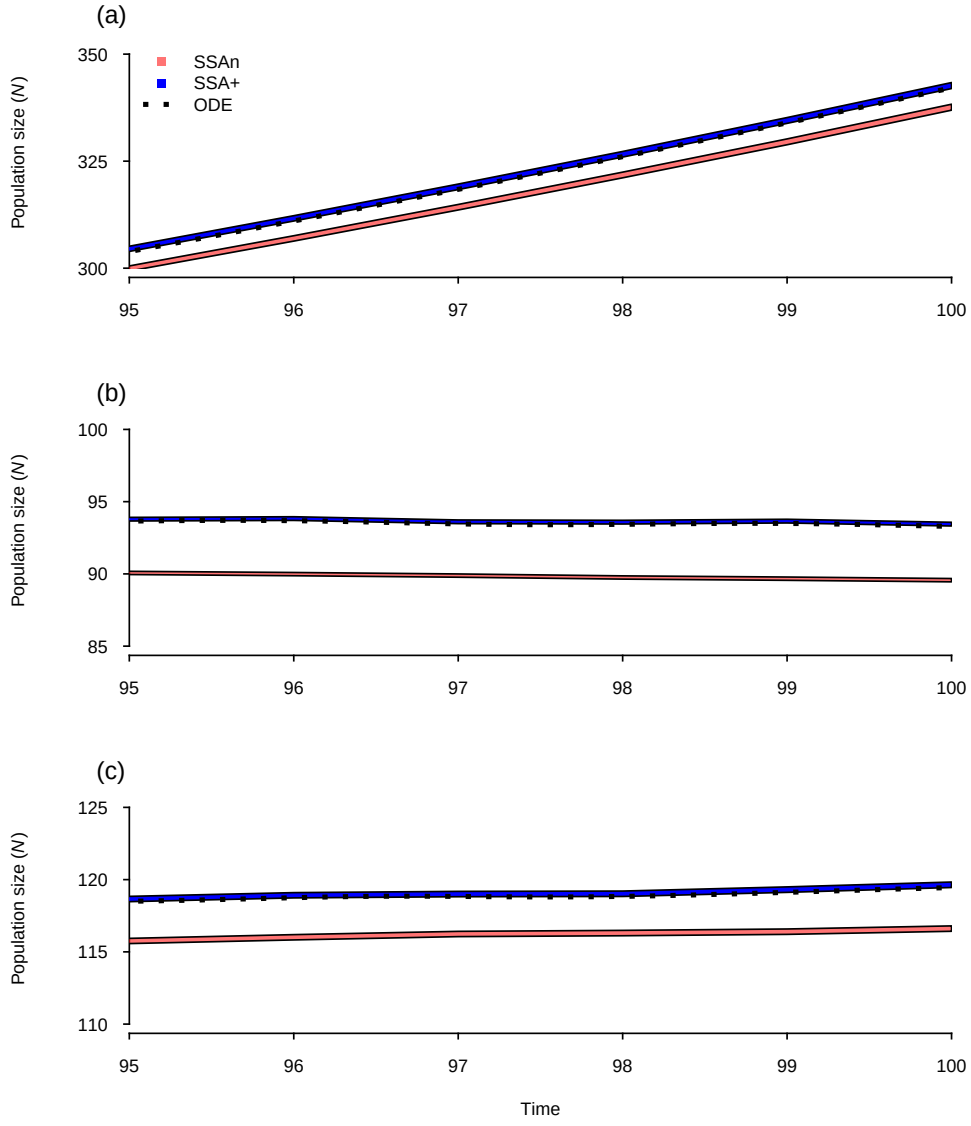

known that demographic traits can and do respond to changing environments. Here we described one method of extending the standard SSA algorithm to account for the added effects of non-stationary demography (i.e., demography that changes through time) and examined a variety of scenarios and ecological models in which accounting for non-stationary demography might be important. For exponential growth and logistic growth models, we found often large differences in the predicted distributions of population sizes between partly stationary (SSAn) versus non-stationary (SSA+) implementations of the algorithm in changing environments. Particularly when demography changed rapidly - as in the case of demography responding to significant environmental variability - SSAn and SSA+ simulations differed markedly in their expected values and distributions (Figures 3.3, 3.4). Moreover, these differences could generally be predicted *a priori* based on comparing the CDFs (Figure 3.2) of both methods.

We do not intend for this paper to be a criticism of stationary SSAs as there are many circumstances in which it is appropriate to treat demography as stationary. Rather, because of the computational cost of fully non-stationary SSAs, one of our goals is to highlight the circumstances in which partly stationary SSAs and fully non-stationary SSAs would differ substantially when the environment is changing (i.e., demography is non-stationary) in a system. Based on our findings, which compare a naive SSA that updates demographic rates only after each event (SSAn) to an SSA that fully accounts for continuously-changing demographic rates (SSA+), these circumstances are: (1) strong coupling between demographic traits and the environment (in our simulations, this coupling was always 1 to 1, with no lag); and (2) large environmental variability.

Research on thermal ecology and thermal performance over several decades suggests strong coupling between demography and environmental conditions, particularly for temperature in ectotherms (e.g., Davidson and Andrewartha, 1948; Huey and Stevenson, 1979; Huey and Kingsolver, 1989; Adolph and Porter, 1993; Deutsch et al., 2008; Angilletta, 2009; Dell et al., 2011; Estay et al., 2011; Meisner et al., 2014). It is therefore already well-known

that condition (1) is often satisfied in the natural world, particularly with respect to temperature. Regarding condition (2), environmental variability is also common in many systems and is likely to increase in the future. For example, inter-annual temperature variability has increased markedly in some regions in the past 50 years (Donat and Alexander, 2012; Huntingford et al., 2013; Hartmann et al., 2013) and will probably continue to increase in the future (Collins et al., 2013). Similarly rainfall, is also variable over time (e.g., Loik et al., 2004) and can strongly influence demography, particularly in arid or semi-arid areas (Knapp and Smith, 2001; Huxman et al., 2004). Thus, many natural systems satisfy the two conditions which favor the use of a non-stationary SSA over less expensive stationary ones.

Understanding the interaction of environmental stochasticity and non-stationary demography could be particularly important going forward. For our simulations, we created a single random trajectory for each of the two random environment functions (random 1 and 2) and compared 10,000 SSAn and SSA+ simulations with those specific trajectories. A fuller accounting of how stationary and non-stationary models differ in the face of environmental variability could extend our approach by running additional simulations for a variety of different realizations of "random" environments. Alternatively, each individual simulation could generate a different realization of a "random" environment. In either case, avoiding significant Monte Carlo error would likely require many times more simulations than used here.

As mentioned previously, various authors have suggested alternatives to the exact approach we used to sample inter-arrival times, most of which use a variation of thinning or rejection sampling (Boguñá et al., 2014; Vestergaard and Gnois, 2015; Ross, 2014; Duan and Liu, 2015). However, we were not concerned with finding the most computationally efficient method for simulating non-stationary SSAs. Indeed, our simulations would have been many times faster if they had been written in a lower-level language such as *C* rather than *R*. Rather, since both our exact approach (SSA+) and current rejection-based methods are quite costly computationally, we were more interested in knowing when it was worth considering

any non-stationary simulation approaches. In doing so for some simple ecological models and environment functions, we also found a fairly general, computationally inexpensive approach - involving the comparison of easily calculated stationary and non-stationary CDFs - for predicting when large differences between SSAn and SSA+ might arise. We suggest comparing such CDFs prior to deciding whether to implement any of the resource-intensive non-stationary methods.

Some caution is necessary when comparing CDFs, as we did, to understand when stationary or non-stationary approaches should be used. We examined initial CDFs (i.e., those beginning at $t = 0$) to gain some intuition about any overlap between the methods, and while that intuition was correct for most models and environments considered, it failed for the random environment. This was because the random environment of our simulations trended down at the beginning of the time interval but on average trended upwards over the full interval. It is straightforward to conceive of other cases, involving both variable environment functions or models with complicated phase spaces (i.e., dynamical trajectories), where examining only the CDFs based on initial conditions would provide incomplete information on possible differences between the methods; for instance: chaotic systems, systems that cycle (e.g., predator-prey models), and community-level models where individual species can go extinct. One way around this problem would be to compare CDFs across a range of time intervals and initial conditions.

We compared the predictions of stationary and non-stationary implementations of Gillespie's stochastic simulation algorithm (SSA) when demography was non-stationary, for two simple ecological models and six different environmental change scenarios. For our simulations, we allowed only a single model parameter (b_1) in the models to be affected by a changing environment. We nevertheless found an important effect of non-stationary demography for these simple, low-dimensional models. In real systems, multiple demographic traits have the potential to respond to the environment in different ways and such systems are also typically high-dimensional (i.e., contain many populations), non-linear, and have

complicated dynamics. Our study should therefore be considered a fairly conservative test of the importance of fully accounting for non-stationary demography in stochastic population models.

Chapter 4

Intrinsic dispersal ability and environment affect trait evolution during range expansion

Geoffrey B. Legault, Brett A. Melbourne

4.1 Introduction

Species geographic ranges are changing markedly as a result of climate change and human activities (Harsch et al., 2009; Chen et al., 2011; Bebber et al., 2013). Such shifts usually begin as ecological responses to changing conditions, including altered local abiotic conditions (e.g., temperature change), habitat destruction, or human-mediated dispersal. As a result, it is common to apply ecological approaches (e.g., models with static growth and dispersal rates) to predict range shifts and their consequences (Gaston, 2009). Recently, however, it has been suggested that evolution may play a significant role in short-term range dynamics (Excoffier et al., 2009; Kubisch et al., 2014). In particular, rapid evolutionary changes during range expansions have been predicted to alter the dispersal and growth rates of shifting populations (Burton et al., 2010; Shine et al., 2011), leading to eco-evolutionary dynamics not fully accounted for in purely ecological models (Kubisch et al., 2014).

Theoretical studies of the consequences of evolutionary changes during range shifts have focused on spatial selection, a process that involves a combination of assortative mating across space (i.e., spatial sorting, Shine et al. (2011)) and differences in selective pressures across the range (Holt, 2003; Dytham, 2009). Spatial selection has been predicted to lead

to differences in dispersal traits across expanding ranges, in particular increasing per-capita dispersal rates at range edges compared to range cores and thereby increasing spread rates (Burton et al., 2010; Shine et al., 2011; Perkins et al., 2013). In the past few years, laboratory experiments across four different taxa (Fronhofer and Altermatt, 2015; Williams et al., 2016; Ochocki and Miller, 2017; Weiss-Lehman et al., 2017) have shown that such effects are real and have the potential to contribute significantly to overall spread rates in expanding populations. However, these studies have focused largely on demonstrating that spatial selection is possible, rather than on exploring the environmental and ecological contexts in which short-term evolutionary changes are expected to have meaningful impacts on range dynamics. This focus on demonstration may over- or under-represent the importance of spatial selection for shifting natural systems. For instance, founding populations may lack the necessary standing genetic variation for evolutionary change (e.g., Dlugosch and Parker, 2008), dispersal traits may be more or less heritable for different species (Ronce, 2007), and differences in gene flow within or between species may affect rates of genetic differentiation (e.g., Henry et al., 2015).

Gene flow may be an especially important determinant of whether short-term evolutionary change during range expansion is possible. When gene flow between populations is high, local adaptation is thought to be hindered (Haldane, 1930; Wright, 1931), an idea that has been largely supported in both models of evolution (e.g., Garca-Ramos and Kirkpatrick, 1997) and in the field (e.g., Moore et al., 2007). Even low levels of gene flow are sufficient to reduce the effects of genetic drift, purge deleterious alleles, or interfere with local selection (Slatkin, 1987; Morjan and Rieseberg, 2004; Ellstrand, 2014; Tigano and Friesen, 2016). Therefore, if gene flow is capable of interferring with other evolutionary processes, it is likely that it can disrupt spatial selection as well. Theoretical and empirical investigations of evolution across space have not yet focused on the interaction between spatial selection and gene flow, but as a first approximation we would expect high levels of gene flow across a range to lead to more transient differences in the dispersal rates of individuals at range

edges.

The likelihood and impact of spatial selection may also depend on the environment experienced by shifting populations. Selection in stressful environments, for example, may select against high dispersing individuals, especially if there are trade-offs between growth in that environment and dispersal ability (Burton et al., 2010). If such selection occurs, it may override any spatial assortment that has occurred as a result of dispersal and limit the evolution of high dispersal ability at range edges. Though not focused on spatial selection per se, eco-evolutionary models have found significant effects of the environment on range dynamics (e.g., Garca-Ramos and Kirkpatrick, 1997; Kirkpatrick and Barton, 1997; Doebeli and Dieckmann, 2003; Atkins and Travis, 2010), suggesting that environmental context can influence evolutionary changes across a range. However, the role of environment on spatial selection has yet to be tested empirically.

In this study, we examine how spatial evolution is affected by both species-specific differences in dispersal rate (a proxy for gene flow) and the environment experienced by expanding populations. In particular, we compare the growth rate and dispersal traits of two closely-related species of flour beetles (*Tribolium castaneum* and *Tribolium confusum*) before and after five generations of experimental range expansion in two different environments. We find that both intrinsic dispersal rates and environment play an important role in determining whether spatial evolution causes differences in traits that impact range dynamics.

4.2 Methods

To examine the evolutionary consequences of range expansion, we used laboratory microcosms of flour beetles from the genus *Tribolium* (Coleoptera: Tenebrionidae). These beetles have a long history as model organisms in ecology (Costantino and Desharnais, 1991) and one of the species, *Tribolium castaneum*, has been used previously to study the ecology and evolution of range expansion (Melbourne and Hastings, 2009; Szücs et al., 2014; Hufbauer et al., 2015; Weiss-Lehman et al., 2017; Szücs et al., 2017). Our experiment (outlined in

Figure 4.1) consisted of two main parts: (1) Five generations of range expansion to establish CORE and EDGE populations; and (2) Expansion of CORE and EDGE populations into empty landscapes to assess how they differed in terms of growth and dispersal.

4.2.1 Details on model system and range expansion phase

We used two beetle species, *Tribolium castaneum* and *Tribolium confusum*, each of which can be easily reared to relatively high population sizes (>150) in individual acrylic boxes (dimensions: 4.0cm x 4.0cm x 6.0cm; herein patches) containing 15g mixtures of 95% wheat flour and 5% brewers yeast. Individual patches can be arranged into linear arrays (herein landscapes), with neighboring patches connected via 2.0 mm holes, which may be blocked to control dispersal. Beginning in one or a small number of patches within these landscapes, flour beetle populations will grow and expand into neighboring patches across multiple generations (see below for details on the beetle life-cycle). To our knowledge, *T. confusum* has not previously been studied in the context of range expansion, though it will also easily spread through experimental landscapes such as ours.

For each species (*T. castaneum* and *T. confusum*), we established 8 experimental landscapes (16 patches long) for each of two environment treatments (WET and DRY). Landscapes were founded by adding 50 adult beetles to the first patch (patch 1) and allowing them to mate and lay eggs for 24 hours before being removed. All founding beetles were taken from large, long-running stock cultures (5,000 - 10,000 individuals) kept under conditions equivalent to the WET environment treatment (see below). We also created 8 individual patches for each species and environment as controls, resulting in a total of 32 landscapes and 32 individual patches. All landscapes and individual patches were kept in temperature-controlled incubators (29.6 C) with different relative humidities for each of the environment treatments (WET = 65% relative humidity; DRY = 10-15% relative humidity).

We controlled the beetle life-cycle in the landscapes so that they dispersed and reproduced only once in their lifetime, and so that populations experienced non-overlapping

Figure 4.1: Experimental design. (1) Two species of beetles, *Tribolium castaneum* (**Sp1**) and *Tribolium confusum* (**Sp2**), each underwent five generations of range expansion in experimental landscapes (WET or DRY conditions) of connected patches (individual squares); (2) At the end of five generations, beetles were taken from CORE (i.e., patch 1) and EDGE patches (i.e., furthest patch) to found new experimental landscapes under common conditions (WET); (3) The F1 generation was allowed to grow and disperse for a single generation; (4) F1 beetles were fully censused; (5) Fifty beetles were randomly sampled (from across entire range) and used to found the F2 generation; and (6) F2 beetles grew, dispersed, and were censused.

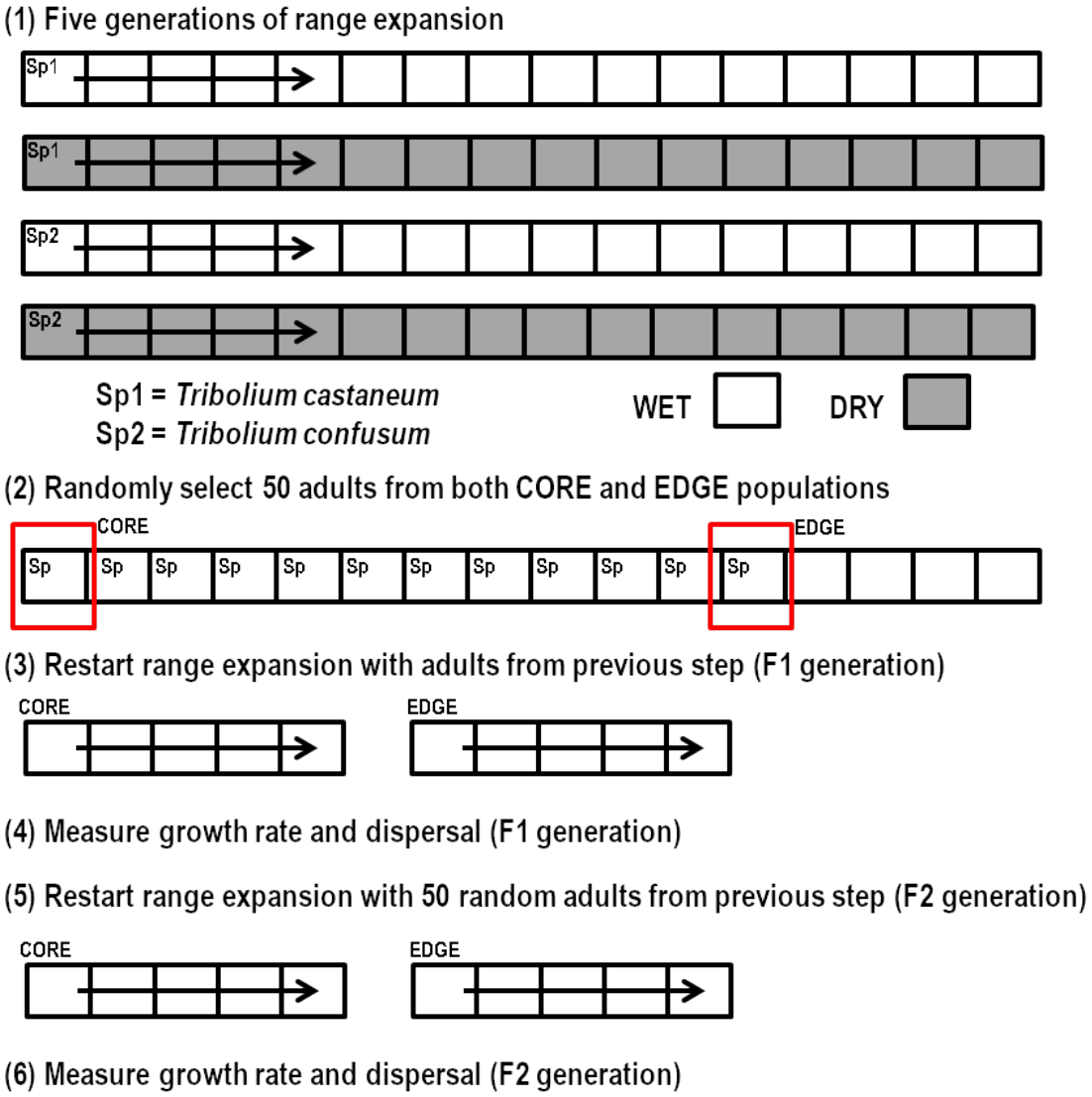

generations. This life-cycle mimics that of seasonal or semelparous organisms such as annual plants and many insect species. For each six-week generation, their life-cycle was as follows: (1) Development: beetle eggs in each patch were left undisturbed to develop into adults for 41 days; (2) Dispersal: Holes connecting neighboring patches were unblocked for a period of 24 hours, allowing adult beetles to move freely between patches in a landscape; (3) Reproduction: Flour media in every patch was replaced, and beetles were given 24 hours to copulate and lay eggs in the new media. Following the reproduction period, all adult beetles were removed from their patches (i.e., 100% mortality at the end of every generation), leaving only the eggs behind to begin the next generation. Full censuses of adult beetles after step (2) and prior to step (3) occurred every generation.

The range expansion phase (Figure 4.1, phase 1) of the experiment began in July 2016 and ended in March 2017, after each landscape and control had experienced five full generations of growth and dispersal. During this period, one control patch went extinct (*T. confusum* DRY) and four control patches (4 of *T. castaneum* DRY) were lost due to handling errors.

4.2.2 Expansion of CORE and EDGE populations

At the end of the fifth generation (Figure 4.1, phase 2), 50 adult beetles were taken randomly from either CORE (i.e., patch 1) or EDGE patches (i.e., the furthest patch in a replicate). If there were fewer than 50 beetles in the furthest patch (there were always at least 50 in the CORE), we sampled beetles randomly from the next furthest patch to the EDGE patch until we had obtained the required number of beetles. In such cases, we rarely had to take beetles from more than 1 patch behind the furthest population. We also took 50 random beetles from the single-patch controls to establish CONTROL populations that had never experienced range expansion, although one CONTROL replicate in the *T. confusum* DRY treatment had only 12 beetles. As in the initial set-up, beetles from CORE, EDGE and CONTROL patches were then added to the first patch of new landscapes (Figure 4.1,

phase 3) and allowed to mate and lay eggs for 24 hours. The eggs laid at this stage were considered the F1 generation.

All F1 beetles were raised from the egg stage to adulthood under identical conditions, equivalent to the WET environment treatment (29.6 C and 65% RH). As in the range expansion phase, F1 beetles were allowed to grow undisturbed for 41 days in an incubator, at which point they were given 24 hours to disperse across their (new) landscapes (Figure 4.1, end of phase 3). After dispersal, we recorded abundances in each patch (Figure 4.1, phase 4). For each of the now 91 experimental landscapes, we then mixed together all beetles (removing any spatial structure that had developed due to dispersal in phase 3), and again randomly selected 50 adults to found an F2 generation (Figure 4.1, phase 5). Only a single replicate had fewer than 50 beetles at this stage (41 beetles in a *T. confusum* DRY CONTROL landscape). The F2 beetles similarly started in empty landscapes and were allowed to grow for 41 days in an incubator, disperse for 24 hours, and, finally, were censused (Figure 4.1, phase 6). The purpose of the F1 generation was to control for maternal effects arising from CORE, EDGE, and CONTROL beetles experiencing different conditions, particularly relating to patch density. It was apparent from comparing F1 and F2 data that there were sometimes strong maternal effects on growth and dispersal ability (see Appendix C), suggesting this was a necessary step; however, here we focus exclusively on the growth and dispersal of the F2s.

The expansion of CORE and EDGE populations (Figure 4.1, phases 2-6) began in March 2017 and lasted until June 2017. During this period, 2 landscapes were lost due to handling errors (a *T. confusum* CORE and EDGE [WET]).

4.2.3 Comparing population growth and dispersal

We quantified the population growth rates and dispersal abilities of beetles from each F2 experimental landscape, allowing us to assess the impact of spatial evolution on these traits after five generations of range expansion and 2 generations in a common garden.

We compared the growth and dispersal of CORE, EDGE, and CONTROL populations. Furthermore, since the set-up of the F2 generation paralleled the initial set-up of the overall experiment (i.e., 50 adult beetles were allowed to lay eggs in patch 1 for Generation 0), we also quantified the growth and dispersal of beetles from Generation 1 of the range expansion phase (herein, INITIAL populations).

Growth rate was calculated as $r = \log(\frac{N_{t+1}}{N_t})$, where N_{t+1} was the number of beetles found in the entire landscape and where N_t was the number of beetles that had originally founded (i.e., laid eggs in) those landscapes. At our starting densities of 50 individuals, both density-independent and density-dependent contributions to overall population growth were likely strong (Melbourne and Hastings, 2008); however our measure of growth rate cannot distinguish between or adjust for these different effects. As a result, and because of a lack of power to fit mechanistic growth models such as the generalized Ricker model (Hufbauer et al., 2015), we compared growth rates between treatments using Wilcoxon Rank Sum tests. Since CORE and EDGE beetle populations either came from shared landscapes (during the range expansion) and were direct descendants of INITIAL populations, we used paired tests for comparisons between these groups. All other comparisons used unpaired tests.

We estimated the dispersal abilities of beetles in the different treatments by fitting a dispersal kernel to all replicates within a treatment. The dispersal kernel we used is a stochastic model of diffusion (Melbourne and Hastings, 2009) that assumes individual beetles move probabilistically from patch 1 to patch x. In the case of density-independent dispersal, the probability of a beetle moving from patch 1 to patch x can be obtained at any given time by solving the following deterministic system of equations:

$$\frac{dN_x}{dt} = D(N_{x-1} - HN_x + N_{x+1}) \tag{4.1}$$

Where N_i is the number of individuals in patch i, D is the diffusion coefficient (i.e., dispersal ability), and H is the number of holes in a patch. In our landscapes, the first and last patch in a landscape have 1 hole, and all other patches have 2 holes connecting them to other

patches. The kernel was fitted to the data by maximum likelihood; specifically, by solving equation 4.1 from $t = 0$ to $t = 1$, with $i = 1, 2, 3, 4, 5$ (i.e., patches 1-5, the dispersal range across all replicates) and initial conditions $N_1 = 1$ and $N_2 = N_3 = N_4 = N_5 = 0$, and setting those solutions as the probabilities p_1 through p_5 of a multinomial distribution (i.e., the probability of finding a beetle in patches 1-5). We then found the value of D that produced the multinomial dispersal model with the highest likelihood given our data. We estimated 95% confidence intervals for our estimates of D using non-parametric bootstrapping (percentile method; Davidson and Hinkley (1997)).

All analyses were conducted using R version 3.4.0 (R Core Team, 2017). We used the package deSolve (Soetaert et al., 2010) to produce numerical solutions to equation 4.1. Sample code for the dispersal kernel and likelihood function is provided in Appendix C.

4.3 Results

4.3.1 Range expansion phase

Over the course of five generations, *T. castaneum* and *T. confusum* populations spread across the experimental landscapes at speeds that varied between species and environments (Figure 4.2).

In both WET and DRY environments, *T. castaneum* spread rapidly, reaching up to patch 13 (WET) or patch 15 (DRY) after five generations (Figure 4.2). In the WET environment, average abundances in CORE patches (i.e, patch 1) were 66.7 after generation 1 (40.4 for DRY) and 171.1 after generation 5 (178.6 for DRY). Abundances in EDGE patches (i.e., the furthest patch containing a beetle within a replicate) were consistently low for both environments, with an average abundance of 6.4 at the end of generation 1 for the WET treatment (23.4 for DRY) and 26.6 after generation 5 (11.9 for DRY).

T. confusum populations spread roughly half as far as *T. castaneum* over the same period of range expansion, reaching only as far as patch 7 (WET) or patch 5 (DRY) (Figure

4.2). Abundances in WET, CORE patches rose from 54.5 at the end of generation 1 (54.8 in DRY) to 264.1 by generation 5 (198.8 in DRY). As with *T. castaneum*, abundances in EDGE patches were consistently low, with an average of 4.0 beetles in the furthest WET patches after generation 1 (1.0 for DRY) and 24.4 beetles after generation 5 (18.5 for DRY).

In CONTROL patches, where beetles were unable to disperse out of the starting patch, *T. castaneum* replicates had an average abundance at generation 5 of 144.1 and 188.5 in WET and DRY environments, respectively (Figure 4.3). *T. confusum* CONTROL replicates had an average abundance of 257.8 and 148.5 in WET and DRY environments. Notably, after generation 4, there was relatively high between-replicate variation in the abundances of *T. confusum* DRY patches (Figure 4.3d).

Figure 4.2: Mean abundances across the experimental landscapes during the five-generation range expansion phase. Shaded lines represent the mean abundance (y-axis) in a patch (x-axis) for *T. castaneum* (a, b) and *T. confusum* (c, d) replicates, with darker colors representing later generations. All landscapes began with 50 individuals in patch 1 (Generation 0; not shown).

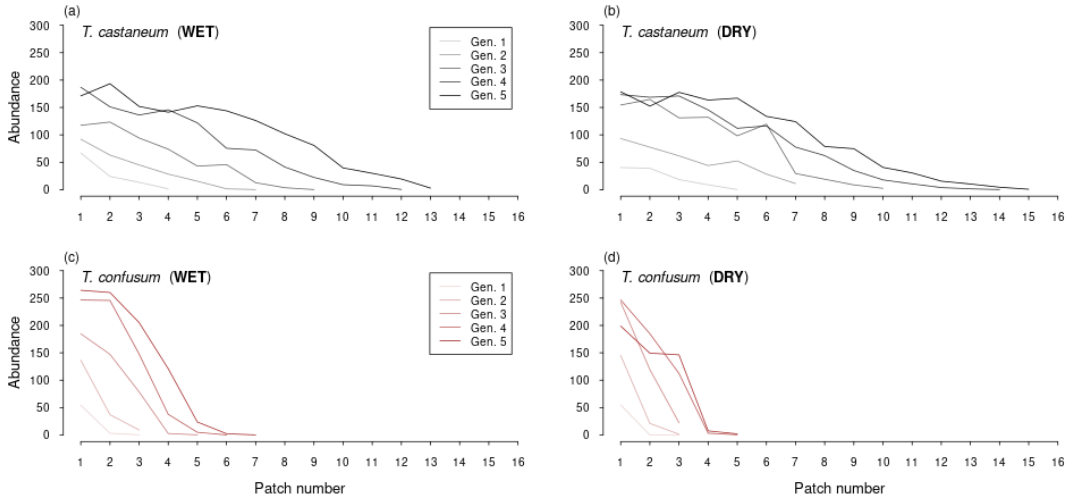

Figure 4.3: Abundances over time in control patches during the five-generation range expansion phase. Solid lines represent the total abundance of adult beetles (y-axis) at the end of each generation (x-axis) for *T. castaneum* (a, b) and *T. confusum* (c, d). Dotted lines (in b and d) represent the abundances over time of replicates lost due to handling errors and not considered in subsequent analyses.

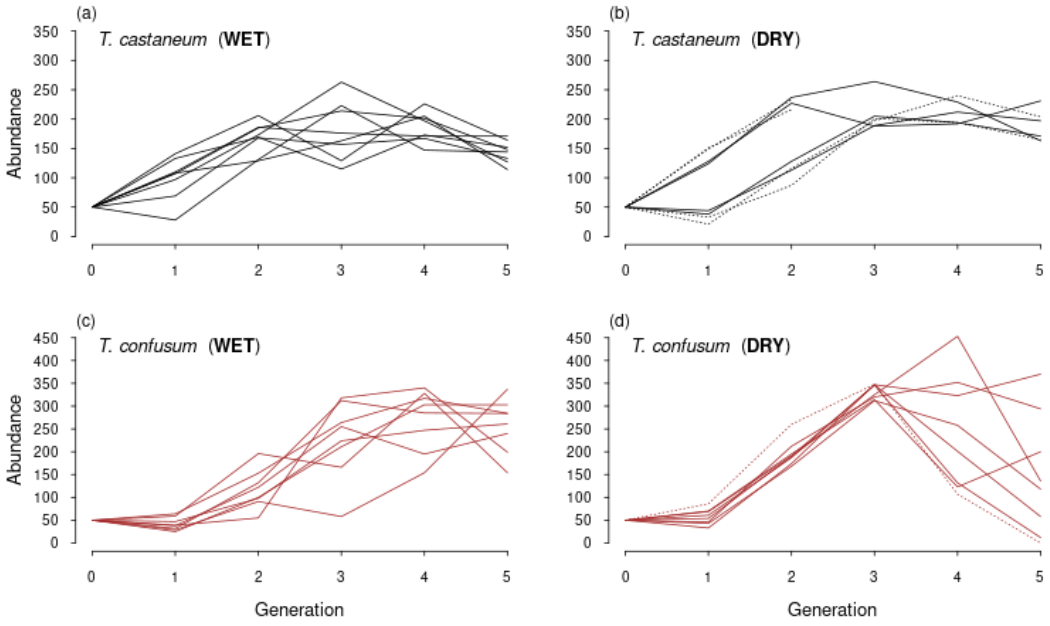

4.3.2 Population growth in CORE and EDGE populations

For *T. castaneum*, mean population growth rates were similar for CORE/EDGE/CONTROL populations and not significantly different (Figure 4.4). INITIAL population growth rates were lower than the other groups, but this difference was not statistically significant.

In contrast, *T. confusum* growth rates were significantly lower in EDGE populations that had expanded in the WET environment, compared to their CORE population pairs (Figure 4.4b; paired Wilcoxon Rank Sum test, $p = 0.03$) and the independent CONTROL populations (unpaired Wilcoxon Rank Sum test, $p = 0.03$). There were no significant differences between EDGE and CORE/CONTROL populations in the DRY environment, however. Finally, for all environmental treatments, INITIAL populations had consistently lower growth rates than all other population types.

4.3.3 Dispersal in CORE and EDGE populations

The 95% confidence intervals for our estimated diffusion coefficents overlapped for all *T. castaneum* populations (Figure 4.5a), suggesting that these populations did not differ significantly in terms of dispersal ability. However, INITIAL and CONTROL populations tended to have larger confidence intervals. For one treatment and environment (CONTROL, DRY), we had only 4 replicates for model-fitting, leading to very large intervals.

In contrast, the confidence intervals of the diffusion coefficients of *T. confusum* CORE and EDGE populations did not overlap for the WET environment (Figure 4.5), suggesting that these populations differed signifcantly in terms of dispersal ability. We found no differences between CORE and EDGE populations in the DRY conditions, however INITIAL populations had significantly lower dispersal ability than all other populations from that environment. Similar to *T. castaneum*, CONTROL populations had larger confidence intervals than other populations.

Figure 4.4: Growth rates of replicates for each type of population in the two environments. Thicker black points represent the mean growth rates (y-axis; log scale) of INITIAL (cross), CORE (square), EDGE (circle), and CONTROL (triangle) populations across the two environmental treatments (x-axis) for *T. castaneum* (a) and *T. confusum* (b). Lighter gray points are the growth rates of replicates within treatments. Bars are estimated 95% confidence intervals of the mean. Asterisks above pairs of points indicate statistically significant differences in the rank distributions of the two groups (Wilcoxon Rank Sum tests: * $p < 0.05$; ** $p < 0.01$; and *** $p < 0.001$).

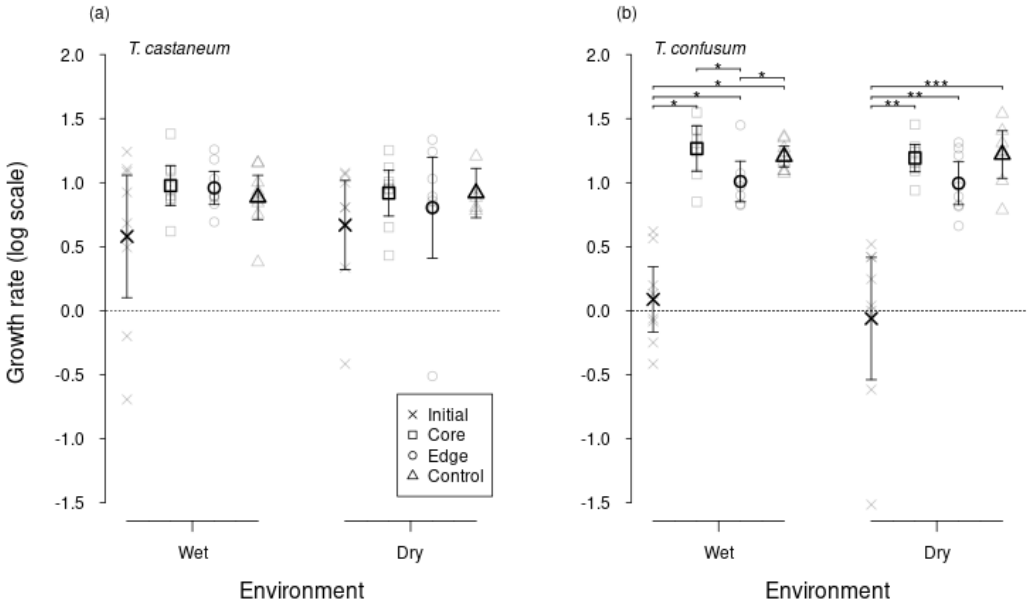

Figure 4.5: Estimated diffusion coefficients for each type of population in the two environments. Points represent the estimated diffusion coefficient (y-axis; higher values indicate better dispersal ability) of INITIAL (cross), CORE (square), EDGE (circle), and CONTROL (triangle) populations across the two environmental treatments (x-axis) for *T. castaneum* (a) and *T. confusum* (b). Bars are boostrapped 95% confidence intervals, meaning that non-overlapping bars (e.g., CORE and EDGE in b, Wet) indicate strongly significant differences in diffusion between groups. In one case, the confidence interval extends well beyond the range of the plot (arrow above last point in a).

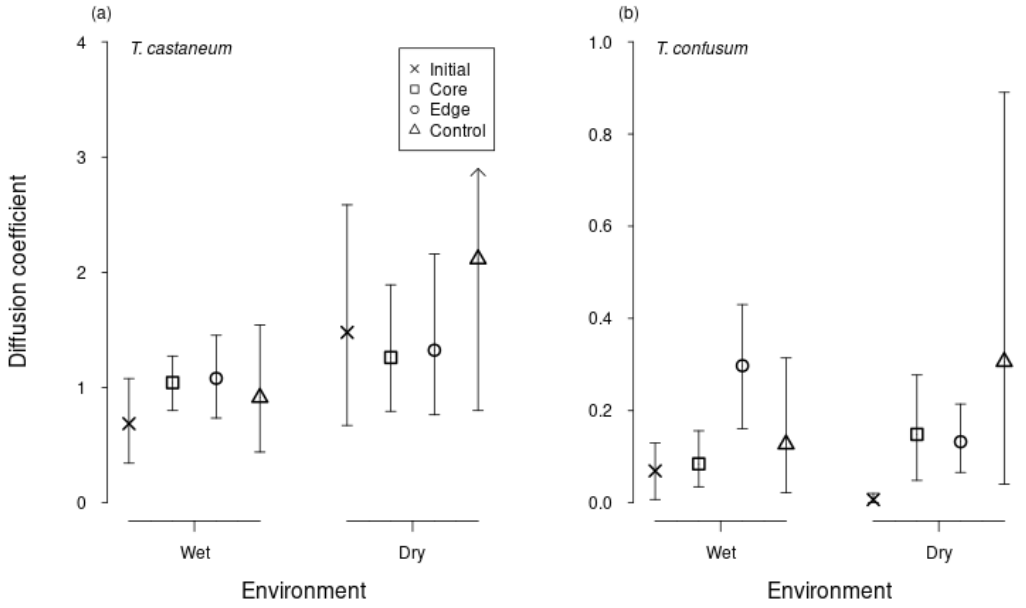

4.4 Discussion

A variety of factors may interfere with the efficacy of spatial evolution during range expansion, including gene flow and habitat quality. Following five generations of experimental expansion into one of two possible habitats, we found no evidence of rapid evolutionary changes to either the population growth rate or dispersal of intrinsically high-dispersing *T. castaneum* beetles across their range (i.e., between CORE and EDGE beetles) or when comparing expanded populations to unexpanded ones (i.e., INITIAL and CONTROL beetles). In contrast, for one of the two environment treatments, we found significant differences in the growth and dispersal traits of CORE and EDGE populations for the low-dispersing species, *T. confusum*, as well as differences between expanded and unexpanded populations. From this, we conclude that both intrinsic dispersal ability and environmental context can affect whether spatial evolution leads to differences in the demographic traits of expanding populations.

The notion that high levels of gene flow can slow or prevent local adaptation is well-known (Haldane, 1930; Wright, 1931). Consistent with this, we observed no evidence of spatial evolution in populations of our high-dispersing species *T. castaneum*. The estimated diffusion rates of INITIAL populations were between 0.75 and 1.5 (Figure 4.5), which translates into approximately 40-60% of beetles leaving their home patch (i.e., the patch in which they developed from eggs) every generation and possibly mating with beetles near or at the range edges. In contrast, *T. confusum* had initial diffusion rates of less than 0.1, translating into less than 5% of beetles leaving their home patch every generation. We are not aware of any studies directly examining the effects of dispersal rates on spatial evolution, but it is likely that high intrinsic dispersal would lead to high levels of gene flow between adjacent patches, thereby slowing or preventing any local adaptation that could have arisen from spatial sorting (Shine et al., 2011) or selection. For longer periods of range expansion where small differences could accumulate over time, or for highly non-linear dispersal kernels, we

would not necessarily expect such effects. However, our experiment lasted only a moderate number of generations and the observed dispersal kernels in our replicates were fairly linear (Appendix C).

T. confusum EDGE populations evolved higher dispersal rates in only one of the two environments. This may have been due to differences in selective pressures between the WET and DRY environments. We did not measure selection on demographic traits in these environments explicitly; however, from Figures 4.2 and 4.3, it is clear that by generation 4 *T. confusum* populations in the DRY environment were beginning to experience large declines in abundance and distance spread. Since conditions in the incubators did not change across generations and since we did not observe similar declines in the WET environment, we infer that such fitness declines were lagged responses to reduced water availability. The seemingly abrupt halt to range expansion in the DRY environment at generation 5 (Figure 4.2d) is also suggestive of the presence of strong selection in that environment (e.g., Garca-Ramos and Kirkpatrick, 1997; Kirkpatrick and Barton, 1997), though it is not clear for which traits. Nevertheless, it is likely that selection in the DRY environment did not favor high-dispersal traits in *T. confusum*, either because of trade-offs between dispersal and drought tolerance or because selection was acting predominantly on traits not related to dispersal. Alternatively, the apparent halt to range expansion in generation 5 of the DRY environment may have enabled sufficient dispersal (i.e., gene flow) from populations behind the EDGE populations to erode any evolutionary changes caused by spatial sorting.

We found no significant differences in the population growth rates of any *T. castaneum* populations but did observe large differences between pre- and post-expansion *T. confusum* populations. This may be partly explained by our metric of population growth (i.e., the number of viable offspring produced from 50 adults), that combines both density-independent and density-dependent mechanisms into a single term. In our system, density-dependent mechanisms are strong at our starting population sizes of 50, and so any increases in this metric of growth could be the result of evolutionary changes to density-dependent mecha-

nisms. We likely did not observe selection for higher growth in *T. castaneum* populations since the maximum densities within individual patches approximately 150 individuals rarely exceeded the artificially maintained densities of the long-running stock cultures used to seed the experiment. In contrast, *T. confusum* densities in the experimental landscapes/patches were often well above the baseline levels of their starting stock cultures (also around 150 individuals). Therefore, selection arising from higher than usual densities could explain why all post-expansion *T. confusum* populations evolved higher population growth. Consistent with this explanation is the fact that in the lower density EDGE populations, selection for higher growth rates was apparently weaker than in the equivalent CORE and CONTROL populations (Figure 4.4b). Alternatively, differences in growth rates could have been driven by selection acting on other life-history traits not measured in the experiment or due to trade-offs between dispersal ability and growth (Burton et al., 2010). The trade-off explanation is unlikely, however, given the lack of consistent directional responses and the minimal correlations between dispersal ability and growth (Appendix C)

A previous study of spatial evolution in *T. castaneum* similarly found no evidence of evolution for increased dispersal at moderate densities (Weiss-Lehman et al., 2017). However, the authors did find evidence of increased low-density dispersal as well as higher mean growth rates in core patches. Our experiment ran for 3 fewer generations, which could explain why we did not observe differences in growth rates across the range and would be in line with our assertion that genetic differentiation between CORE and EDGE populations requires more time for species with high intrinsic dispersal rates. The experiment had other important differences as well, including a 1-week longer development period to accomodate the slower development time of *T. confusum* and the use of effectively in situ trait assays where growth and dispersal were measured together (not as separate trials) and under nearly the same conditions beetles experienced in experimental landscapes (e.g., developing in a patch prior to dispersing, age at dispersal, and a single reproductive period).

Spatial evolution has been shown to have the potential to change demographic traits

across an expanding range, effects that could in turn affect the speed and nature of range expansion. In this study, we extended such work to consider how different intrinsic and extrinsic factors could affect the likelihood of spatial evolution contributing to range dynamics. In particular, we examined how spatial evolution affected trait differentiation between core and edge populations for two closely related species of flour beetles with significantly different dispersal abilities. We found no evolved differences in dispersal abilities across the range of the high-dispersing species, compared to significant differences in dispersal abilities of the low-dispersing species. Environment also played a role in determining whether spatial evolution produced meaningful changes in expanding populations. This work highlights the importance of considering the species- and evironment-specific contexts of shifting populations when deciding whether to account for the effects of spatial evolution in natural systems.

Chapter 5

Interspecific competition halts range expansions in an experimental system

Geoffrey B. Legault, Brett A. Melbourne

5.1 Introduction

A species range - where it is found in geographic space - depends on a combination of local and regional factors. At the local level, species may be affected by biotic (e.g., species interactions) and/or abiotic (e.g., temperature) constraints on population growth rates (Gause, 1934; Connell, 1961; Silvertown, 2004; Levine and HilleRisLambers, 2009). Regional factors, particularly dispersal from other areas, can also affect the presence of species and, in some cases (e.g., source-sink dynamics), lead to long-term persistence in geographic areas even when local growth rates are not positive (e.g., Huffaker, 1958; Crowder and Cooper, 1982; Tilman, 1994). While ecologists largely recognize the importance of such local and regional processes on species distributions (Chesson, 2000; Leibold et al., 2004), and in many cases have knowledge about which specific factors seem most important in particular areas (e.g., Hargreaves et al., 2014; Ettinger et al., 2011; Cunningham et al., 2016), it has nevertheless been difficult to use this information to predict how species ranges change over time (Kubisch et al., 2014).

Some of the difficulty of predicting how ranges change over time, or in response to environment change, is that we often lack the demographic data necessary to parameterize mechanistic population models. Moreover, we may not even know which models are most

appropriate for a given species or environmental context. Recent work on understanding and predicting range shifts has focused on parameterizing single-species population models with highly replicated experimental trials (e.g., Melbourne and Hastings, 2008, 2009; Fronhofer and Altermatt, 2015; Szücs et al., 2017, 2014). These approaches have had some success in using fitted population models to predict how individual species can expand into unoccupied habitat (but in some cases, evolution complicates matters, see Weiss-Lehman et al. (2017); Ochocki and Miller (2017), and Chapter 4), and suggest that such an approach can be fruitful for understanding some of the many climate- or human-induced range shifts that are occuring worldwide (e.g., Harsch et al., 2009; Chen et al., 2011; Bebber et al., 2013). However, we are aware of no studies that extend beyond the single-species perspective and explore how ranges can change in the presence of other species. Given that significant biotic interactions between species are found nearly anytime we look for them in nature (e.g., Sexton et al., 2009), this represents a serious gap in our ability to understand and forecast range shifts.

In this chapter, we describe an experiment that aims to address some of these limitations by providing replicated, high resolution data on how ranges change with and without species interactions. In particular, we examine how interspecific competition between two species of flour beetles (genus *Tribolium*) affects range expansion dynamics over multiple generations. Here, we focus on results from the first six generations of the experiment, which show strong effects of interspecific competition on the speed of range spread and, furthermore, suggest that species interactions may have long-term effects on range boundaries.

5.2 Methods

To examine the role of interspecific competition on range expansion, we used laboratory microcosms of flour beetles from the genus Tribolium (Coleoptera: Tenebrionidae). In particular we tested how competition between two species, *Tribolium castaneum* and *Tribolium confusum*, affected the spread of *T. castaneum* (focal species) across different experimental landscapes. As previously discussed, *T. castaneum* has been used before to study single-

species range expansion (Melbourne and Hastings, 2009; Szücs et al., 2014; Hufbauer et al., 2015; Weiss-Lehman et al., 2017). Further, in Chapter 4, I used *T. confusum* (in addition to *T. castaneum*) to examine the eco-evolutionary dynamics of single-species range expansion and found that it too will expand across artificial landscapes in a similar way as *T. castaneum*, albeit at a slower rate.

Not only will *T. castaneum* and *T. confusum* readily expand across experimental landscapes, they are also known to compete strongly with each other, both directly via chemical interference (e.g. Ghent, 1963), and indirectly for shared resources. Thomas Parks seminal work on competition between these species (Park, 1948, 1954, 1957) found that over the long-term (¿1800 days in continuous culture, 1 patch only), one species tended to exclude the other (¿70% of the time) and that the identity of the winner depended on the environment. Therefore, flour beetles have already been used as a model system for both range expansion and competition in ecology, and thus it is advantageous to use them to examine how the two processes interact.

The design of our experiment is partly inspired by Park (1954), and examines range expansion in monoculture and in competition with another species, under two environmental conditions similar to those in Parks original study, specifically WET (29.6 C, 65% relative humidity) and DRY (29.6 C, 10-15% relative humidity) environments, equivalent to Parks treatments III (*T. castaneum* usually wins) and IV (*T. confusum* usually wins). However, while we use similar environments, we do not necessarily expect similar outcomes in terms of competitive exclusion, as our system is in discrete-time and, unlike Parks, does not have overlapping generations or strong stage structure. Also, Park did not investigate range expansion, only competition within a single container.

5.2.1 Design of range expansion experiment

We used the same media, acrylic boxes, and linear landscape as described in Chapter 4. Further, we imposed the same 6-week discrete-time life-cycle of Growth (41 days), Dispersal

(24 hours), and Reproduction (24 hours, then removal of adults).

For each of two environments (WET and DRY), we established 20 replicate landscapes (16 patches long) where *T. castaneum* could disperse into unoccupied, monoculture landscapes (i.e., single-species treatments) or into landscapes with subsequent patches occupied by its competitor, *T. confusum* (i.e., two-species treatments). All replicates started by adding 50 *T. castaneum* (Generation 0) to the left-most patch (patch 1) and allowing them to mate and lay eggs for 24 hours prior to being removed. Additionally, for all two-species treatments, 50 adult *T. confusum* were added to each of patches 9 through 16 and similarly allowed to mate and lay eggs for 24 hours. We also established 20 replicates for each of 6 one-patch controls in which beetles could not disperse away from their starting patch. The design of our experiment is outlined in Figure 5.1.

The experiment began in December 2016 and here we include data from up to October 2017, representing 6 full generations of range expansion. During this period, a number of landscapes were lost due to handling errors or were intentionally removed (at random) due to logistical constraints. As a result, by Generation 6, we had 14-15 complete replicates for each treatment.

5.3 Results

In single-species one-patch controls, where beetles were unable to disperse out of their initial patch, *T. castaneum* populations had similar abundances in both environments, with averages of 224.6 (WET) and 220.1 (DRY) adult beetles by generation 6 (Figure 5.2a, b). Competition with *T. confusum* generally reduced long-term abundances, with Generation 6 averages of 138.6 (WET) and 132.6 (DRY) in the two-species patches (Figure 5.2c, d; approximately 60% of the abundances of single-species patches).

T. confusum abundances in the single-species one-patch controls were generally higher than *T. castaneum* after generation 1 (compare Figures 5.2 and 5.3). By Generation 6, average abundances of *T. confusum* were 285.6 and 313.3 in WET and DRY environments,

Figure 5.1: Experimental design. We established 20 replicates for each of four landscape treatments (each 16 patches long) and six one-patch treatments. There were two kinds of landscape treatments: (1) single-species landscapes, where every patch was in a WET or DRY environment and all patches beyond the first were unoccupied; and (2) two-species landscapes with the same environments as (1), but with patches 9-16 initially occupied by a competitor (Sp2, *T. confusum*). All replicates began with 50 adult *T. castaneum* (Sp1) beetles reproducing in the left-most patch (or the only patch in the case of controls) and, where approproriate, 50 adult *T. confusum* beetles (Sp2) reproducing in patches 9 through 16. We then followed the growth and dispersal of one or both species as they spread across the landscapes over six generations.

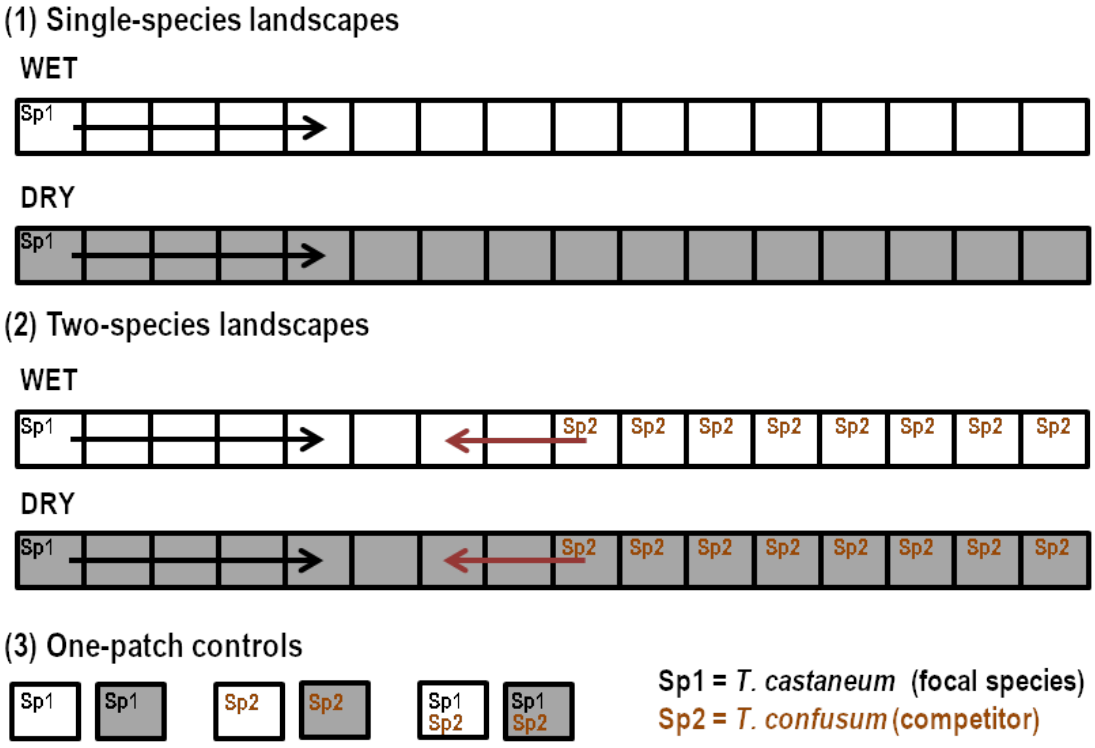

respectively (Figure 5.3a, b). Competition with another species similarly reduced long-term abundances, with Generation 6 averages of 124.0 (WET) and 135.6 (DRY) when competing with *T. castaneum* (Figure 5.3c, d; approximately 40% of the abundances of single-species patches).

There was generally higher variation between replicates in DRY environments for both species, regardless of whether they were alone or competing (Figure 5.2b, d, Figure 5.3,b, d).

T. castaneum populations in single-species and two-species landscapes had similar rates of spread and similar abundances across their ranges until around Generation 4, the first generation in which *T. castaneum* beetles at range edges developed alongside *T. confusum* adults (Figures 5.4, 5.5, 5.6).

By Generation 4, the presence of another species clearly affected the average spread of *T. castaneum* populations across the landscapes (Figures 5.4, 5.5). For instance, average abundances in patch 8 of single-species WET landscapes were 28.8 (Generation 4), 95.1 (Generation 5), and 144.8 (Generation 6) compared to 4.2 (Generation 4), 8.7 (Generation 5), and 17.0 (Generation 6) in two-species landscapes. Similarly, average abundances in patch 8 of single-species DRY landscapes were 27.0 compared to 11.4 in two-species landscapes (Generation 4), 57.3 compared to 24.7 (Generation 5) and 115.8 compared to 31 (Generation 6).

Finally, while small numbers of beetles continued to spread into two-species landscapes despite the presence of competing species, after Generation 4 populations greater than 10 individuals were generally not found beyond patches 7 or 8 (Figure 5.7).

5.4 Discussion

Interspecific competition is likely an important driver of species ranges in nature, however we currently lack the empirical data necessary to quantify its effects on range dynamics. Here we presented data from the first six generations of a laboratory microcosm experiment

Figure 5.2: Abundances over time of *T. castaneum* in control patches during the six generations of range expansion. Solid lines represent the total abundance of adult beetles (y-axis) at the end of each generation (x-axis) when in monoculture (a, b) or in competition (c, d) for each of two environments (left column = WET, right column = DRY).

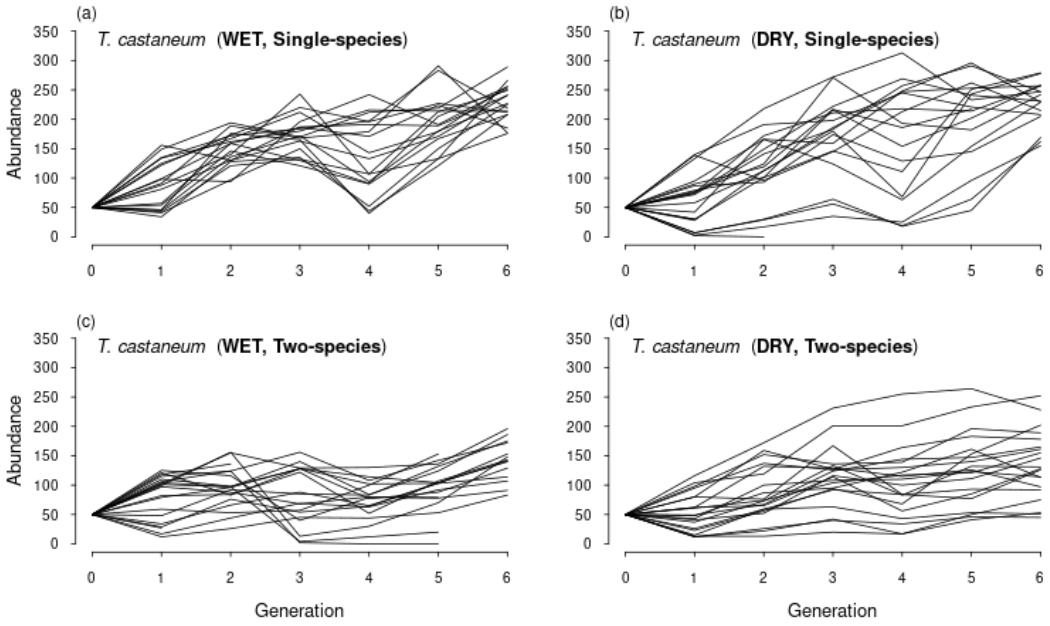

Figure 5.3: Abundances over time of *T. confusum* in control patches during the six generations of range expansion. Solid lines represent the total abundance of adult beetles (y-axis; scale is larger than in Figure 2) at the end of each generation (x-axis) when in monoculture (a, b) or in competition (c, d) for each of two environments (left column = WET, right column = DRY).

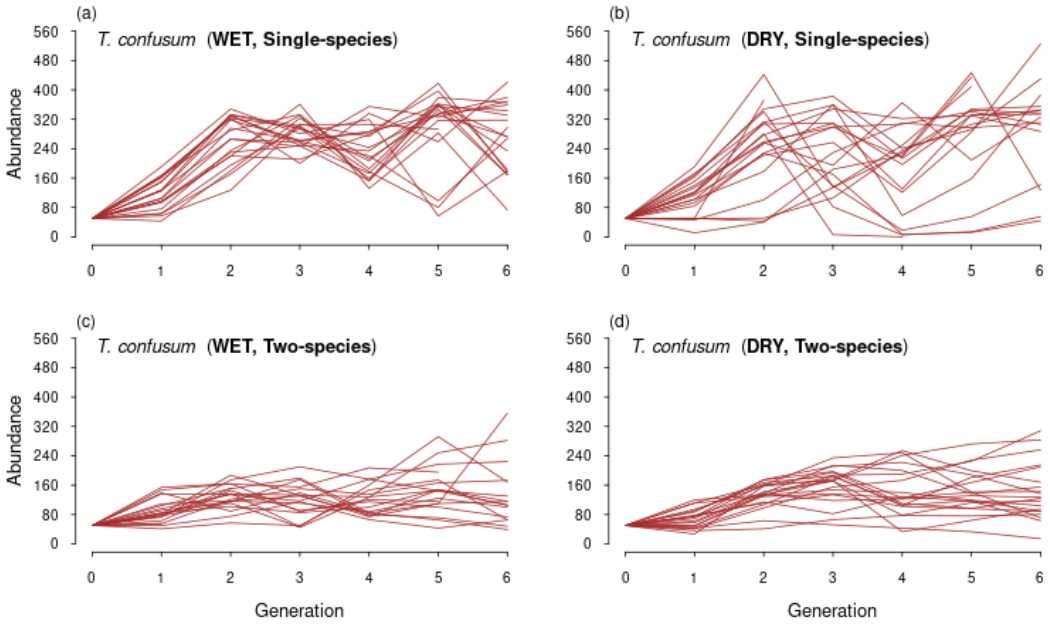

Figure 5.4: Abundances over time and across space of *T. castaneum* in WET single-species (a) or two-species (b) landscapes. Filled in polygons represent the standard error intervals of the mean abundances (y-axis) in each patch (x-axis). Different colored polygons represent different generations, from light (generation 1) to dark (generation 6). *T. confusum* abundances have been omitted from (b) for clarity (shown in Figure 5.6).

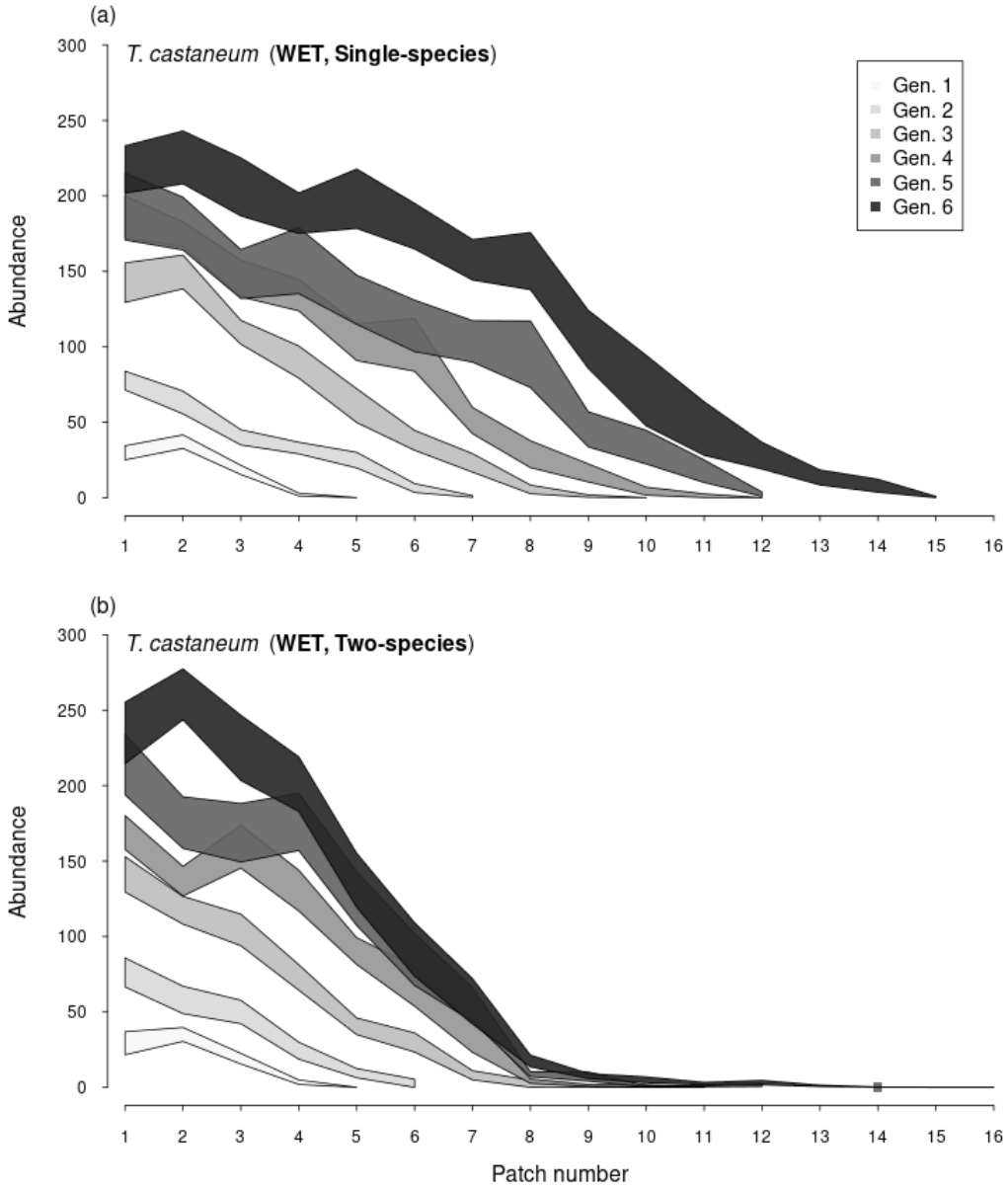

Figure 5.5: Abundances over time and across space of *T. castaneum* in DRY single-species (a) or two-species (b) landscapes. Filled in polygons represent the standard error intervals of the mean abundances (y-axis) in each patch (x-axis). Different colored polygons represent different generations, from light (generation 1) to dark (generation 6). *T. confusum* abundances have been omitted from (b) for clarity (shown in Figure 5.6).

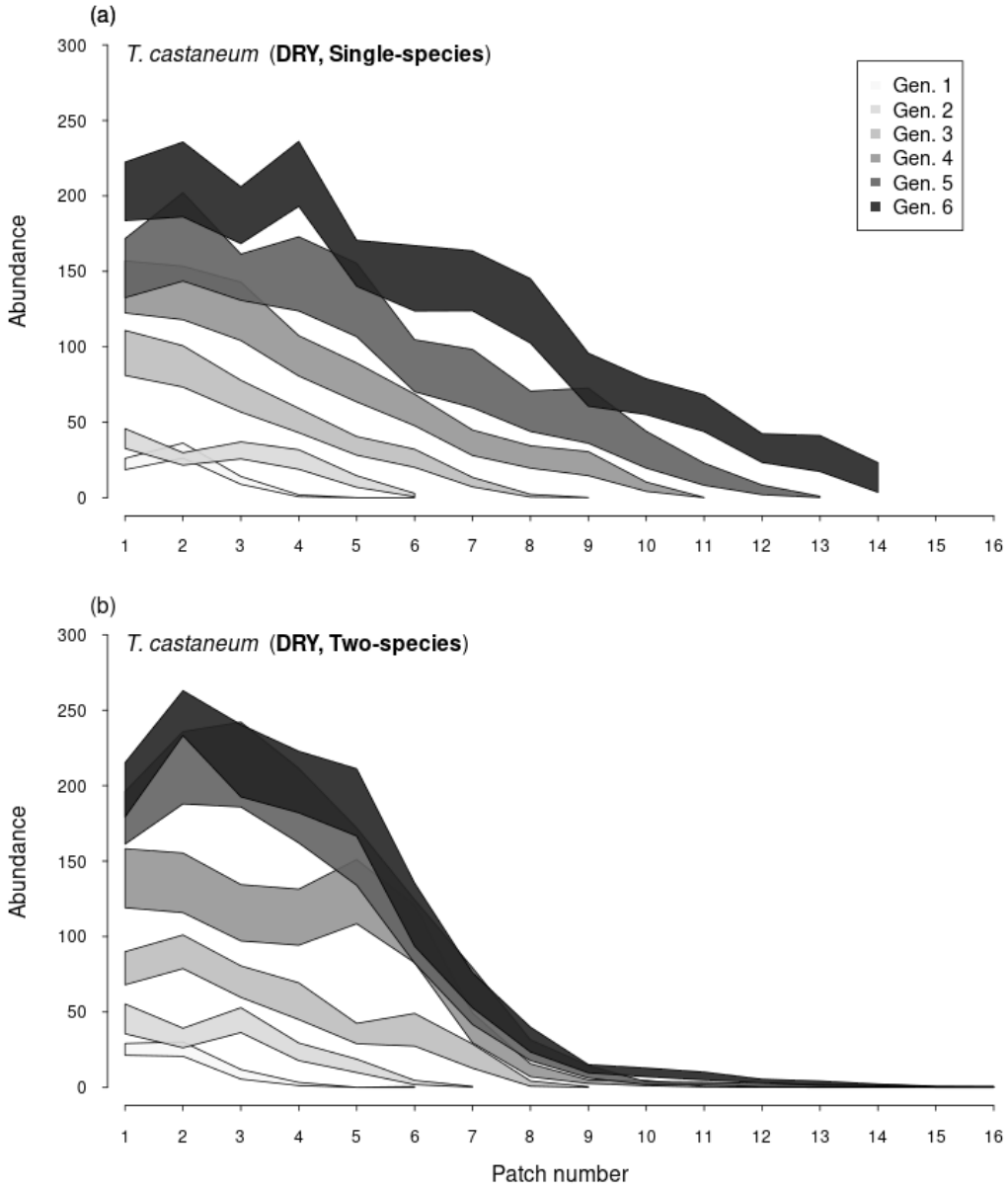

Figure 5.6: Abundances over time and across space of *T. confusum* in the two-species landscapes. Filled in polygons represent the standard error intervals of the mean abundances (y-axis) in each patch (x-axis) in the WET (a) or DRY (b) environments. Different colored polygons represent different generations, from light (generation 1) to dark (generation 6). Note that *T. castaneum* abundances (largely concentrated in the first 8 patches) have been omitted for clarity (shown in Figures 5.4 and 5.4).

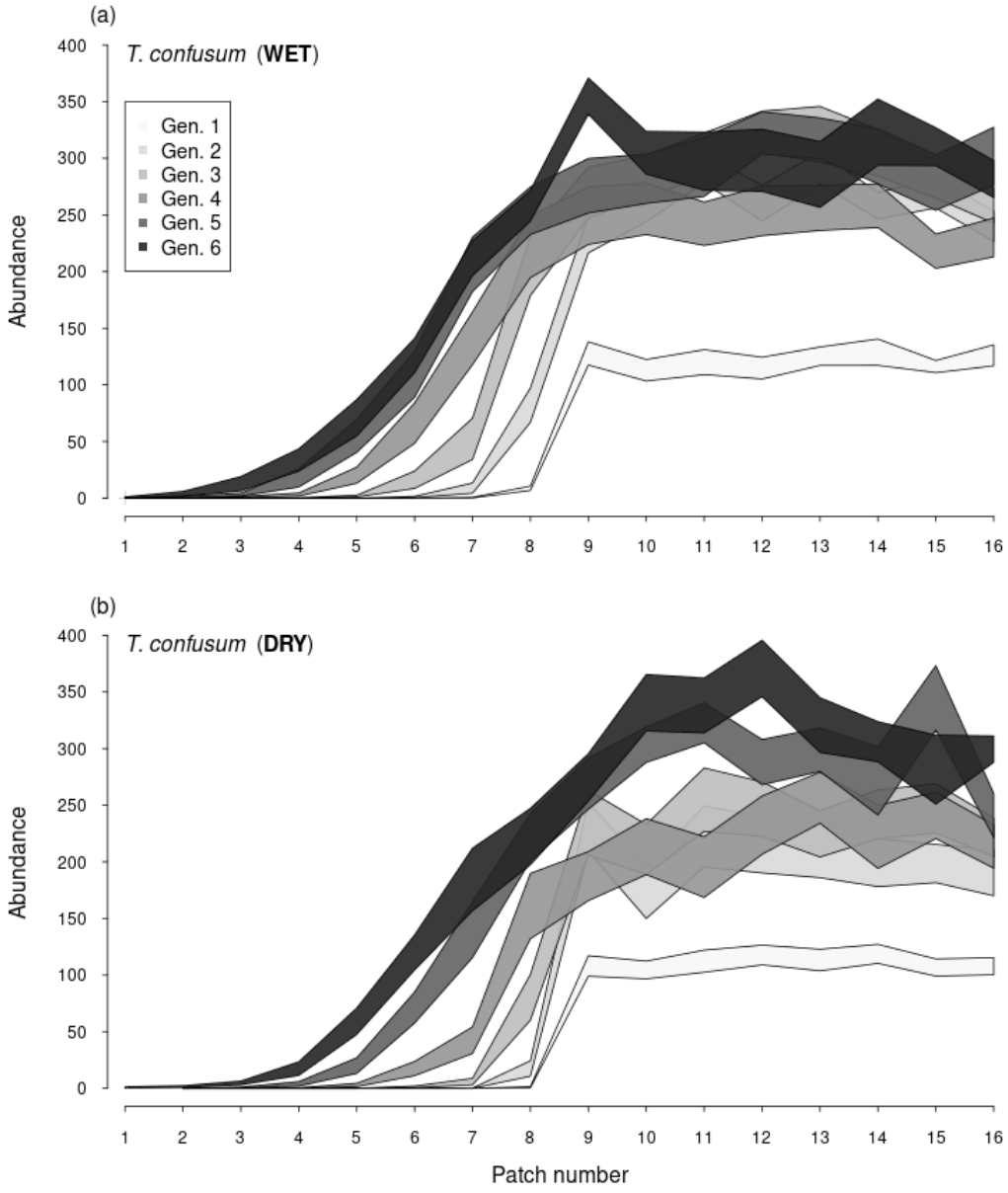

Figure 5.7: Maximum spatial extent of *T. castaneum* in experimental landscapes. Points represent the mean furthest patch (among replicates) occupied by at least 10 beetles within a landscape (y-axis) for each generation (x-axis) for WET (a) or DRY (b) environments. Black diamonds are the single-species landscapes and crosses are the two-species landscapes. Bars above and below the points are the 95% confidence intervals of the means.

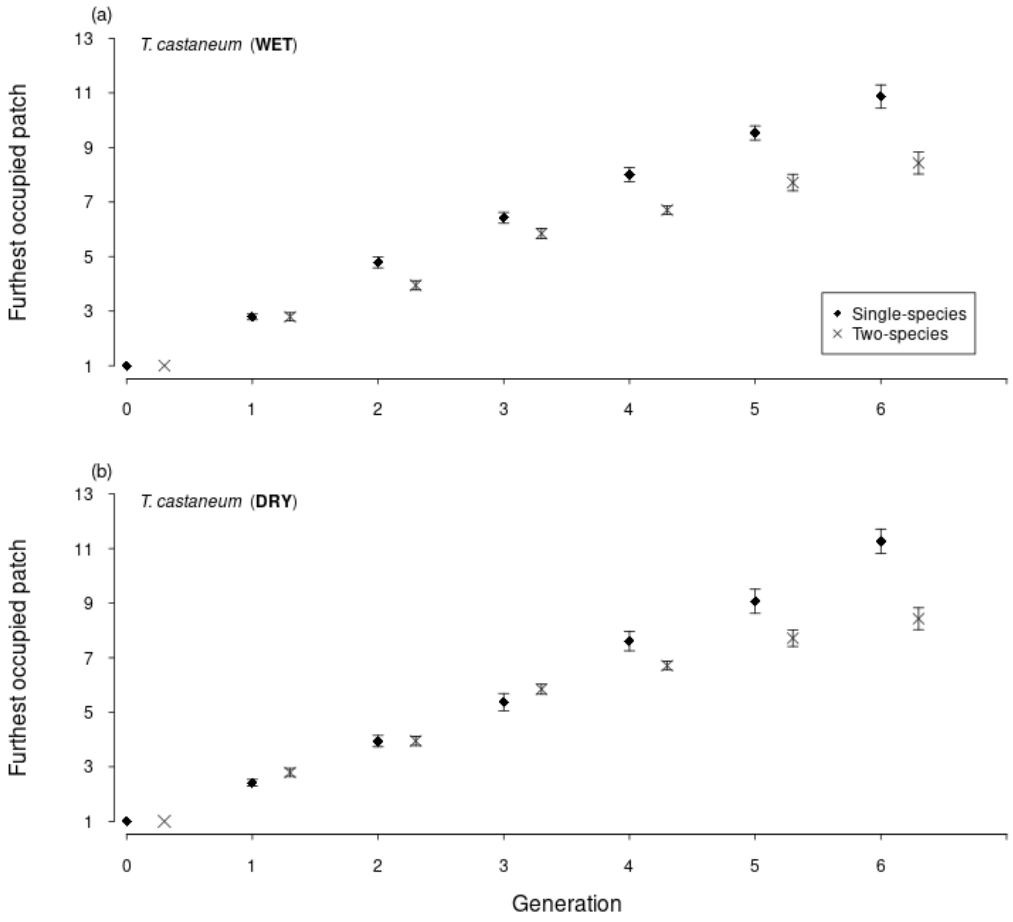

examining how competition affects range expansion. We found effects of competition on range dynamics across two different environments. Specifically, the presence of an interspecific competitor (*T. confusum*) in adjacent patches within a landscape strongly limited the continued spread of the focal species (*T. castaneum*) compared to the single-species cases. This effect lasted for 3 generations and seems likely to last in future generations of the experiment.

While competition is known to play a role in species abundances locally (e.g., Gause, 1934; Park, 1954) and regionally (e.g., Reitz and Trumble, 2002; Bertolino, 2008), to our knowledge this is the first study to demonstrate a clear effect of competition on range dynamics. In our experiment, *T. confusum* effectively stopped the expansion of *T. castaneum* into new patches for the three generations in which the two species met up in the two-species landscapes (Generation 4-6). However, whether or not this halt to range expansion will continue for subsequent generations is unknown, especially given the possibility of evolutionary change, which has already been shown to occur for *T. confusum* growth rates in Chapter 4 (after five generations of range expansion), and for dispersal and growth in other laboratory experiments over longer periods (Fronhofer and Altermatt, 2015; Williams et al., 2016; Weiss-Lehman et al., 2017; Ochocki and Miller, 2017). Due to the high replication in this study, it may be possible with more data (i.e., more generations) to disentangle ecological from evolutionary effects via model-fitting.

Future work involving this growing dataset will move towards fitting stochastic models to the full time series (Generations 1 to the end of the experiment), so as to fully quantify the influence of interspecific competition on demographic processes during range expansion. An appropriate two-species growth model of our flour beetle system has not yet been published, though Dallas et al (2017, unpublished) has fitted a two-species Ricker model (Cushing et al., 2004) to similar data on competition between *T. castaneum* and *T. confusum* in individual patches. However, two-species Ricker models are not able to account for direct chemical interference between species (e.g., Ghent, 1963), which may be occurring in our populations.

A separate study has been undertaken to better understand the possible effects of such chemicals (Bullock et al 2017, unpublished). The dispersal component of any expansion model will also likely need refinement. The most recently published dispersal model for the T. cataneum system (Melbourne and Hastings, 2009) assumes that dispersal is either density-independent or depends on the density of beetles in the current patch; however, if beetles are releasing chemicals into the flour or otherwise affecting habitat quality, this may not hold. For instance, the average abundance in patch 2 of the single-species DRY landscapes is higher than the average in patch 1 (Figure 5.5a, Generation 1), which is unlikely for models of dispersal/diffusion that depend only on density.

The data presented here supports the notion that interspecific competition can be an important driver of range expansion, at least over the short-term. We examined the effects of competition between two closely related species with nearly identical niches (in the lab) and that can exhibit fairly rapid competitive exclusion (in our case, we observed 2 cases of exclusion after six generations [in the DRY environment]), representing an extreme case. In cases where competition between species is less strong (perhaps because of small population sizes, as in Chapter 2), competition may not be able to halt range expansion, even temporarily. However, as range expansion in the context of multiple species is likely to be a highly non-linear phenomenon, the impact of reduced competition is difficult to predict without well-developed models or empirical data. As a result, we hope this study will be the first of many in this system and others that attempts to account for the potentially significant impact of species interactions during range expansions.

Chapter 6

Conclusions

My dissertation examined both basic and applied questions in ecology, each motivated by an interest in improving our understanding of complex, stochastic biological phenomena.

In Chapter 2, I examined how demographic stochasticity affected competitive outcomes and dynamics in simple two-species communities. In particular, I tested the theory that demographic stochasticity can alter competitive outcomes when fitness differences between competitors are small, but not when they are large. Using experimental two-species protist communities, I found that competitive outcomes in small communities (associated with strong stochasticity) were significantly different than outcomes in larger communities when fitness differences were small, but not when they were large. Furthermore, I found that absolute population size could alter **mean** competitive dynamics over time, a result not discussed by existing theory. To explore whether demographic stochasticity alone could explain these experimental findings, I also simulated continuous-time models of the protist system and found similar results for different community sizes. Moreover, model-fitting to the simulated data suggested that the effects of demographic stochasticity on outcomes and dynamics may be caused by changes to the effective demographic rates of populations.

Chapter 3 also dealt with a basic question about stochasticity in populations, specifically the issue of integrating non-stationary (i.e., environment-dependent) demography into continuous-time stochastic population models. I described an extension of Gillespie's stochastic simulation algorithm that allows for non-stationary demography and examined how its

predictions differed from a method that is partly naive to environmental change. I found significant differences in the predicted population sizes of the two implementations for two ecological models (exponential and logistic growth), particularly when demography responded to fluctuating and variable environments. Further, I outlined a computationally inexpensive approach for estimating when and under what circumstances it can be important to fully account for non-stationary demography for any class of model.

Chapters 4 and 5 centered on the applied issue of range expansions, a difficult phenomenon to predict precisely, in part because it is the ultimate outcome of many different stochastic demographic processes occurring across space and time (and other processes as well (e.g., American Acclimatization Society, 1877)). In order to create effective models of expansion that account for such stochasticity, ecologists first require better data on the myriad of processes involved during such expansions. In this case, better means both high temporal resolution (which is also necessary for fitting deterministic population models) and because individual demographic processes are either inherently or effectively samples from probability distributions highly replicated. Thus, as in Chapter 2, I employed laboratory microcosms to address this general topic.

In Chapter 4, I examined the role of evolutionary change (i.e., spatial selection) during the expansion of two species of flour beetles into artificial landscapes maintained in two different environments. I found that evolutionary change during range expansion may not occur or at least not affect some of the relevant demographic traits that drive expansion (population growth and dispersal), particularly if the intrinsic dispersal ability (a proxy for gene flow between populations) of the focal organism is high. Furthermore, I found that the environment experienced by expanding populations can also affect the occurrence of meaningful evolutionary change. This work highlights the importance of considering intrinsic dispersal ability and environmental context when attempting to predict range shifts.

Chapter 5 examined how range expansion occurred in the presence of a competing species, likely a common occurrence in nature but one for which we largely lack empiricial

data. In this study, a focal flour beetle species, *T. castaneum*, was allowed to expand left to right across artificial landscapes (the same kind used in Chapter 4) that were either unoccupied or contained a competing species, *T. confusum*. For two different environments, the effect of competition after six generations of range expansion was clear: interspecific competition severely limited the spread of the focal species. Thus, competition can be an important driver of range dynamics in the short-term and should be accounted for in predictive models of expansion.

In addition to these specific findings, each chapter highlights the importance of taking seriously the idea that demography is stochastic. Chapter 2 demonstrates that such stochasticity can change how we expect competition to proceed in communities. Chapter 3 highlights the importance of recognizing that demography can be simultaneously stochastic **and** environment-dependent. Chapters 4 and 5 take it as a given that demographic processes are stochastic by employing both the experimental control and replication necessary for dealing with multiple, independent stochastic processes acting on populations spreading across a range. Further, they provide baseline data on the importance of evolution and competition during range expansion, data that is essential for creating and parameterizing stochastic models of range expansion.

What does it mean to take demographic stochasticity seriously for natural populations? This is a difficult question to answer, but one that is important to ask given the work presented here. I used models and data from controlled laboratory experiments to understand the impacts of demographic stochasticity, approaches that greatly simplify (e.g., fewer species, static environments, low genetic variation) the immense complexity of natural systems. Nevertheless, there are commonalities between these experiments/simulations and real populations that I hope will motivate more applied ecologists to think about demographic stochasticity in their work. First, many natural populations are small at scales that are relevant to important ecological questions, and thus many natural may be strongly affected by demographic stochasticity. Second, even for those populations that are not small,

intra- and interspecific interactions between individuals will often happen at small spatial scales, and thus are likely to involve both a small number individuals and a small number of species. For instance, the highly speciose and abundant forests in Barro Colorado Island (Panama) have only an average of 0.3 individual plants above 1 cm per square meter (Condit et al., 2012). As a result, individual trees only compete with a few dozen individuals of a handful of species. The effects of stochasticity in such cases would be strong and relatively straightforward to predict using methods and experiments similar to those described above. Finally, recognizing that demographic processes are stochastic does not necessarily entail the use of highly-parameterized stochastic models to understand ecological phenomena. Rather, simply accepting that there is inherent or effective uncertainty in the outcomes of biological processes (whether they demographic processes or cellular processes or ecosystem processes) can change many aspects of how one might choose to answer ecological questions, including: experimental design (e.g., determining how many replicates are necessary for differentiating between probability distributions), analysis (e.g., using probability distributions of stochastic processes rather than normal distributions), and interpration (e.g., large variability in outcomes can be a real property of the system). The relevance of a stochastic conception of biology is therefore not relegated merely to artificial systems, and is worthy of careful consideration by ecologists of all varieties and concern.

Bibliography

Adiciptaningrum, A., M. Osella, M. C. Moolman, M. C. Lagomarsino, and S. J. Tans. 2015. Stohcasticity and homeostasis in the E. coli replication and division cycle. Scientific Reports **5**:18261.

Adler, P. B., J. HilleRisLambers, and J. M. Levine. 2007. A niche for neutrality. Ecology Letters **10**:95–104.

Adolph, S. C., and W. P. Porter. 1993. Temperature, Activity, and Lizard Life Histories. The American Naturalist **142**:273–295.

American Acclimatization Society. 1877. American Acclimatization Society. New York Times .

Andrewartha, H. G., and L. C. Birch. 1954. The distribution and abundance of animals. University of Chicago Press.

Angert, A. L., T. E. Huxman, G. A. Barron-Gafford, K. L. Gerst, and D. L. Venable. 2007. Linking growth strategies to long-term population dynamics in a guild of desert annuals. Journal of Ecology **95**:321–331.

Angilletta, M. 2009. Thermal Adaptation: A Theoretical and Empirical Synthesis. Oxford University Press.

Atkins, K. E., and J. M. J. Travis. 2010. Local adaptation and the evolution of species' ranges under climate change. Journal of Theoretical Biology **266**:449–457.

Avery, S. 2006. Microbial cell individuality and the underlying sources of heterogeneity. Nature Reviews Microbiology **4**:577–587.

Balčiūnas, D., and S. P. Lawler. 1995. Effects of Basal Resources, Predation, and Alternative Prey in Microcosm Food Chains. Ecology **76**:1327–1336.

Bar-Even, A., J. Paulsson, N. Maheshri, M. Carmi, E. O'Shea, Y. Pilpel, and N. Barkai. 2006. Noise in protein expression scales with natural protein abundance. Nature Genetics **38**:636–643.

Bartlett, M. 1960. Stochastic population models in ecology and epidemiology. Methuen and Company, Ltd.

Bartlett, M. S. 1957. Measles Periodicity and Community Size. Journal of the Royal Statistical Society. Series A (General) **120**:48–70.

Bebber, D., M. A. T. Ramotowski, and S. Gurr. 2013. Crop pests and pathogens move poleward in a warming world. Nature Climate Change **3**:985–988.

Beddington, J. R. 1975. Mutual Interference Between Parasites or Predators and its Effect on Searching Efficiency. Journal of Animal Ecology **44**:331–340.

Bell, G. 2000. The Distribution of Abundance in Neutral Communities. The American Naturalist **155**:606–617.

Belovsky, G. E., C. Mellison, C. Larson, and P. A. Van Zandt. 1999. Experimental Studies of Extinction Dynamics. Science **286**:1175–1177.

Bertolino, S. 2008. Introduction of the American grey squirrel (Sciurus carolinensis) in Europe: a case study in biological invasion. Current Science **95**:903–906.

Bjrnstad, O. N., M. Begon, N. C. Stenseth, W. Falck, S. M. Sait, and D. J. Thompson. 1998. Population dynamics of the Indian meal moth: demographic stochasticity and delayed regulatory mechanisms. Journal of Animal Ecology **67**:110–126.

Black, A. J., and A. J. McKane. 2012. Stochastic formulation of ecological models and their applications. Trends in Ecology & Evolution **27**:337–345.

Boguñá, M., L. F. Lafuerza, R. Toral, and M. A. Serrano. 2014. Simulating non-Markovian stochastic processes. Phys. Rev. E **90**:042108.

Bolnick, D. I., P. Amarasekare, M. S. Arajo, R. Brger, J. M. Levine, M. Novak, V. H. Rudolf, S. J. Schreiber, M. C. Urban, and D. A. Vasseur. 2011. Why intraspecific trait variation matters in community ecology. Trends in Ecology & Evolution **26**:183–192.

Buffon, G. L. L. 1774. Histoire naturelle, gnrale et particulire servant de suite la thorie de la terre, & d'introduction l'histoire des min raux. De l'Imprimerie royale a Paris.

Burkey, T. V. 1997. Metapopulation Extinction in Fragmented Landscapes: Using Bacteria and Protozoa Communities as Model Ecosystems. The American Naturalist **150**:568–591.

Burton, O. J., B. L. Phillips, and J. M. J. Travis. 2010. Trade-offs and the evolution of life-histories during range expansion. Ecology Letters **13**:1210–1220.

Cao, Y., H. Li, and L. Petzold. 2004. Efficient formulation of the stochastic simulation algorithm for chemically reacting systems. The Journal of Chemical Physics **121**:4059–4067.

Chase, J. 2007. Drought mediates the importance of stochastic community assembly. Proceedings of the National Academy of Sciences of the United States of America **104**:17430–17434.

Chase, J. M., and J. A. Myers. 2011. Disentangling the importance of ecological niches from stochastic processes across scales. Philosophical Transactions of the Royal Society of London B: Biological Sciences **366**:2351–2363.

Chen, I.-C., J. K. Hill, R. Ohlemüller, D. B. Roy, and C. D. Thomas. 2011. Rapid Range Shifts of Species Associated with High Levels of Climate Warming. Science **333**:1024–1026.

Chesson, P. 2000. Mechanisms of maintenance of species diversity. Annual Review of Ecology and Systematics **31**:343–366.

Chesson, P., M. J. Donahue, B. A. Melbourne, and A. L. Sears, 2005. Scale transition theory for understanding mechanisms in metacommunities. Chapter 12, pages 279–306 in M. A. Leibold and R. D. Holt, editors. Metacommunities: Spatial dynamics and ecological communities. University of Chicago Press.

Clark, J. S. 2009. Beyond neutral science. Trends in Ecology & Evolution **24**:8–15.

Clavero, M., and E. Garcia-Berthou. 2005. Invasive species are a leading cause of animal extinctions. Trends in Ecology & Evolution **20**:110.

Collins, M., R. Knutti, J. Arblaster, J.-L. Dufresne, T. Fichefet, P. Friedlingstein, X. Gao, W. Gutowski, T. Johns, G. Krinner, M. Shongwe, C. Tebaldi, A. Weaver, and M. Wehner, 2013. Long-term Climate Change: Projections, Commitments and Irreversibility. Chapter 12, pages 1029–1136 in T. Stocker, D. Qin, G.-K. Plattner, M. Tignor, S. Allen, J. Boschung, A. Nauels, Y. Xia, V. Bex, and P. Midgley, editors. Climate Change 2013: The Physical Science Basis. Contribution of Working Group I to the Fifth Assessment Report of the Intergovernmental Panel on Climate Change. Cambridge University Press.

Condit, R., S. Lao, R. Perez, S. B. Dolins, R. Foster, and S. Hubbell, 2012. Dataset: Barro Colorado Forest Census Plot Data (Version 2012). `https://doi.org/10.5479/data.bci.20130603`.

Connell, J. H. 1961. The Influence of Interspecific Competition and Other Factors on the Distribution of the Barnacle Chthamalus Stellatus. Ecology **42**:710–723.

Costantino, R. F., and R. A. Desharnais. 1991. Population dynamics and the Tribolium model : genetics and demography. Springer-Verlag New York.

Crowder, L. B., and W. E. Cooper. 1982. Habitat Structural Complexity and the Interaction Between Bluegills and Their Prey. Ecology **63**:1802–1813.

Cunningham, H. R., L. J. Rissler, L. B. Buckley, and M. C. Urban. 2016. Abiotic and biotic constraints across reptile and amphibian ranges. Ecography **39**:1–8.

Cushing, J., S. Levarge, N. Chitnis, and S. M. Henson. 2004. Some Discrete Competition Models and the Competitive Exclusion Principle. Journal of Difference Equations and Applications **10**:1139–1151.

David, T. 2004. Niche tradeoffs, neutrality, and community structure:A stochastic theory of resource competition, invasion, and community assembly. Proceedings of the National Academy of Sciences of the United States of America **101**:10854–10861.

Davidson, A. C., and D. V. Hinkley. 1997. Bootstrap methods and their application. Cambridge University Press.

Davidson, J., and H. G. Andrewartha. 1948. The Influence of Rainfall, Evaporation and Atmospheric Temperature on Fluctuations in the Size of a Natural Population of Thrips imaginis (Thysanoptera). Journal of Animal Ecology **17**:200–222.

DeAngelis, D. L., R. A. Goldstein, and R. V. O'Neill. 1975. A Model for Tropic Interaction. Ecology **56**:881–892.

Dell, A. I., S. Pawar, and V. M. Savage. 2011. Systematic variation in the temperature dependence of physiological and ecological traits. Proceedings of the National Academy of Sciences **108**:10591–10596.

DeLong, J. P., and D. A. Vasseur. 2012. Size-density scaling in protists and the links between consumerresource interaction parameters. Journal of Animal Ecology **81**:1193–1201.

Desharnais, R. A., R. F. Costantino, J. M. Cushing, S. M. Henson, B. Dennis, and A. A. King. 2006. Experimental support of the scaling rule for demographic stochasticity. Ecology Letters **9**:537–547.

Deutsch, C. A., J. J. Tewksbury, R. B. Huey, K. S. Sheldon, C. K. Ghalambor, D. C. Haak, and P. R. Martin. 2008. Impacts of climate warming on terrestrial ectotherms across latitude. Proceedings of the National Academy of Sciences **105**:6668–6672.

Dickerson, J. E., and J. V. Robinson. 1985. Microcosms as Islands: A Test of the Macarthur-Wilson Equilibrium Theory. Ecology **66**:966–980.

Diehl, S., and M. Feiel. 2000. Effects of Enrichment on ThreeLevel Food Chains with Omnivory. The American Naturalist **155**:200–218.

Dlugosch, K. M., and I. M. Parker. 2008. Founding events in species invasions: genetic variation, adaptive evolution, and the role of multiple introductions. Molecular Ecology **17**:431–449.

Dobzhansky, T., and O. Pavlovsky. 1957. An Experimental Study of Interaction between Genetic Drift and Natural Selection. Evolution **11**:311–319.

Doebeli, M., and U. Dieckmann. 2003. Speciation along environmental gradients. Nature **421**:259–264.

Doering, C. R., K. V. Sargsyan, and L. M. Sander. 2005. Extinction Times for Birth-Death Processes: Exact Results, Continuum Asymptotics, and the Failure of the Fokker–Planck Approximation. Multiscale Modeling & Simulation **3**:283–299.

Donat, M. G., and L. V. Alexander. 2012. The shifting probability distribution of global daytime and night-time temperatures. Geophysical Research Letters **39**.

Duan, Q., and J. Liu. 2015. A first step to implement Gillespie's algorithm with rejection sampling. Statistical Methods & Applications **24**:85–95.

Dytham, C. 2009. Evolved dispersal strategies at range margins. Proceedings of the Royal Society of London B: Biological Sciences **276**:1407–1413.

Ellstrand, N. C. 2014. Is gene flow the most important evolutionary force in plants? American Journal of Botany **101**:737–753.

Engen, S., R. Lande, B.-E. Sther, and H. Weimerskirch. 2005. Extinction in relation to demographic and environmental stochasticity in age-structured models. Mathematical Biosciences **195**:210–227.

Estay, S. A., S. Clavijo-Baquet, M. Lima, and F. Bozinovic. 2011. Beyond average: an experimental test of temperature variability on the population dynamics of Tribolium confusum. Population Ecology **53**:53–58.

Estay, S. A., M. Lima, and F. Bozinovic. 2014. The role of temperature variability on insect performance and population dynamics in a warming world. Oikos **123**:131–140.

Ettinger, A. K., K. R. Ford, and J. HilleRisLambers. 2011. Climate determines upper, but not lower, altitudinal range limits of Pacific Northwest conifers. Ecology **92**:1323–1331.

Excoffier, L., M. Foll, and R. J. Petit. 2009. Genetic Consequences of Range Expansions. Annual Review of Ecology, Evolution, and Systematics **40**:481–501.

Fay, P. A., J. D. Carlisle, A. K. Knapp, J. M. Blair, and S. L. Collins. 2003. Productivity responses to altered rainfall patterns in a C4-dominated grassland. Oecologia **137**:245–251.

Feller, W. 1939. Die Grundlagen der Volterraschen Theorie Des Kampfes Ums Dasein in Wahrscheinlichkeitstheoretischer Behandlung. Acta Biotheoretica **5**:11–40.

Fisher, C., and P. Mehta. 2014. The transition between the niche and neutral regimes in ecology. Proceedings of the National Academy of Sciences of the United States of America **111**:13111–13116.

Fox, J. W. 2002. Testing a Simple Rule for Dominance in Resource Competition. The American Naturalist **159**:305–319.

Fox, J. W., and D. C. Smith. 1997. Variable Outcomes of Protist-Rotifer Competition in Laboratory Microcosms. Oikos **79**:489–495.

Fronhofer, E. A., and F. Altermatt. 2015. Eco-evolutionary feedbacks during experimental range expansions. Nature Communications **6**:6844.

Fukami, T. 2004. Assembly history interacts with ecosystem size to influence species diversity. Ecology **85**:3234–3242.

Garca-Ramos, G., and M. Kirkpatrick. 1997. Genetic models of adaptation and gene flow in peripheral populations. Evolution **51**:21–28.

Gaston, K. J. 2009. Geographic range limits: achieving synthesis. Proceedings of the Royal Society of London B: Biological Sciences **276**:1395–1406.

Gause, G. 1934. The struggle for existence. Williams and Wilkins Company.

Gause, G. 1935. Vrifications exprimentales de la thorie mathmatiques de la lute pour la vie. Actualites Scientifiques et Industrielles **277**.

Ghent, A. W. 1963. Studies of Behavior of the Tribolium Flour Beetles. I. Contrasting Responses of T. castaneum and T. confusum to Fresh and Conditioned Flours. Ecology **44**:269–283.

Gilbert, B., and J. M. Levine. 2017. Ecological drift and the distribution of species diversity. Proceedings of the Royal Society of London B: Biological Sciences **284**.

Gill, D. E. 1972. Intrinsic Rates of Increase, Saturation Densities, and Competitive Ability. I. An Experiment with Paramecium. The American Naturalist **106**:461–471.

Gillespie, D. T. 1977. Exact stochastic simulation of coupled chemical reactions. The Journal of Physical Chemistry **81**:2340–2361.

Gillespie, D. T. 2001. Approximate accelerated stochastic simulation of chemically reacting systems. The Journal of Chemical Physics **115**:1716–1733.

Gokhale, C. S., A. Papkou, A. Traulsen, and H. Schulenburg. 2013. Lotka–Volterra dynamics kills the Red Queen: population size fluctuations and associated stochasticity dramatically change host-parasite coevolution. BMC Evolutionary Biology **13**:254.

Gravel, D., F. Guichard, and M. E. Hochberg. 2011. Species coexistence in a variable world. Ecology Letters **14**:828–839.

Griffen, B. D., and J. M. Drake. 2008. A Review of Extinction in Experimental Populations. Journal of Animal Ecology **77**:1274–1287.

Habte, M., and M. Alexander. 1978. Protozoan Density and the Coexistence of Protozoan Predators and Bacterial Prey. Ecology **59**:140–146.

Haldane, J. B. S. 1930. Theoretical genetics of autopolyploids. Journal of Genetics **22**:359–372.

Hansen, S. R., and S. P. Hubbell. 1980. Single-nutrient microbial competition: qualitative agreement between experimental and theoretically forecast outcomes. Science **207**:1491–1493.

Hargreaves, A. L., K. E. Samis, and C. G. Eckert. 2014. Are Species Range Limits Simply Niche Limits Writ Large? A Review of Transplant Experiments beyond the Range. The American Naturalist **183**:157–173.

Harsch, M. A., P. E. Hulme, M. S. McGlone, and R. P. Duncan. 2009. Are treelines advancing? A global meta-analysis of treeline response to climate warming. Ecology Letters **12**:1040–1049.

Hart, S. P., S. J. Schreiber, and J. M. Levine. 2016. How variation between individuals affects species coexistence. Ecology Letters **19**:825–838.

Hartmann, D., A. KleinTank, M. Rusticucci, L. Alexander, S. Bronnimann, Y. Charabi, F. Dentener, E. Dlugokencky, D. Easterling, A. Kaplan, B. Soden, P. Thorne, M. Wild, and P. Zhai, 2013. Observations: Atmosphere and Surface. Book section 2, pages 159–254 in T. Stocker, D. Qin, G.-K. Plattner, M. Tignor, S. Allen, J. Boschung, A. Nauels, Y. Xia, V. Bex, and P. Midgley, editors. Climate Change 2013: The Physical Science Basis. Contribution of Working Group I to the Fifth Assessment Report of the Intergovernmental Panel on Climate Change. Cambridge University Press, Cambridge, United Kingdom and New York, NY, USA.

Heisler-White, J. L., A. K. Knapp, and E. F. Kelly. 2008. Increasing precipitation event size increases aboveground net primary productivity in a semi-arid grassland. Oecologia **158**:129–140.

Henry, R. C., A. Coulon, and J. M. J. Travis. 2015. Dispersal asymmetries and deleterious mutations influence metapopulation persistence and range dynamics. Evolutionary Ecology **29**:833–850.

Henson, S. M., R. F. Costantino, J. M. Cushing, R. A. Desharnais, B. Dennis, and A. A. King. 2001. Lattice Effects Observed in Chaotic Dynamics of Experimental Populations. Science **294**:602–605.

Holling, C. S. 1959. The Components of Predation as Revealed by a Study of Small-Mammal Predation of the European Pine Sawfly. The Canadian Entomologist **91**:293320.

Holt, R. D. 2003. On the evolutionary ecology of species ranges. Evolutionary Ecology Research pages 159–178.

Huang, W., C. Hauert, and A. Traulsen. 2015. Stochastic game dynamics under demographic fluctuations. Proceedings of the National Academy of Sciences **112**:9064–9069.

Hubbell, S. P. 2001. The unified neutral theory of biodiversity and biogeography. Princeton University Press.

Huey, R. B., and J. G. Kingsolver. 1989. Evolution of thermal sensitivity of ectotherm performance. Trends in Ecology & Evolution **4**:131–135.

Huey, R. B., and R. Stevenson. 1979. Integrating Thermal Physiology and Ecology of Ectotherms: A Discussion of Approaches. American Zoologist **19**:357–366.

Hufbauer, R. A., M. Szcs, E. Kasyon, C. Youngberg, M. J. Koontz, C. Richards, T. Tuff, and B. A. Melbourne. 2015. Three types of rescue can avert extinction in a changing environment. Proceedings of the National Academy of Sciences **112**:10557–10562.

Huffaker, C. B. 1958. Experimental studies on predation: Dispersion factors and predator-prey oscillations. Hilgardia **27**:343–383.

Huntingford, C., P. D. Jones, V. N. Livina, T. M. Lenton, and P. M. Cox. 2013. No increase in global temperature variability despite changing regional patterns. Nature **500**:327–330.

Huxman, T. E., K. A. Snyder, D. Tissue, A. J. Leffler, K. Ogle, W. T. Pockman, D. R. Sandquist, D. L. Potts, and S. Schwinning. 2004. Precipitation pulses and carbon fluxes in semiarid and arid ecosystems. Oecologia **141**:254–268.

Inouye, B. D. 2005. The importance of the variance around the mean effect size of ecological processes: comment. Ecology **86**:262–265.

Jensen, J. 1906. Sur les fonctions convexes et les ingalits entre les valeurs moyennes. Acta Mathematica **3**:175–193.

Kærn, M., T. C. Elston, W. J. Blake, and J. J. Collins. 2005. Stochasticity in gene expression: from theories to phenotypes. Nature Reviews Genetics **6**:451–464.

Keeling, M., and J. Ross. 2008. On methods for studying stochastic disease dynamics. Journal of The Royal Society Interface **5**:171–181.

Kendall, D. G. 1949. Stochastic Processes and Population Growth. Journal of the Royal Statistical Society. Series B (Methodological) **11**:230–282.

Kermack, W. O., and A. G. McKendrick. 1927. A Contribution to the Mathematical Theory of Epidemics. Proceedings of the Royal Society of London A: Mathematical, Physical and Engineering Sciences **115**:700–721.

Kessler, D. A., and N. M. Shnerb. 2007. Extinction Rates for Fluctuation-Induced Metastabilities: A Real-Space WKB Approach. Journal of Statistical Physics **127**:861–886.

Kilpatrick, A. M., and A. R. Ives. 2003. Species interactions can explain Taylor's power law for ecological time series. Nature **422**:65–68.

Kingsolver, J. G., S. E. Diamond, and L. B. Buckley. 2013. Heat stress and the fitness consequences of climate change for terrestrial ectotherms. Functional Ecology **27**:1415–1423.

Kingsolver, J. G., J. K. Higgins, and K. E. Augustine. 2015. Fluctuating temperatures and ectotherm growth: distinguishing non-linear and time-dependent effects. Journal of Experimental Biology **218**:2218–2225.

Kirkpatrick, M., and N. H. Barton. 1997. Evolution of a Species' Range. The American Naturalist **150**:1–23.

Knapp, A. K., and M. D. Smith. 2001. Variation Among Biomes in Temporal Dynamics of Aboveground Primary Production. Science **291**:481–484.

Kolmogorov, A. 1931. ber die analytischen Methoden in der Wahrscheinlichkeitsrechnung. Mathematische Annalen **104**:415–458.

Kolpas, A., and R. M. Nisbet. 2010. Effects of Demographic Stochasticity onPopulationPersistence in Advective Media. Bulletin of Mathematical Biology **72**:1254–1270.

Kramer, A. M., and J. M. Drake. 2010. Experimental demonstration of population extinction due to a predator-driven Allee effect. Journal of Animal Ecology **79**:633–639.

Kubisch, A., R. D. Holt, H.-J. Poethke, and E. A. Fronhofer. 2014. Where am I and why? Synthesizing range biology and the eco-evolutionary dynamics of dispersal. Oikos **123**:5–22.

Kurtz, T. G. 1970. Solutions of Ordinary Differential Equations as Limits of Pure Jump Markov Processes. Journal of Applied Probability **7**:49–58.

Kusch, J., L. Czubatinski, S. Nachname, M. Hbner, M. Alter, and P. Albrecht. 2002. Competitive Advantages of Caedibacter-Infected Paramecia. Protist **153**:47–58.

Lande, R. 1993. Risks of Population Extinction from Demographic and Environmental Stochasticity and Random Catastrophes. The American Naturalist **142**:911–927.

Landis, W. G. 1981. The ecology, role of the killer trait, and interactions of five species of the Paramecium aurelia complex inhabiting the littoral zone. Canadian Journal of Zoology **59**:1734–1743.

Leibold, M. A., M. Holyoak, N. Mouquet, P. Amarasekare, J. M. Chase, M. F. Hoopes, R. D. Holt, J. B. Shurin, R. Law, D. Tilman, M. Loreau, and A. Gonzalez. 2004. The metacommunity concept: a framework for multi-scale community ecology. Ecology Letters **7**:601–613.

Levine, J., and J. HilleRisLambers. 2009. The importance of niches for the maintenance of species diversity. Nature **461**:254–257.

Levins, R. 1969. Some demographic and genetic consequences of environmental heterogeneity for biological control. Bulletin of the Entomological Society of America **15**:237–240.

Loik, M. E., D. D. Breshears, W. K. Lauenroth, and J. Belnap. 2004. A multi-scale perspective of water pulses in dryland ecosystems: climatology and ecohydrology of the western USA. Oecologia **141**:269–281.

Lotka, A. 1925. Elements of Physical Biology. Williams and Wilkins Company.

Louthan, A. M., D. F. Doak, and A. L. Angert. 2015. Where and when do species interactions set range limits? Trends in Ecology & Evolution **30**:780–792.

Luckinbill, L. S. 1979. Regulation, stability, and diversity in a model experimental microcosm. Ecology **60**:1098–1102.

Lynch, M., and J. S. Conery. 2003. The Origins of Genome Complexity. Science **302**:1401–1404.

MacArthur, R. 1970. Species packing and competitive equilibrium for many species. Theoretical Population Biology **1**:1–11.

Macarthur, R., and R. Levins. 1967. The Limiting Similarity, Convergence, and Divergence of Coexisting Species. The American Naturalist **101**:377–385.

Matis, J., and T. Kiffe. 2000. Stochastic population models: a compartmental perspective. Springer Verlag.

May, R. 1973. Stability and complexity in model ecosystems. Princeton University Press.

Meisner, M. H., J. P. Harmon, and A. R. Ives. 2014. Temperature effects on long-term population dynamics in a parasitoidhost system. Ecological Monographs **84**:457–476.

Melbourne, B. A., 2012. Demographic stochasticity. Page 848 in Encyclopedia of Theoretical Ecology. University of California Press.

Melbourne, B. A., and A. Hastings. 2008. Extinction risk depends strongly on factors contributing to stochasticity. Nature **454**:100–103.

Melbourne, B. A., and A. Hastings. 2009. Highly Variable Spread Rates in Replicated Biological Invasions: Fundamental Limits to Predictability. Science **325**:1536–1539.

Miquel, J., P. R. Lundgren, K. G. Bensch, and H. Atlan. 1976. Effects of temperature on the life span, vitality and fine structure of Drosophila melanogaster. Mechanisms of Ageing and Development **5**:347–370.

Moore, J.-S., J. L. Gow, E. B. Taylor, and A. P. Hendry. 2007. Quantifying the constraining influence of gene flow on adaptive divergence in the lake-stream threespine stickleback system. Evolution **61**:2015–2026.

Morjan, C. L., and L. H. Rieseberg. 2004. How species evolve collectively: implications of gene flow and selection for the spread of advantageous alleles. Molecular Ecology **13**:1341–1356.

Müller, J. P., C. Hauzy, and F. D. Hulot. 2012. Ingredients for protist coexistence: competition, endosymbiosis and a pinch of biochemical interactions. Journal of Animal Ecology **81**:222–232.

Murdoch, W. W., C. J. Briggs, and R. M. Nisbet. 2003. Consumer-resource dynamics. Princeton University Press.

Nisbet, R., and W. Gurney. 1982. Modelling fluctuating populations. Wiley.

Nisbet, R. M., B. T. Martin, and A. M. de Roos. 2016. Integrating ecological insight derived from individual-based simulations and physiologically structured population models. Ecological Modelling **326**:101–112.

Norman, T. M., N. D. Lord, J. Paulsson, and R. Losick. 2013. Memory and modularity in cell-fate decision making. Nature **503**:481–486.

Novick, A., and M. Weiner. 1957. Enzyme induction as an all-or-none phenomenon. Proceedings of the National Academy of Sciences **43**:553–566.

Novoplansky, A., and D. E. Goldberg. 2001. Effects of water pulsing on individual performance and competitive hierarchies in plants. Journal of Vegetation Science **12**:199–208.

Nsell, I. 2001. Extinction and Quasi-stationarity in the Verhulst Logistic Model. Journal of Theoretical Biology **211**:11–27.

Ochocki, B. M., and T. E. X. Miller. 2017. Rapid evolution of dispersal ability makes biological invasions faster and more variable. Nature Communications **8**:14315.

Okuyama, T. 2015. Demographic stochasticity alters the outcome of exploitation competition. Journal of Theoretical Biology **365**:347–351.

Orrock, J. L., and R. J. Fletcher. 2005. Changes in Community Size Affect the Outcome of Competition. The American Naturalist **166**:107–111.

Orrock, J. L., and J. I. Watling. 2010. Local community size mediates ecological drift and competition in metacommunities. Proceedings of the Royal Society of London B: Biological Sciences **277**:2185–2191.

Ovaskainen, O., and B. Meerson. 2010. Stochastic models of population extinction. Trends in Ecology & Evolution **25**:643–652.

Paaijmans, K. P., R. L. Heinig, R. A. Seliga, J. I. Blanford, S. Blanford, C. C. Murdock, and M. B. Thomas. 2013. Temperature variation makes ectotherms more sensitive to climate change. Global Change Biology **19**:2373–2380.

Paland, S., and B. Schmid. 2003. Population size and the nature of genetic load in Gentianella Germanica. Evolution **57**.

Park, T. 1948. Experimental studies of interspecies competition. I. Competition between populations of the flour beetles Tribolium confusum Duval and Tribolium castaneum Herbs. Ecological Monographs **18**:265–308.

Park, T. 1954. Experimental Studies of Interspecies Competition II. Temperature, Humidity, and Competition in Two Species of Tribolium. Physiological Zoology **27**:177–238.

Park, T. 1957. Experimental studies of interspecies competition. III. Relation of initial species proportion to the competitive outcome in populations of Tribolium. Physiological Zoology **30**:166–184.

Parmesan, C. 2006. Ecological and Evolutionary Responses to Recent Climate Change. Annual Review of Ecology, Evolution, and Systematics **37**:637–669.

Pearl, R., and L. J. Reed. 1920. On the Rate of Growth of the Population of the United States Since 1790 and its Mathematical Representation. Proceedings of the National Academy of Sciences of the United States of America **6**:275–288.

Pedruski, M. T., G. F. Fussmann, and A. Gonzalez. 2015. Predicting the outcome of competition when fitness inequality is variable. Royal Society Open Science **2**.

Perkins, T. A., B. L. Phillips, M. L. Baskett, and A. Hastings. 2013. Evolution of dispersal and life history interact to drive accelerating spread of an invasive species. Ecology Letters **16**:1079–1087.

Petit, N., and A. Barbadilla. 2009. Selection efficiency and effective population size in Drosophila species. Journal of Evolutionary Biology **22**:515–526.

Pimentel, D., R. Zuniga, and D. Morrison. 2005. Update on the environmental and economic costs associated with alien-invasive species in the United States. Ecological Economics **52**:273–288.

R Core Team, 2017. R: A Language and Environment for Statistical Computing. R Foundation for Statistical Computing, Vienna, Austria.

Reitz, S. R., and J. T. Trumble. 2002. Competitive displacement among insects and arachnids. Annual Review of Entomology **47**:435–465.

Renshaw, E. 1991. Modelling biological populations in space and time. Cambridge University Press.

Rohani, P., M. J. Keeling, and B. T. Grenfell. 2002. The Interplay between Determinism and Stochasticity in Childhood Diseases. The American Naturalist **159**:469–481.

Ronce, O. 2007. How Does It Feel to Be Like a Rolling Stone? Ten Questions About Dispersal Evolution. Annual Review of Ecology, Evolution, and Systematics **38**:231–253.

Rosindell, J., S. P. Hubbell, F. He, L. J. Harmon, and R. S. Etienne. 2012. The case for ecological neutral theory. Trends in Ecology & Evolution **27**:203–208.

Ross, S. 2014. Introduction to Probability Models. Eleventh edition. Academic Press.

Ruel, J. J., and M. P. Ayres. 1999. Jensen's inequality predicts effects of environmental variation. Trends in Ecology & Evolution **14**:361–366.

Ruxton, G., W. Gurney, and A. de Roos. 1992. Interference and generation cycles. Theoretical Population Biology **42**:235–253.

Schaffer, W. M. 1984. Stretching and Folding in Lynx Fur Returns: Evidence for a Strange Attractor in Nature? The American Naturalist **124**:798–820.

Sexton, J. P., P. J. McIntyre, A. L. Angert, and K. J. Rice. 2009. Evolution and Ecology of Species Range Limits. Annual Review of Ecology, Evolution, and Systematics **40**:415–436.

Shaffer, M. L. 1981. Minimum Population Sizes for Species Conservation. BioScience **31**:131–134.

Shine, R., G. P. Brown, and B. L. Phillips. 2011. An evolutionary process that assembles phenotypes through space rather than through time. Proceedings of the National Academy of Sciences **108**:5708–5711.

Silvertown, J. 2004. Plant coexistence and the niche. Trends in Ecology & Evolution **19**:605–611.

Simonis, J. L. 2012. Demographic stochasticity reduces the synchronizing effect of dispersal in predatorprey metapopulations. Ecology **93**:1517–1524.

Slatkin, M. 1987. Gene flow and the geographic structure of natural populations. Science **236**:787–792.

Soetaert, K., T. Petzoldt, and R. W. Setzer. 2010. Solving Differential Equations in R: Package deSolve. Journal of Statistical Software **33**:1–25.

Spencer, M., and P. H. Warren. 1996. The Effects of Habitat Size and Productivity on Food Web Structure in Small Aquatic Microcosms. Oikos **75**:419–430.

Spudich, J. L., and D. E. Kosland. 1976. Non-genetic individuality: chance in the single cell. Nature **262**:467–471.

Stroustrup, N., W. E. Anthony, Z. M. Nash, V. Gowda, A. Gomez, I. F. Lpez-Moyado, J. Apfeld, and W. Fontana. 2016. The temporal scaling of Caenorhabditis elegans ageing. Nature **530**:103–107.

Szücs, M., B. A. Melbourne, T. Tuff, and R. A. Hufbauer. 2014. The roles of demography and genetics in the early stages of colonization. Proceedings of the Royal Society of London B: Biological Sciences **281**.

Szücs, M., B. A. Melbourne, T. Tuff, C. Weiss-Lehman, and R. A. Hufbauer. 2017. Genetic and demographic founder effects have long-term fitness consequences for colonising populations. Ecology Letters **20**:436–444.

Taylor, L. R., I. P. Woiwod, and J. N. Perry. 1980. Variance and the Large Scale Spatial Stability of Aphids, Moths and Birds. Journal of Animal Ecology **49**:831–854.

Tigano, A., and V. L. Friesen. 2016. Genomics of local adaptation with gene flow. Molecular Ecology **25**:2144–2164.

Tilman, D. 1982. Resource competition and community structure. Princeton University Press.

Tilman, D. 1994. Competition and Biodiversity in Spatially Structured Habitats. Ecology **75**:2–16.

van Kampen, N. G. 1992. Stochastic Processes in Physics and Chemistry. Elsevier Science.

Vellend, M. 2010. Conceptual Synthesis in Community Ecology. The Quarterly Review of Biology **85**:183–206.

Vellend, M., D. S. Srivastava, K. M. Anderson, C. D. Brown, J. E. Jankowski, E. J. Kleynhans, N. J. B. Kraft, A. D. Letaw, A. A. M. Macdonald, J. E. Maclean, I. H. Myers-Smith, A. R. Norris, and X. Xue. 2014. Assessing the relative importance of neutral stochasticity in ecological communities. Oikos **123**:1420–1430.

Verhulst, P. 1845. Recherches mathmatiques sur la loi d'accroissement de la population. Nouveaux mmoires de l'Acadmie Royale des Sciences et Belles-Lettres de Bruxelles **18**:14–54.

Vestergaard, C. L., and M. Gnois. 2015. Temporal Gillespie Algorithm: Fast Simulation of Contagion Processes on Time-Varying Networks. PLOS Computational Biology **11**:1–28.

Vindenes, Y., S. Engen, and B. Sther. 2008. Individual Heterogeneity in Vital Parameters and Demographic Stochasticity. The American Naturalist **171**:455–467.

Volkov, I., J. R. Banavar, S. P. Hubbell, and A. Maritan. 2003. Neutral theory and relative species abundance in ecology. Nature **424**:1035–1037.

Volterra, V. 1926. Variazioni e fluttuazioni del numero dindividui in specie animali conviventi. Memoires of the Accademia dei Lincei **2**:31–113.

Von Neumann, J. 1951. Various Techniques Used in Connection With Random Digits. Appl. Math Ser **12**:36–38.

Wang, X., T. Wiegand, N. J. B. Kraft, N. G. Swenson, S. J. Davies, Z. Hao, R. Howe, Y. Lin, K. Ma, X. Mi, S.-H. Su, I.-F. Sun, and A. Wolf. 2016. Stochastic dilution effects weaken deterministic effects of niche-based processes in species rich forests. Ecology **97**:347–360.

Weber, K. E. 1990. Increased selection response in larger populations. I. Selection for wingtip height in Drosophila melanogaster at three population sizes. Genetics **125**:579–584.

Weiss-Lehman, C., R. A. Hufbauer, and B. A. Melbourne. 2017. Rapid trait evolution drives increased speed and variance in experimental range expansions. Nature Communications **8**:14303.

Wilcox, C., and H. Possingham. 2002. Do life history traits affect the accuracy of diffusion approximations for mean time to extinction? Ecological Applications **12**:1163–1179.

Williams, J. L., B. E. Kendall, and J. M. Levine. 2016. Rapid evolution accelerates plant population spread in fragmented experimental landscapes. Science **353**:482–485.

Wright, S. 1931. Evolution in Mendelian populations. Genetics **16**:97–159.

Yaari, G., Y. Ben-Zion, N. M. Shnerb, and D. A. Vasseur. 2012. Consistent scaling of persistence time in metapopulations. Ecology **93**:1214–1227.

Yule, G. U. 1925. A Mathematical Theory of Evolution, Based on the Conclusions of Dr. J. C. Willis, F.R.S. Philosophical Transactions of the Royal Society of London B: Biological Sciences **213**:21–87.

Appendix A

Supplemental information for Chapter 2

A.1 Monocultures

A.1.1 Experimental procedures

In parallel with the main experiment, we established 10 replicate monocultures of each protist species (*Paramecium aurelia*, *Paramecium caudatum*, *Philodina americanum*) in large (80 mL) jars. The preparation of the jars and the media matched that of the two-species competition trials..

Each jar started with initial densities of 4.5-5.5 individuals per mL of media, or approximately 360-440 individuals total. Added individuals were not counted directly, rather a fixed volume of media from stock cultures of known densities was added to each replicate.

Subsequent sampling and media replacement also matched that of the two-species competition trials. Jars were sampled until day 42, well after a stable population size had been observed for each species.

A.1.2 Consumer-resource models

We were interested in quantifying the dynamics in our monocultures (and, subsequently, in the two-species trials) by fitting mechanistic population models to our data. The dynamics of *P. aurelia* were not consistent with a continuous-time logistic growth model because their abundances did not increase monotonically to a carrying capacity but instead

increased then decreased (Figure A.1). This, as well as knowledge that protists consume an explicit biological resource (bacteria) in our system, led us to consider consumer-resource models (MacArthur, 1970) of the form:

$$\begin{aligned} \frac{dR}{dt} &= Rf(R) - N_1 g(R, N_1) \\ \frac{dN_i}{dt} &= N_i e_i g(R, N_i) - h(N_i) \end{aligned} \tag{A.1}$$

where $f(R)$ is the growth function of the resource (prey), $g(R, N_i)$ is the consumption function of the consumer (i.e., the rate at which the consumer removes the resource), $h(N_i)$ is the death function of the consumer, e_i is the efficiency (i.e., assimilation rate) of the consumer, while i indexes the consumer species.

Protists within culture vessels compete indirectly via exploitative competition for shared bacterial resources and may also compete directly via interference competition. Interference within and between protist species is thought to occur as a result of allelopathic compounds released into the media or interactions with bacterial endosymbionts (Gause, 1935; Gill, 1972; Habte and Alexander, 1978; Landis, 1981; Balčiūnas and Lawler, 1995; Kusch et al., 2002; Müller et al., 2012). Such interactions could affect consumption rates or death rates. As a result, we fit model A.1 to our data, specifying a variety of different consumption and death functions

For the five models we considered, we assumed that the bacterial resource exhibited logistic growth, such that:

$$f(R) = r(1 - \frac{R}{K}) \tag{A.2}$$

where r is the density-independent growth rate of the resource and K is the carrying capacity. Models differed in their consumption functions $g(R, N_1)$ and death functions $h(N_1)$. The consumption and death functions considered are outlined in Table A.1.

Table A.1: Details of the consumption and death functions used in the consumer-resource models. A total of 5 models were fit to monoculture data for each species.

Description	Function	Models	Reference(s)
Consumption $g(R, N_1)$			
A. Linear type I	$a_1 R$	1, 5	
B. Handling time (type II)	$\frac{a_1 R}{1+a_1 h_1 R}$	2	Holling (1959)
C. Handling time + consumer-dependent	$\frac{a_1 R}{1+a_1 h_1 R+u_1 N_1}$	3	Beddington (1975) DeAngelis et al. (1975)
D. Consumer-dependent	$\frac{a_1 R}{1+u_1 N_1}$	4	Ruxton et al. (1992)
Death $h(N_1)$			
E. Linear	d_1	1-4	
F. Non-linear	$d_1 + m_1 N_1$	5	Murdoch et al. (2003)

A.1.3 Model-fitting

We assumed that the bacterial resource was at carrying capacity at the beginning of the experiment, and, based on previous experimental studies using similar conditions (e.g. (Diehl and Feiel, 2000; Fox, 2002; DeLong and Vasseur, 2012)), set the carrying capacity K to 10^8 bacterial cells per mL. Under our lab conditions, half saturation of the bacteria occurs after approximately 30 hours, so we estimated r_1 using the analytical solution of the logistic growth equation:

$$R(t) = \frac{KR(0)}{R(0) + (K - R(0))e^{-rt}}$$

and solving for r given that $R_0 =$ (number of loops of added bacteria) $*$ (cells per loopful) $= 4 * 10^8$, $K =$ (mL of prepared media) $*$ (cells per mL at K) $= 2000 * 10^8$, and $R(1.25) = 1000$. From this, we estimated r_1 (4.970) and set it constant across all models.

Using a one-step ahead maximum likelihood approach where the consumer-resource models above were the means of normal distributions (i.e., incorporating both process error and a normal approximation of stochasticity), we fitted to the monoculture data from the first 30 days of observations for each species. Replicates which did not persist for 30 days were omitted from the model fitting, such that we fit the models to data from 9 replicates for *P. aurelia* and *P. americanum*, and 8 replicates for *P. caudatum*.

For each set of monocultures, we first performed a broad search of likelihood space, calculating the likelihood of each model for parameter values ranging from e^-10 to e^2 in increments of e^1, resulting in a search across 2197 unique parameter combinations for model 1 (3 parameters); 28561 parameter combinations for models 2, 4, and 5 (4 parameters); and 371293 parameter combinations for model 3 (5 parameters).

From this set of parameters, the top 100 parameter combinations (i.e., with the highest maximum likelihood scores) became the starting values for a numerical optimization routine using the Nelder-Mead method, as implemented in the function ‘mle2‘ from the package ‘bbmle‘ for R.

A.1.4 Results

For the *P. aurelia* monocultures, model-fitting was possible for all models considered, with model 3 having the lowest negative log-likelihood and AIC scores (Table A.2, below). However, it was not possible to obtain reasonable parameter estimates for any of the models for either *P. caudatum* or *P. americanum* due to one or more of the following issues: (1) lack of convergence in the optimization; (2) unrealistic parameter estimates (e.g. efficiency [e_1] estimates > 1); 3) confidence intervals spanning 3 or more orders of magnitude; and (4) flat likelihood surfaces, preventing reasonable estimation of confidence intervals. Some of these problems can likely be attributed to a lack of data on the bacterial resource as well as insufficient coverage of state space due to the fast dynamics of the protist system and our 2-day sampling resolution (e.g., *P. caudatum* monocultures reached equilibrium after only 6 days and remained there for the duration of our observations). Times series data and model fits are shown in Figure A.1 below. As a result of these aforementioned issues with model-fitting, we did not fit mechanistic population models to our two-species trials.

A.2 Stochastic consumer-resource model

Here we outline some of the assumption made in our formulation of the stochastic version of the consumer-resource model discussed in the manuscript. The deterministic model is:

$$\begin{aligned} \frac{dR}{dt} &= r_1 R(1 - \frac{R}{K}) - a_1 R N_1 - a_2 R N_2 \\ \frac{dN_1}{dt} &= e_1 a_1 R N_1 - d_1 N_1 \\ \frac{dN_2}{dt} &= e_2 a_2 R N_2 - d_2 N_2 \end{aligned} \tag{A.3}$$

We expect the following demographic events in this system: (1) resource growth; (2) resource death by consumer N_1; (3) resource death by consumer N_2; (4) consumer N_1 growth; (5) consumer N_2 growth; (6) consumer N_1 death; (7) consumer N_2 death. Therefore, the goal

Figure A.1: Monoculture time series data for the three protist species *Paracemium aurelia*, *Paramecium caudatum*, *Philodina americanum*. Thin lines represent individual replicate populations, and in the case of *P. aurelia* thicker lines represent the population trajectories predicted by the fitted models.

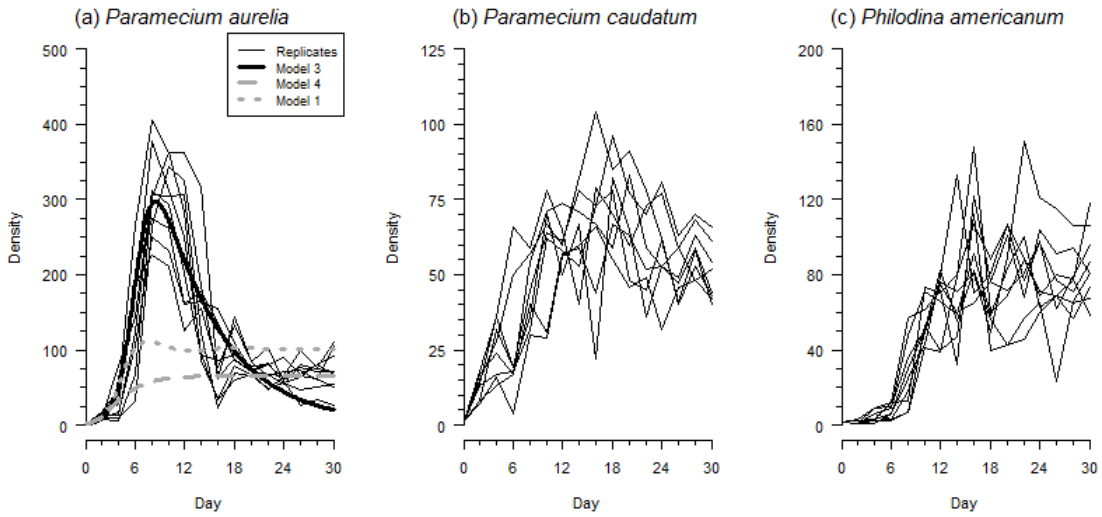

Table A.2: Estimated parameter values (on the natural log scale) and confidence intervals (CI) for models 1 through 6 for *Paramecium aurelia*. The table includes AIC scores from the Nelder-Mead optimization for each model. Asterisks (*) indicate when confidence intervals were estimated from a quadratic approximation of the likelihood surface.

Model / Parameter	Estimate	95% CI	AIC
1. Linear consumption + death			1434.32
Consumer attack rate, a_1	-3.11	(-3.19,-3.01)	
Consumer efficiency, e_1	-14.10	(-14.22,-14.00)	
Consumer death rate, d_1	-2.31	(-2.53,-2.12)	
2. Type II consumption + death			1379.30
Consumer attack rate, a_1	-3.10	(-3.14,-2.55)*	
Consumer efficiency, e_1	-12.66	(-12.83,-12.51)*	
Resource handling time, h_1	-12.74	(-12.93,-12.51)*	
Consumer death rate, d_1	-2.17	(-2.37,-1.99)	
3. Consumer-dependent consumption + death			1355.68
Consumer attack rate, a_1	-0.93	(-0.94,-0.41)*	
Consumer efficiency, e_1	-13.04	(-13.23,-12.93)*	
Density-dependence (consumption), u_1	-2.77	(-3.09,-1.99)*	
Resource handling time, h_1	-13.14	(-13.34,-13.08)*	
Consumer death rate, d_1	-2.01	(-2.19,-1.85)*	
4. Consumer-dependent consumption + death			1412.90
Consumer attack rate, a_1	-2.15	(-2.37,-1.88)*	
Consumer efficiency, e_1	-14.81	(-15.04,-14.61)*	
Density-dependence (consumption), u_1	-4.04	(-4.36,-3.68)*	
Consumer death rate, d_1	-1.66	(-1.96,-1.45)*	
5. Linear consumption + non-linear death			1432.16
Consumer attack rate, a_1	-3.10	(-3.18,-2.99)*	
Consumer efficiency, e_1	-14.15	(-14.28,-14.04)*	
Consumer death rate, d_1	-2.88	(-5.74,-2.29)*	
Density-dependence (death), m_1	-7.95	(-11.32,-7.12)*	

in our top-down approach for constructing a stochastic model (Black and McKane, 2012) is to determine which terms in model A.3 correspond to these different events.

Resource growth corresponds well with the first set of terms in the first equation ($r_1 R(1-\frac{R}{K})$ as it does not appear anywhere else in the model and is the only term which can add resources to the system. Here we assume that the resource growth rate, r_1 represents the net growth rate and thus we do not specify individual birth (b) and death (d) rates. In small populations, this assumption would be problematic, as the particular values of b and d - rather than their sum - could be important for population dynamics. However, in our system, the resource population is large ($> 10^4$) and so births and consumer-independent deaths happen frequently enough that it is appropriate to consider only their net effect.

Determining the probability of consumer death is also relatively straightforward, as for each consumer the last term in each consumer equation is the only one capable of subtracting consumers from the system.

Accounting for consumer growth and resource death is less straightforward since both are linked via the consumption functions, $a_i R N_i$. Moreover, efficiences (e_i) may be less than 1, meaning that the death of a resource may not always corresponds to the birth of a consumer. As in (Simonis, 2012), we therefore discriminate between three kinds of resource consumptions: (1) resource consumption with no corresponding consumer growth; (2) resource consumption with consumer N_1 growth; (3) resource consumption with consumer N_2 growth. For (2) and (3), we assume that e_i represents the probability that the consumption of a single (final) resource leads to the birth of a consumer. For (1), we assume that all other consumptive events (by either consumer) lead only to the death of a resource. Thus, resource death with consumer i growth occurs with probability:

$$e_i a_i R N_i$$

and resource death with no consumer growth occurs with probability:

$$(1-e_1)a_1 R N_1 + (1-e_2)a_2 R N_2$$

For the latter, we have lumped the two different kinds of resource death (by N_1 and by N_2) without associated consumer births, since from the perspective of the overall system, both kinds of events simply subtract a resource. Specifying separate no-birth death events would have no effect on the final outcome of stochastic simulations. From the above, we obtain 6 final demographic events with the following transition probabilities and state changes (reprinted from Chapter 1):

$$\begin{aligned}
\text{R birth: } R &\xrightarrow{r_1 R(1-\frac{R}{K})} R+1 \\
\text{R death: } R &\xrightarrow{(1-e_1)a_1 R N_1 + (1-e_2)a_2 R N_2} R-1 \\
\text{R death, N1 birth: } R,\, N_1 &\xrightarrow{e_1 a_1 R N_1} R-1,\, N_1+1 \\
\text{R death, N2 birth: } R,\, N_2 &\xrightarrow{e_2 a_2 R N_2} R-1,\, N_2+1 \\
\text{N1 death: } N_1 &\xrightarrow{d_1 N_1} N_1-1 \\
\text{N2 death: } N_2 &\xrightarrow{d_2 N_2} N_2-1
\end{aligned} \tag{A.4}$$

We used R to simulate the model A.4 using the direct version of the Gillespie algorithm. For details on the Gillespie algorithm (i.e., the stochastic simulation approximation) we refer readers to Gillespie (1977); Cao et al. (2004); Black and McKane (2012). Sample code with annotations can be found in section 3 of Appendix A, below.

A.3 R code for Gillespie's stochastic simulation algorithm

```
## This section contains a function capable of simulating 1 run of the
   Gillespie algorithm (SSA). This implementation of the SSA in R is
   largely based on Ben Bolker's excellent code, some of which can be
   seen here: https://rpubs.com/bbolker/SIRgillespie

## The function 'gillespie' takes as input the following:
## * 'init' = Array containing all initial conditions (e.g. initial
   population size)
```

```
## * `times` = Sequence of times over which you wish the function to report/record population size
## * `param` = Array containing all intrinsic demographic rates required for calculating intensities in `inten`(below)
## * `inten` = Function which returns all intensities/probabilities of the point processes
## * `pproc` = Array containing the state changes caused by the point process (in the same order as `intenfun`)
gillespie <- function(init, times, param, inten, pproc){
    tottime <- times[1]
    tinc <- length(times)
    N <- init
    results <- matrix(nrow = tinc, ncol = length(init))
    results[1, ] <- N
    for(i in 2:tinc){
        results[i, ] <- results[i - 1, ]
        while(tottime <= times[i]){
            intentemp <- inten(tottime, N, param)
            if(all(intentemp == 0) | min(intentemp) < 0) {
                results[i, ] <- N
                break
            }
            deltat <- rexp(1, sum(intentemp))
            tottime <- tottime + deltat
            which.pproc <- sample(1:nrow(pproc),
                                  size = 1,
                                  prob = intentemp)
            if(tottime > times[i]){
                results[i, ] <- N
                N <- N + pproc[which.pproc, ]
                break
            }
```

```
33              N <- N + pproc[which.pproc, ]
34          }
35      }
36      cbind(times, results)
37  }
38  ## Initial population sizes
39  init <- c(1000, 5, 5)
40  ## Sequence of times
41  times <- seq(0, 20, by = 1)
42  ## Parameter values
43  param <- list(r = 1,
44                k = 10000,
45                a1 = 0.02,
46                a2 = 0.04,
47                e1 = 0.07,
48                e2 = 0.02,
49                d1 = 0.3,
50                d2 = 0.1)
51  ## Function for returning transition probabilities
52  comp1 <- function(tottime, X, param){
53      with(as.list(c(param)), {
54          Rbirth <- r * X[1] * (1 - X[1] / k)
55          Rdeath <- (1 - e1) * (a1 * X[1] * X[2]) + (1 - e2) * (a2 * X[1] *
        X[3])
56          RdeathN1birth <- e1 * (a1 * X[1] * X[2])
57          RdeathN2birth <- e2 * (a2 * X[1] * X[3])
58          N1death <- d1 * X[2]
59          N2death <- d2 * X[3]
60          c(Rbirth, Rdeath, RdeathN1birth, RdeathN2birth, N1death, N2death)
61      })
62  }
63  ## State changes (corresponding to the transitions above)
```

```
pproc <- matrix(c(
    1, 0, 0,
    -1, 0, 0,
    -1, 1, 0,
    -1, 0, 1,
    0, -1, 0,
    0, 0, -1), ncol = 3, nrow = 6, byrow = T)
## Simulate one run
gillespie(init, times, param, comp1, pproc)
```

A.4 R code for model-fitting

```
## This section contains some of the model-fitting code used to estimate the effective model parameters of the stochastic simulations. Here, I fit the deterministic consumer-resource model to data generated by the deterministic `desolve` function `ode`

## Source essential library
library(deSolve)

## `comp1det` function for simulating the consumer-resource model with r (1) and K (10000) already set
comp1det <- function(t, y, parms){
    with(as.list(c(y, parms)),{
        dR <- R * (1 - R / 10000) - (a1 * R * N1) - (a2 * R * N2)
        dN1 <- e1 * (a1 * R * N1) - d1 * N1
        dN2 <- e2 * (a2 * R * N2) - d2 * N2
        list(c(dR, dN1, dN2))
    })
}
## Model parameters (neutral scenario; no niche differences between consumers)
param1 <- list(a1 = 0.04,
```

```
                a2 = 0.04,
                e1 = 0.02,
                e2 = 0.02,
                d1 = 0.2,
                d2 = 0.2)
## Run deterministic model using above parameters until time = 100
detmodel <- ode(y = c(
                    R = 1000,
                    N1 = 5,
                    N2 = 5),
                times = seq(0, 100, by = 0.01),
                func = comp1det,
                parms = param1)
## Keep values at times 0, 1, 2, etc. and round to discrete states
detmodel.sub <- subset(detmodel, time %in% seq(0, 100, 1))

## `least` function for calculating least-squares difference between
    model results (above) and the same model (`comp1det`) simulated using
    parameters in list `x`. Here I focus on the consumers only (columns 2
    and 3 of detmodel.sub)
least <- function(x){
    mtemp <- ode(y = c(
                    R = 1000,
                    N1 = 5,
                    N2 = 5),
                times = seq(0, 100, by = 0.01),
                func = comp1det,
                parms = c(
                    a1 = x[1],
                    a2 = x[2],
                    e1 = x[3],
                    e2 = x[4],
```

```
                        d1 = x[5],
                        d2 = x[6]))
    mtemp <- subset(mtemp, time %in% seq(0, 100, 1))
    sum(c((mtemp[, 2] - detmodel.sub[, 2])^2), c((mtemp[, 3] - detmodel.
    sub[, 3])^2), na.rm = T)
}

## Set starting values for optimization (in this case, the true values)
startingvalues <- c(param1[[1]],
                    param1[[2]],
                    param1[[3]],
                    param1[[4]],
                    param1[[5]],
                    param1[[6]])
## Use optim to minimize least-squares difference (default method is
    Nelder-Mead)
mtemp <- optim(startingvalues,
               least,
               hessian = TRUE)
## Print actual versus estimated parameters
### Actual
unlist(param1)
### Estimated (same order as above)
mtemp$par

## Try again with different starting values
startingvalues <- c(param1[[1]] * .95,
                    param1[[2]] * .95,
                    param1[[3]] * .95,
                    param1[[4]] * .95,
                    param1[[5]] * .95,
                    param1[[6]] * .95)
```

```
76 ## Use optim to minimize least-squares difference (default method is
       Nelder-Mead)
77 mtemp <- optim(startingvalues,
78                 least,
79                 control = list(maxit = 10000),
80                 hessian = TRUE)
81 ## Print actual versus estimated parameters
82 ### Actual
83 unlist(param1)
84 ### Estimated (same order as above)
85 mtemp$par
```

A.5 Model fits to simulated data

This section contains Figures (A.2 and A.3), showing the simulation data along with their best-fit models.

A.6 Coefficients of variation

If founder effects were a significant influence on dynamics in our microcosms, we would expect to see greater variation between replicates in the smaller jars than in the larger ones. We observed no consistent trend in the coefficients of variation (CV) across time for the experimental data A.4. However, there was a trend in the simulation data A.5, in particular: small simulations sizes had consistently higher CVs than large simulation sizes

Figure A.2: Model fits and conditional mean densities over time for consumer 1 (weak competitor). Shown are the 95% confidence intervals of consumer 1 densities (y-axis) over time (x-axis) for large (blue) and small (red) simulations, along with deterministic versions of the model using the true parameter values (solid line), and the parameter values estimated from the large (dashed) and small (dotdash) simulations

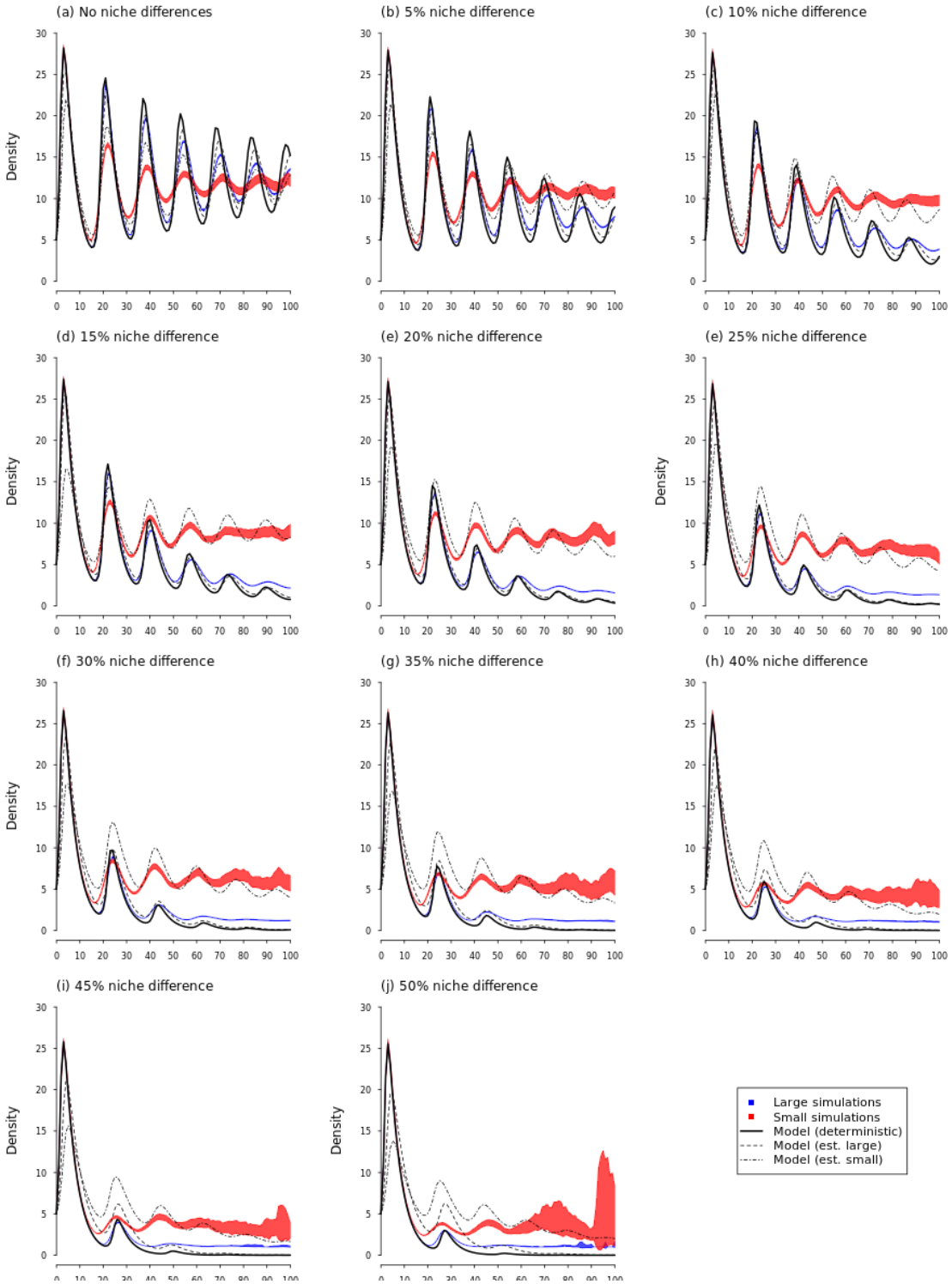

Figure A.3: Model fits and conditional mean densities over time for consumer 2 (superior competitor). Shown are the 95% confidence intervals of consumer 2 densities (y-axis) over time (x-axis) for large (blue) and small (red) simulations, along with deterministic versions of the model using the true parameter values (solid line), and the parameter values estimated from the large (dashed) and small (dotdash) simulations.

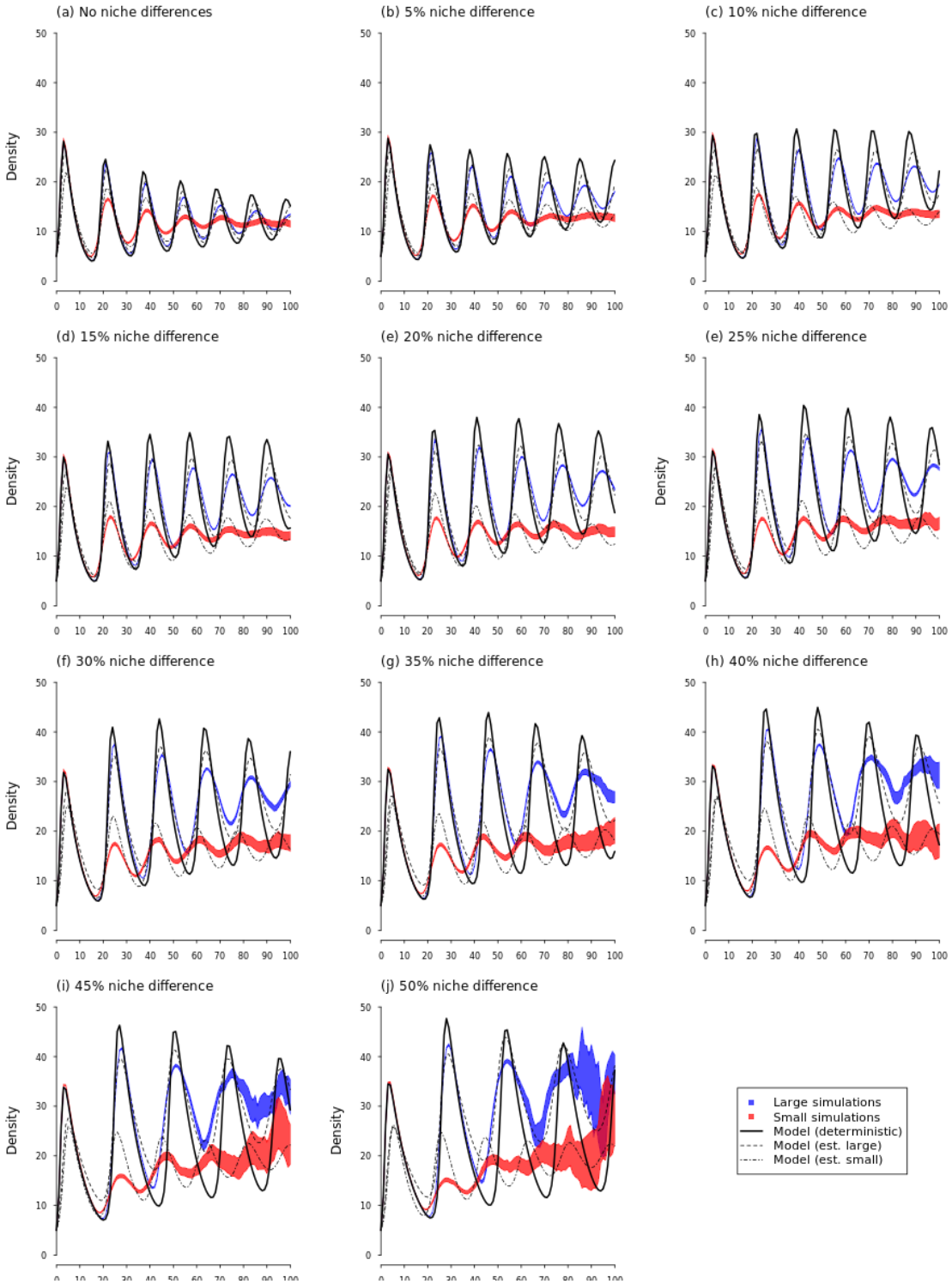

Figure A.4: Coefficients of variation (CV) across time for each competitor in the small (red), medium (gray), and large (blue) experimental jars. Figures are overlaid so that each column represents a competitive treatment: (a) and (b) show results for *Paramecium aurelia* and *Paramecium caudatum* (AC pairing), respectively; (c) and (d) for *P. aurelia* and *Philodina americanum*; (e) and (f) for *P. americanum* and *P. caudatum*.

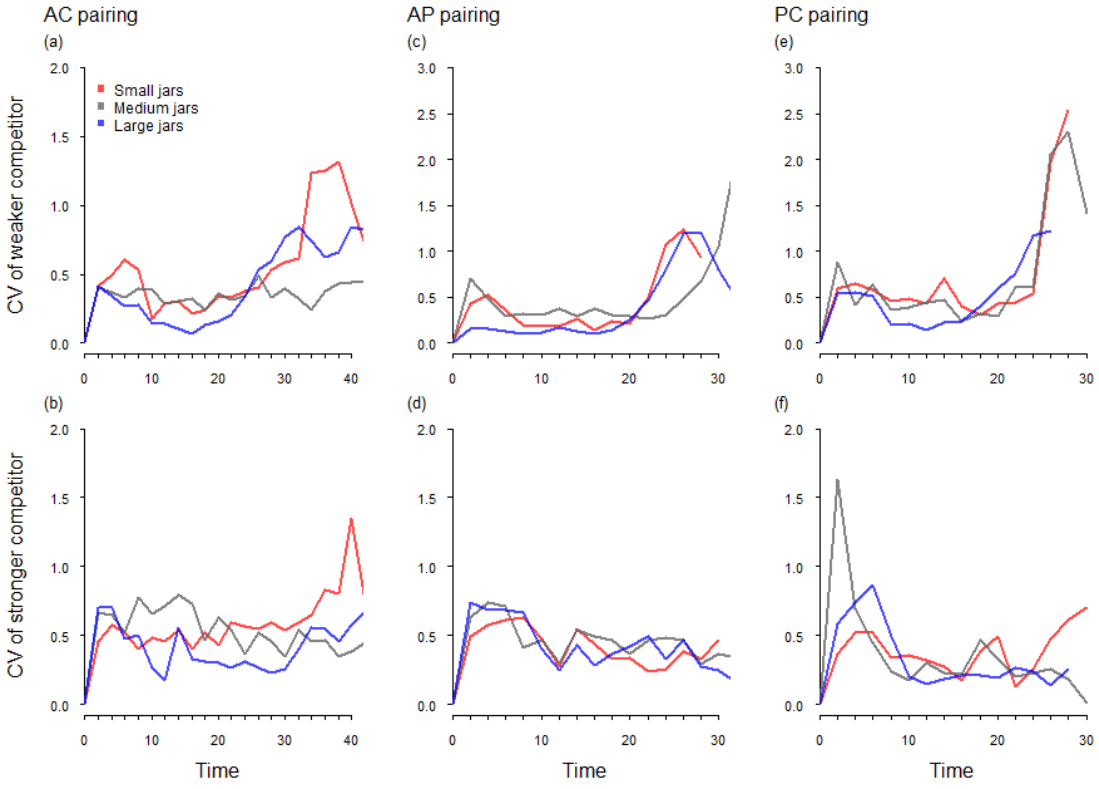

Figure A.5: Coefficients of variation (CV) across time for each competitor in the small (red), and large (blue) simulations. Figures are overlaid so that each column represents a different parameter set (i.e., fitness inequality).

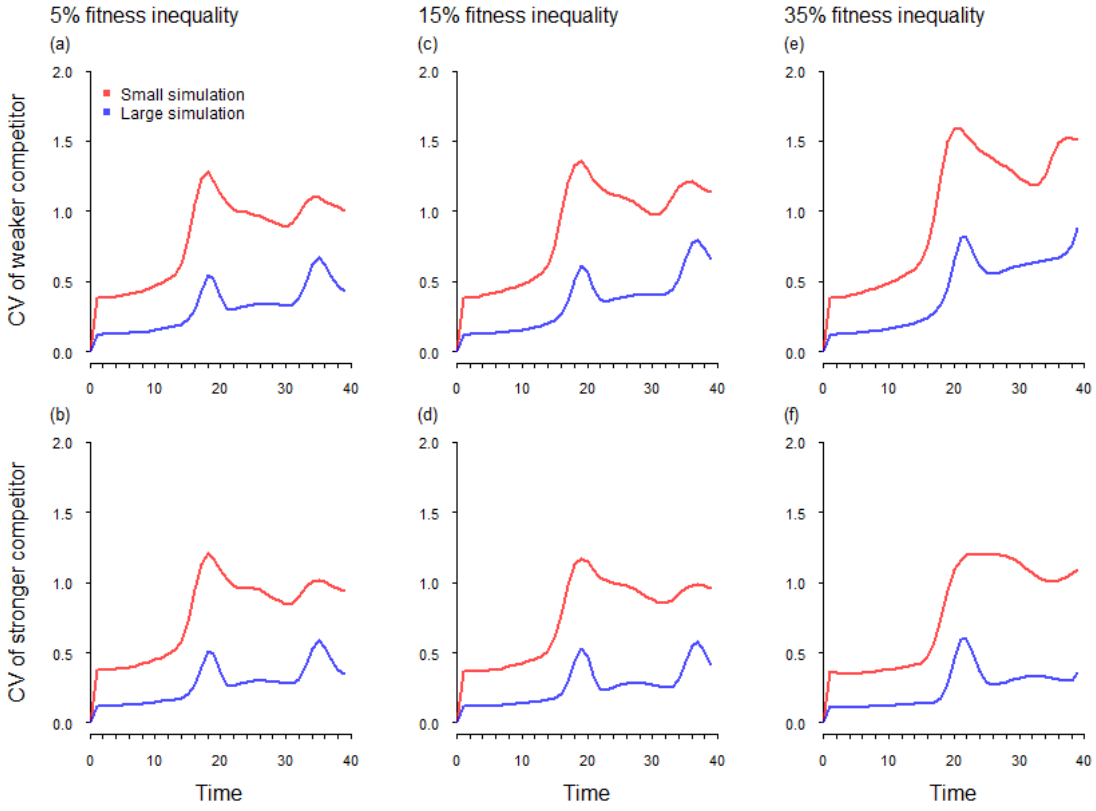

Appendix B

Supplemental information for Chapter 3

B.1 Diagnostic tests of SSA+ method

To ensure we were generating appropriate inter-arrival times, τ, using our implementation of the SSA+ method, we performed two diagnostic tests:

(1) We simulated a non-stationary exponential growth model using our SSA+ implementation with a rate function of $F(t) = \alpha t^{-\beta}$ (a power law function) and compared our results to taking samples from a Weibull distribution with parameters α and β, as discussed in the main text. These results should align nearly exactly if our implementation is correct, which appears to be the case (Figure B.1).

(2) We set the environment function to a constant value (i.e., demography was stationary) and compared the results of 50,000 simulations of the SSA+ method to an independent SSA implementation (since demography is stationary in this case, we refer to it simply as the SSA rather than the SSAn, though both use the same methods). With a constant environment, the SSA+ method should match the SSA method, which appears to be the case (Figure B.2).

Finally, we also examined the extent to which 10,000 simulations was sufficient to capture the ensemble mean and variance of the stochastic simulations. To do so, we examined how the means and variances of the exponential growth models were affected by the number

of simulations used. We found only very small differences in the means and variances from 1,000 to 10,000 simulations used (see Figure B.3 for this comparison).

Figure B.1: The probability density of 1,000,000 arrival times, obtained by sampling from a Weibull distribution with scale parameter α and shape parameter β (black), or using our SSA+ method for a non-stationary stochastic process with rate function $F(t) = \alpha t^{-\beta}$ (blue). In both cases, $\alpha = 1$ and $\beta = 1.5$.

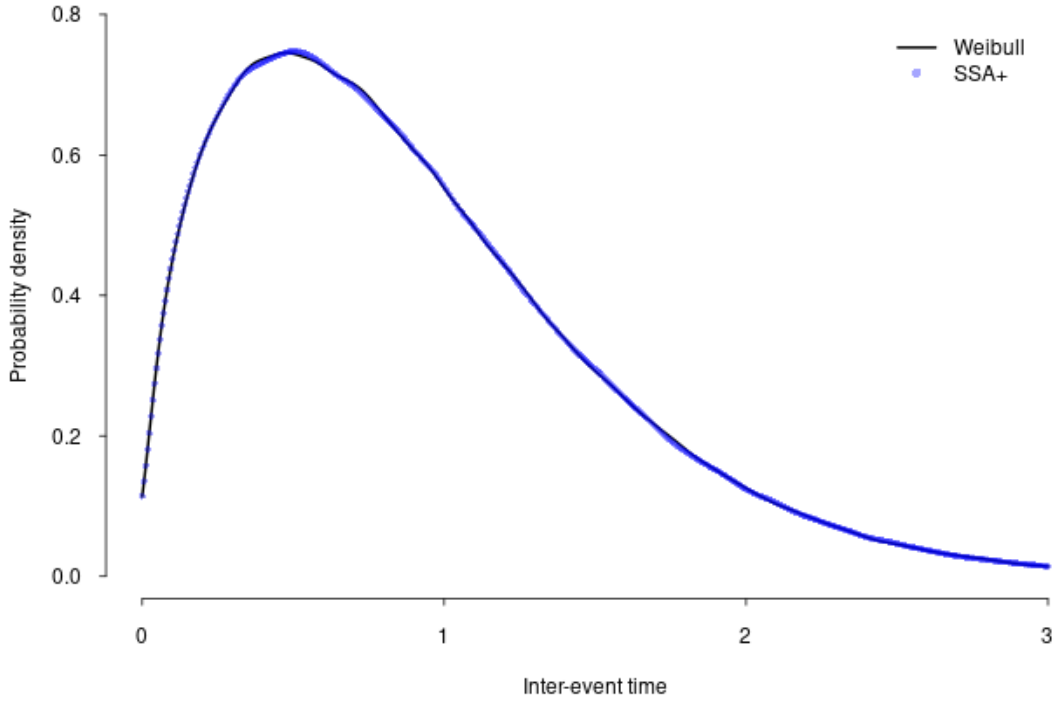

Figure B.2: The frequency distribution of population sizes at $t = 100$ for 50,000 simulations of exponential growth (a) and logistic growth (b), simulated using the SSA (red) or SSA+ (blue) methods with a constant environment. Colors are transparent, so the color purple indicates overlap between the SSA and SSA+ methods. Also displayed are the (overlapping) expected values, $\bar{N}$ (rounded) for each simulation method.

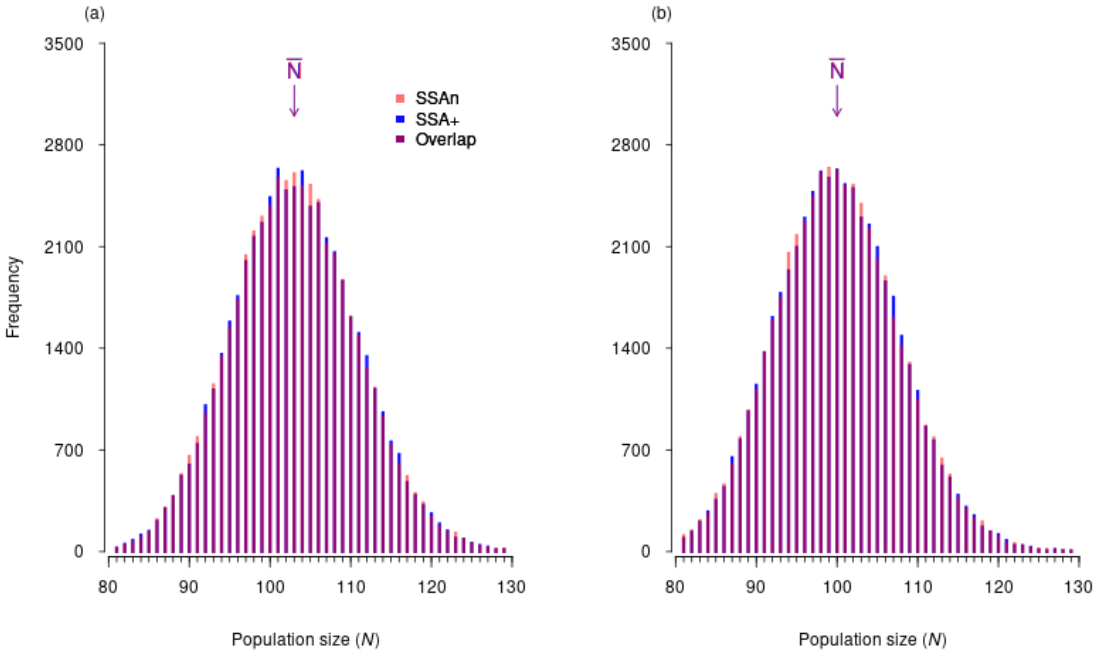

Figure B.3: The expected population sizes at $t = 100$ of the SSA+ method (exponential growth) for different numbers of simulations (x-axis). Displayed are the population sizes for the increasing (a), fluctuating (b), and random (c) environment functions. Points represent the mean population size (across simulations), while bars are the standard deviations of the simulations.

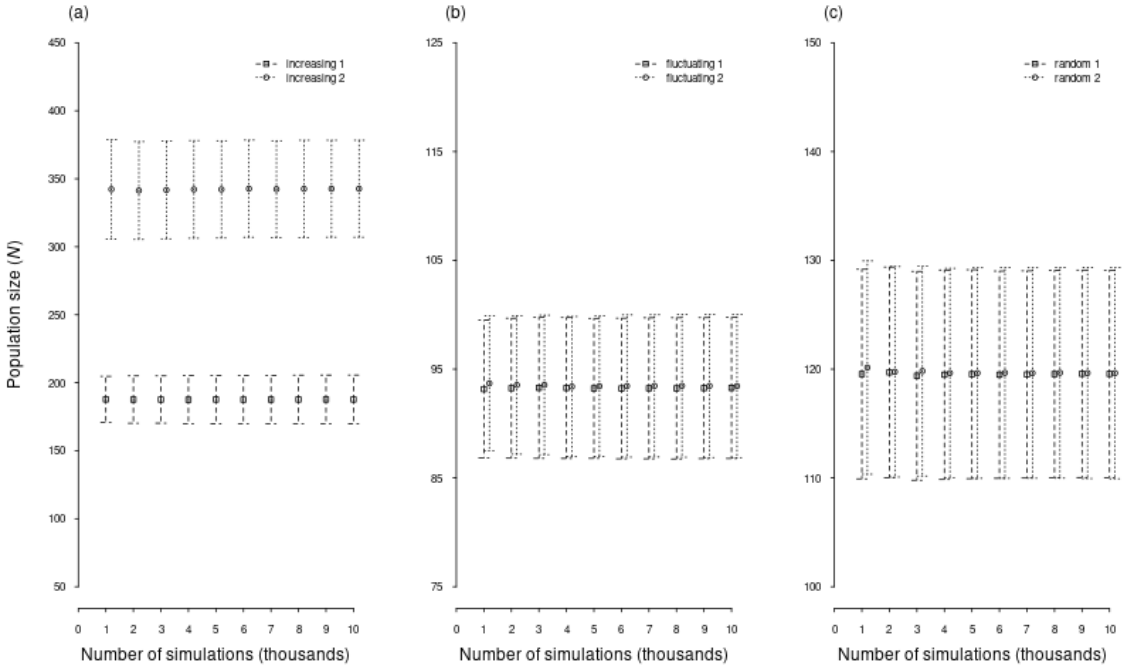

B.2 R code for SSA+ method

This section contains sample code for simulating 1 run of the Gillespie algorithm (SSA or SSAn in the main text) and 1 run of the extended, non-stationary version of the algorithm (SSA+) for an exponential growth model. The code is specifically designed to allow for environment- or time-dependent demography, but in this example the environment is constant. In this code, transition rates are specified separately from intensity functions. This modularity makes running (and debugging) large numbers of simulations easier.

```
1 # SSA function (grid version)
2 ## We refer to this as the grid version of the SSA because it does not
    keep all events that occur during a simulation (or their timing).
    Instead, the grid version records the state of the system for a
    provided vector, or grid, of monotonically increasing time points.
    This vector must include 0 as the first term, but can otherwise be of
    any size and need not be regular. The grid of times does not affect
    the accuracy of the simulation.
3 ## Below, we also include a version of the SSA which stores all events.
    However, the grid version can be much easier to work with (and is
    still exact) for the following reasons: (1) It is often unnecessary to
     know precisely when different events occurred; rather, ecologists are
     often more interested in the state of a system at particular times;
    (2) Because it is not constantly writing to a storage array, it is
    often faster than the full version (even when memory is pre-allocated
    for the storage array); (3) Precise plots of the time course of the
    system may still be achieved in the grid version with a fine gradient
    of time points; (4) It simplifies storage issues when running many
    simulations, by both reducing the size of stored data and by allowing
    better prediction of the required storage.
4
5 ## Function 'gillespie' takes as input the following (examples of which
    will be provided below):
```

```
## * `init` = Array containing all initial conditions (e.g., initial
    population size)
## * `times` = Vector of times over which you wish the function to record
     the system state
## * `param` = Array containing all intrinsic demographic parameters,
    rate functions, and the environment function required for calculating
    intensities in `inten`(below)
## * `inten` = Function which returns all intensities/probabilities of
    the point processes
## * `pproc` = Array containing the state changes caused by the point
    process (in the same order as `inten`; one row per state change)
## * `hpp` = Function for sampling inter-arrival times
gillespie <- function(init, times, param, inten, pproc, hpp){
    if(length(times) == 0){
        stop("No time points provided `times`")
    } else if(times[1] != 0){
        stop("First time point is not 0")
    } else {
        tottime <- times[1]
        tinc <- length(times)
        N <- init
        results <- matrix(nrow = tinc, ncol = length(init))
        results[1, ] <- N
        for(i in 2:tinc){
            results[i, ] <- results[i - 1, ]
            while(tottime <= times[i]){
                intentemp <- inten(tottime, N, param)
                if(all(intentemp == 0)){
                    results[i:tinc, ] <- N
                    i <- tinc
                    warning("Exiting with all intensities equal to 0")
                    break
```

```
32                } else if(min(intentemp) < 0) {
33                    results[i:tinc, ] <- NA
34                    i <- tinc
35                    warning("Exiting with intensity less than 0")
36                    break
37                } else {
38                    tau <- hpp(intentemp)
39                    tottime <- tottime + tau
40                    which.pproc <- sample(1:nrow(pproc),
41                                          size = 1,
42                                          prob = intentemp)
43                    if(tottime > times[i]){
44                        results[i, ] <- N
45                        N <- N + pproc[which.pproc, ]
46                        break
47                    } else{
48                        N <- N + pproc[which.pproc, ]
49                    }
50                }
51            }
52            if(i == tinc) break
53        }
54        cbind(times, results)
55    }
56 }
57
58 ## Initial population size
59 init <- 100
60
61 ## Grid of time points across which we wish to record the system state
62 times <- seq(0, 10, 1)
63
```

```
64 ## Terms for 'param' list
65 ### Function which returns the value of the environment at the current
       time (tottime) [here, constant]
66 constant <- function(t){
67     1
68 }
69 ### List of transition rate functions (birth is environment-dependent and
        therefore multiplied by envres (the result of env(t) in the next
       function)
70 exponentialfun <- list(
71     births = function(b, envres) b * envres,
72     deaths = function(d, envres) d
73 )
74 ## Create a list containing relevant parameter values (b, d) as well as
       transition rates and environment function (now called 'env')
75 param <- list(b = .03,
76               d = .027,
77               exponentialfun,
78               env = constant)
79 param <- unlist(param) # collapse to one-dimensional list
80
81 ## Intensity functions which use above transition rates (function env is
       'constant' above, but is defined as 'env' in the list of parameters
       below)
82 inten <- function(t, X, param){
83     with(as.list(c(param)),{
84         bint <- X * births(b, env(t))
85         dint <- X * deaths(d, env(t))
86         c(bint, dint)})
87 }
88
```

```
## Array containing the state changes caused by the point processes (
    birth = N + 1, death = N - 1)
pproc <- matrix(c(1,
                  -1), nrow = 2)

## Inter-arrival time sampling function (homogenous Poisson process)
hpp <- function(intentemp){
    rexp(1, sum(intentemp))
}


set.seed(20170915)
## Run 1 simulation
ssa.result <- gillespie(init, times, param, inten, pproc, hpp)
ssa.result

# SSA function (full accounting of events and times)
## Function `gillespie_full` takes as input the following (most defined
    above):
## * `init` = Array containing all initial conditions (e.g., initial
    population size)
## * `maxtime` = Desired end time of simulation
## * `param` = Array containing all intrinsic demographic parameters,
    rate functions, and the environment function required for calculating
    intensities in `inten`(below)
## * `inten` = Function which returns all intensities/probabilities of
    the point processes
## * `pproc` = Array containing the state changes caused by the point
    process (in the same order as `inten`; one row per state change)
## * `store_size` = The initial size of the storage array
gillespie_full <- function(init, maxtime, param, inten, pproc, hpp,
    store_size=10000) {
```

```
113     N <- init
114     nvars <- length(N)
115     # Create storage matrix
116     results <- matrix(nrow = store_size, ncol = nvars + 1 )
117     colnames(results) <- c("t", paste(rep("N", nvars), 1:nvars, sep = ""))
118     # Initialize
119     tottime <- 0
120     # Row index to keep track of rows in storage matrix
121     row <- 1
122     while(tottime <= maxtime){
123         # Expand storage if necessary
124         if(row > nrow(results)){
125             results <- rbind(results, matrix(NA, nrow = store_size, ncol = nvars + 1))
126         }
127         results[row,] <- c(tottime, N) # Store result
128         intentemp <- inten(tottime, N, param) # Calculate intensity
129         if(all(intentemp == 0)){
130             warning("Exiting with all intensities equal to 0")
131             break
132         } else if(min(intentemp) < 0) {
133             warning("Exiting with intensity less than 0")
134             break
135         } else {
136             tau <- hpp(intentemp)
137             tottime <- tottime + tau
138             which.proc <- sample(1:nrow(pproc),
139                                  size = 1,
140                                  prob = intentemp) # Which process
141             N <- N + pproc[which.proc, ] # Carry out events
142             row <- row + 1
```

```
143         }
144
145     }
146     if(tottime > maxtime){
147         results[1:(row - 1), ]
148     } else {
149         results[1:row, ]
150     }
151 }
152
153 ## Set maxtime
154 maxtime <- 10
155
156 ## Run 1 simulation
157 set.seed(20170915)
158 ssafull.result <- gillespie_full(init, maxtime, param, inten, pproc, hpp)
159 colnames(ssafull.result) <- c("times", "N")
160 ssafull.result
161
162 # SSA+ function (grid version)
163 ## This is the non-stationary algorithm (SSA+) for a grid of times.
    version of the SSA grid function. The only major difference with the
    SSA function (gillespie(), above) is that this function uses a
    different inter-arrival time sampler (nhpp(), below).
164
165 ## Function `gillespie_plus` takes as input the following:
166 ## * `init` = Array containing all initial conditions (e.g., initial
    population size)
167 ## * `times` = Vector of times over which you wish the function to record
     the system state
168 ## * `param` = Array containing all intrinsic demographic parameters,
    rate functions, and the environment function required for calculating
```

```
    intensities in `inten`(below)
## * `inten` = Function which returns all intensities/probabilities of
    the point processes
## * `pproc` = Array containing the state changes caused by the point
    process (in the same order as `inten`)
## * `nhpp` = Function for sampling inter-arrival times (non-homogeneous
    Poisson process)
gillespie_plus <- function(init, times, param, inten, pproc, nhpp){
    if(length(times) == 0){
        stop("No time points provided `times`")
    } else if(times[1] != 0){
        stop("First time point is not 0")
    } else{
        tottime <- times[1]
        tinc <- length(times)
        N <- init
        results <- matrix(nrow = tinc, ncol = length(init))
        results[1, ] <- N
        for(i in 2:tinc){
            results[i, ] <- results[i - 1, ]
            while(tottime <= times[i]){
                intentemp <- inten(tottime, N, param)
                if(all(intentemp == 0)){
                    results[i:tinc, ] <- N
                    i <- tinc
                    warning("Exiting with all intensities equal to 0")
                    break
                } else if(min(intentemp) < 0) {
                    results[i:tinc, ] <- NA
                    i <- tinc
                    warning("Exiting with intensity less than 0")
                    break
```

```
197                 } else{
198                     tau <- nhpp(tottime, N, param, inten, (times[tinc] -
    tottime))
199                     tottime <- tottime + tau
200                     intentemp <- inten(tottime, N, param) # recalculate
    for new tottime
201                     which.pproc <- sample(1:nrow(pproc),
202                                           size = 1,
203                                           prob = intentemp)
204                     if(tottime > times[i]){
205                         results[i, ] <- N
206                         N <- N + pproc[which.pproc, ]
207                         break
208                     } else{
209                         N <- N + pproc[which.pproc, ]
210                     }
211                 }
212             }
213             if(i == tinc) break
214         }
215         cbind(times, results)
216     }
217 }
218
219
220 ## Function `nhpp` (below) is the workhorse of the SSA+ method and uses
    the inverse transform method to generate appropriate inter-arrival
    times. For performance reasons, the function does not look for a root
    to the inverse function beyond the remaining time in the simulation (`
    timeleft`). If it fails to find a root, the `tryCatch` function makes
    any such failure produce an inter-arrival time greater than the
    remaining time of the simulation, rather than stopping and producing
```

```
    an error message (among other things, this allows `gillespie_plus` to
    correctly record the last state of the system prior to exiting).
    Subdivisions and tolerances may be tweaked to speed up the function or
     to increase precision, but will generally need to be larger than
    defaults.
nhpp <- function(tottime, N, param, inten, timeleft){
    tryCatch(uniroot(function(X, Y) {
        1 - exp(-integrate(Vectorize(function(X){
            sum(inten(tottime + X, N, param))}), 0, X, subdivisions =
    200)$value) - Y},
                     lower = 0, upper = timeleft, tol = 1e-5, Y = runif
    (1))$root,
             error = function(c) timeleft + 1)
}

set.seed(20170915)
## Run 1 simulation
ssaplus.result <- gillespie_plus(init, times, param, inten, pproc, nhpp)
ssaplus.result

## Compare all results
### But first trim ssafull.result
ssafull.result[, 1] <- ceiling(ssafull.result[, 1])
ssafull.result <- aggregate(ssafull.result[, 2] ~ ssafull.result[, 1],
    FUN = function(X) tail(X, 1))
colnames(ssafull.result) <- c("times", "N")
### Comparison
ssa.result
ssafull.result
ssaplus.result

```

```
244 ## Note that the gillespie_plus result is different from the others,
    despite identical seeds. This is because function `hpp` uses `rexp` to
     sample waiting times, while `nhpp` uses `runif`. We can make `hpp`
    use `runif` instead by applying the inverse transform to the CDF of
    the exponential distribution, leaving:
245 hpp <- function(intentemp){
246     -(1 / (sum(intentemp))) * log(1 - runif(1))
247 }
248
249 ## Now run `gillespie` again:
250 set.seed(20170915)
251 ssa.result <- gillespie(init, times, param, inten, pproc, hpp)
252 ssa.result
253 ssaplus.result # They match
```

B.3 Comparison of SSAn and SSA+ for slower environment functions

In Figure B.4, we compare SSAn and SSA+ predictions for the slower environment functions, specifically: increasing 1, fluctuating 1, and random 1. The qualitative results are similar to those in Figure 3 (in main text), albeit with more overlap between the distributions.

Figure B.4: The frequency distribution of population sizes at $t = 100$ for the exponential growth (a-c) and logistic growth (d-f) models, simulated using either the SSAn (red) or SSA+ (blue) method. Displayed are the population size distributions for environment functions: increasing 1 (a, d), fluctuating 1 (b, e), and random 1 (c, f). Colors are transparent, so purple indicates overlap between the SSAn and SSA+ methods. Also displayed are the expected values, $\bar{N}$ (rounded to nearest integer), for each simulation method (same coloration as above). Note the different scales on both axes for each panel.

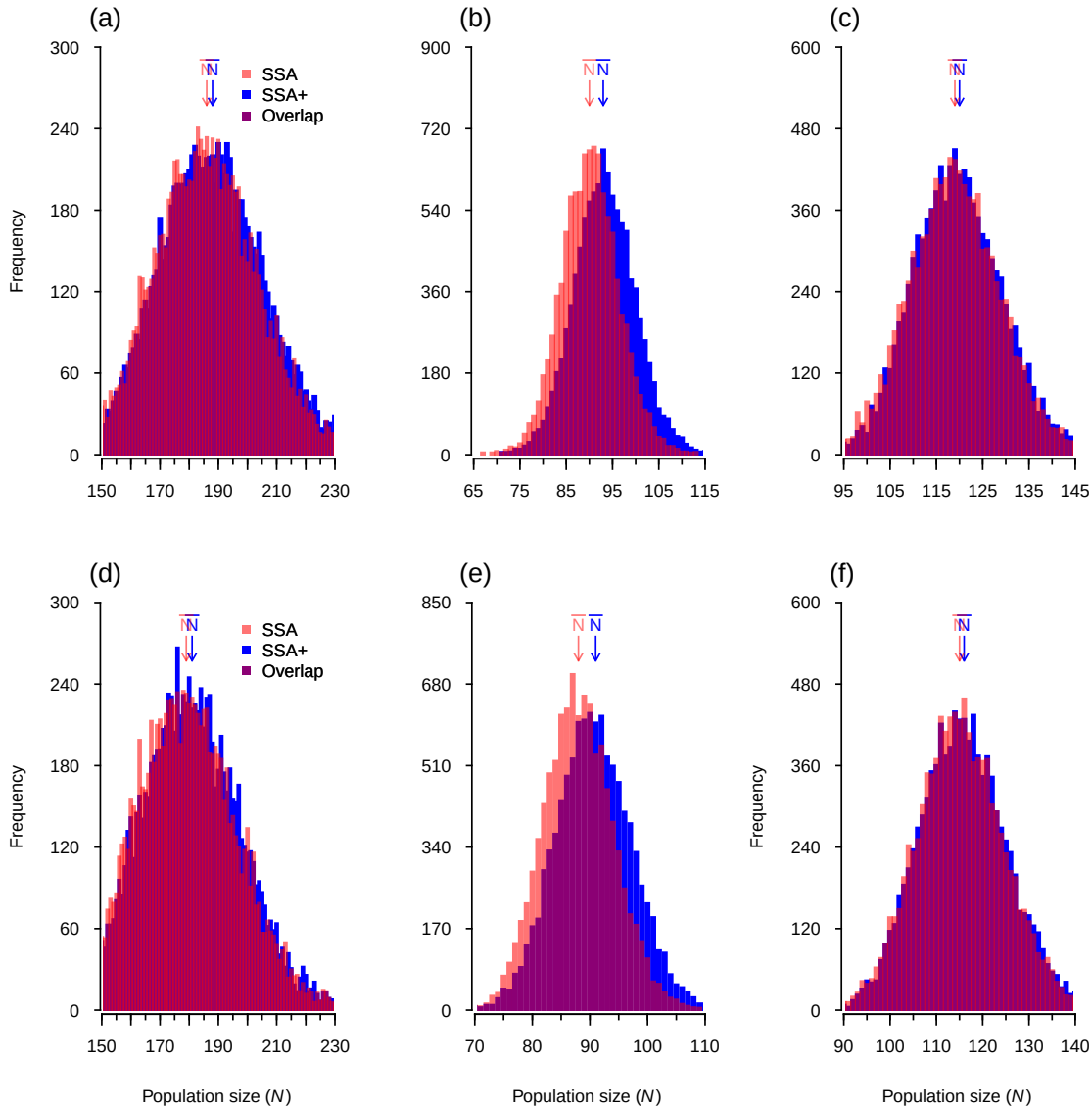

Appendix C

Supplemental information for Chapter 4

C.1 Comparison of F1 and F2 populations

C.1.1 Background

Since population growth and dispersal traits might be plastic, we raised all descendents of CORE, EDGE, and CONTROL replicates under common conditions (29.C and 65% relative humidity) for two generations (F1 and F2 generations). Development under these common conditions was meant to reduce differences in plastic responses due to the environment experienced by F1 and F2 beetles; however, phenotypes of the F1 beetles could still have been affected by maternal effects (i.e., trans-generational plasticity) passed on to them before they were laid as eggs in the common landscapes. We did not know a priori what these effects would be, however we expected some differences in plastic responses to arise from the often large differences in adult densities between, for example, CORE and EDGE populations (see Figure 4.2 in the main text). As a result, in the main text we focus only on the growth and dispersal of the F2 beetles, the generation where both plastic responses and maternal effects were minimized.

Since F1 and F2 beetles experienced identical growth periods (41 days) and dispersal phases (24 hours) into new landscapes, their growth and dispersal traits may be compared directly to assess the impacts of maternal effects. To compare growth rates between gener-

ations, we calculated the relative difference between the two generations as follows:

$$\text{Relative difference} = \frac{x_{F2} - x_{F1}}{\bar{x}} \tag{C.1}$$

where x_{Fi} was the growth rate of a replicate for generation i and $\bar{x}$ was the mean across generations. Relativizing in this way allows for trait values to be zero (relevant for dispersal rates, see below).

In the main text, we estimated dispersal rates at the treatment level by fitting a mechanistic diffusion model of dispersal to all replicates within a treatment. To assess the impacts of maternal effects, however, we were interested in differences in dispersal across generations within individual replicates. Therefore, we calculated an index of dispersal ability - the proportion of beetles that left patch 1 - for the F1s and F2s and looked at the relative differences between them, as above.

C.1.2 Results

As seen in Figure C.1, *Tribolium castaneum* F2 population growth rates were typically higher than F1 growth rates in CORE and CONTROL replicates. In contrast, growth rates in EDGE replicates were generally lower in the F2 generation. *Tribolium confusum* growth rates were higher in the F2 generation for CORE and CONTROL replicates in both environments, while EDGE replicates were consistently lower . Such results may reflect plastic effects on F1 growth rates driven by either the patch densities or the environment experienced by the maternal generation; for instance, beetles that grew in high density CORE/CONTROL patches may have had fewer resources to provision to offspring compared to beetles that grew in low density EDGE patches.

As seen in Figure C.2, there were no consistent differences in *T. castaneum* dispersal between F2 and F1 CORE, EDGE, and CONTROL populations. In contrast, *T. confusum* dispersal appeared higher in F2 EDGE patches. Such a difference suggests a maternal effect on dispersal associated with patch density, though we lack the data to test this further.

Figure C.1: The relative differences in growth rates between F1 and F2 generations. Thicker black points represent the mean differences in growth rates (y-axis) of CORE (square), EDGE (circle), and CONTROL (triangle) populations across the two environmental treatments (x-axis) for (a) *T. castaneum* and (b) *T. confusum*. Lighter gray points are the relative differences for individual replicates within treatments. Bars are the standard errors of the means.

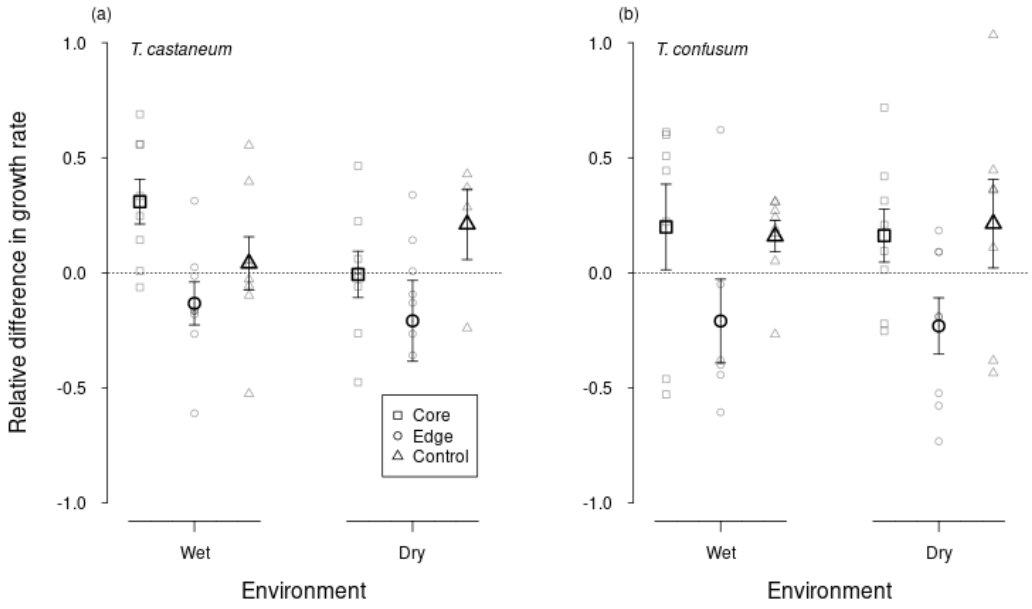

Figure C.2: The relative differences in the proportion of beetles that dispersed between F1 and F2 generations. Thicker black points represent the mean differences in dispersal (y-axis) of CORE (square), EDGE (circle), and CONTROL (triangle) populations across the two environmental treatments (x-axis) for (a) *T. castaneum* and (b) *T. confusum*. Lighter gray points are the relative differences for individual replicates within treatments. Bars are the standard errors of the means.

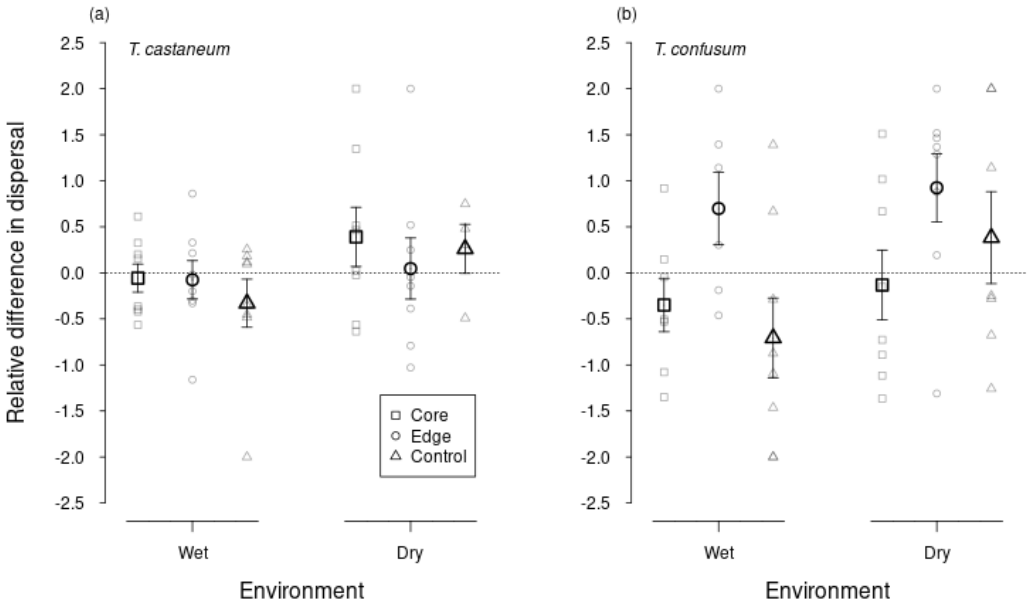

C.2 R code for dispersal kernel and likelihood function

This section contains the function used for calculating dispersal kernels for a given diffusion coefficient (D) and the likelihood function used to determine the best-fit value of D for a given dataset.

```
## Function 'Diffsolver' is used to calculate the dispersal kernel (i.e., the set of probabilities a beetle will be found in a given patch after 24 hours of dispersal) for a given value of D, the diffusion coefficient.
Diffsolver <- function(N, tt, D) {
    diffuse <- function(t, N, D) {
        np <- length(N)
        dN <- N * D  #Number dispersing per hole
        holes <- c(1, rep(2, (np - 2)), 1) #Number of holes
        dNfrR <- c(dN[2:np], 0)         #Number disperse from right
        dNfrL <- c(0, dN[1:(np - 1)])     #Number disperse from left
        list(dNfrR + dNfrL - holes * dN)
    }
    out <- lsoda(N, c(0, tt), diffuse, D, rtol=1e-4, atol=1e-6)
    out[2, 2:ncol(out)]
}

## Function 'dispsearch' is the likelihood function used in conjunction with 'optim' to calculate the likelihood of the dispersal model (the above dispersal kernel embedded in a multinomial model) given the data (a vector called 'counts')
dispsearch <- function(D, counts){
    tempkernel <- Diffsolver(c(1, rep(0, 4)), 1, D)
    templike <- c()
    for(j in 1:nrow(counts)){
        templike2 <- dmultinom(counts[j, ], prob = tempkernel, log = T)
        templike <- c(templike, templike2)
```

```
22      }
23      -sum(templike)
24  }
```

C.3 Fitted dispersal kernels

This section contains Figures C.3, C.4, C.5, C.6, each showing the proportion of beetles found in each patch following dispersal of the F2 experimental landscapes and their best-fit dispersal kernels (see main text for model-fitting details).

C.4 Correlation of dispersal and growth rate

This section examines the correlations between dispersal and growth rate for each species and environmental treatment (Figure C.7). Dispersal ability was estimated by fitting dispersal kernels to individual replicates, using the same dispersal model described in the main text.

In two cases, *T. castaneum* WET (Figure C.7a) and *T. confusum* DRY (Figure C.7d), we found correlations significantly different from zero.

Figure C.3: Proportion of *T. castaneum* beetles found in each patch of the WET experimental landscapes and the best-fit dispersal kernels for each set of populations. Lines represent the proportion of beetles (y-axis) found across patches (x-axis) for each replicate population from before range expansion (a), and following five generations of expansion for CORE, CONTROL, and EDGE populations (b, c, d, respectively). Dashed lines are the expected proportions of beetles found across patches for the fitted dispersal kernels.

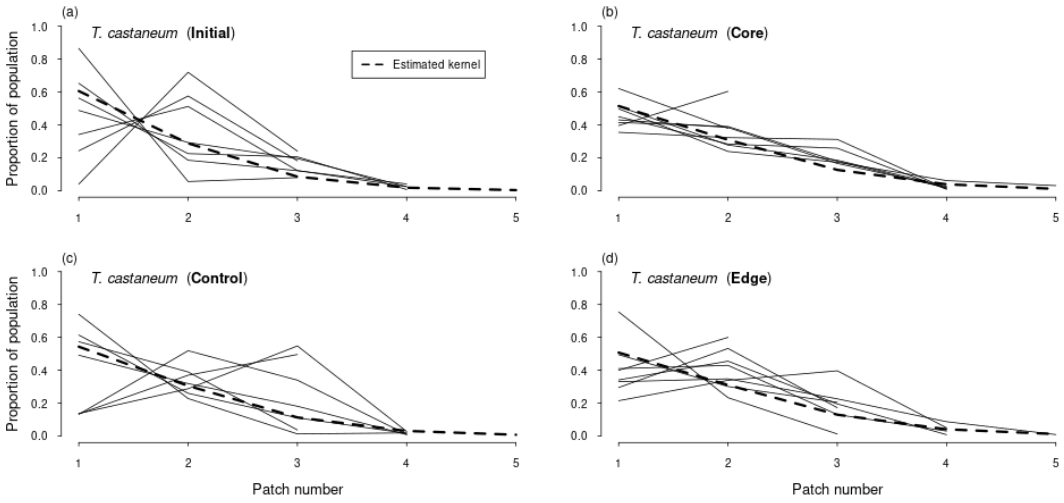

Figure C.4: Proportion of *T. castaneum* beetles found in each patch of the DRY experimental landscapes and the best-fit dispersal kernels for each set of populations. Lines represent the proportion of beetles (y-axis) found across patches (x-axis) for each replicate population from before range expansion (a), and following five generations of expansion for CORE, CONTROL, and EDGE populations (b, c, d, respectively). Dashed lines are the expected proportions of beetles found across patches for the fitted dispersal kernels.

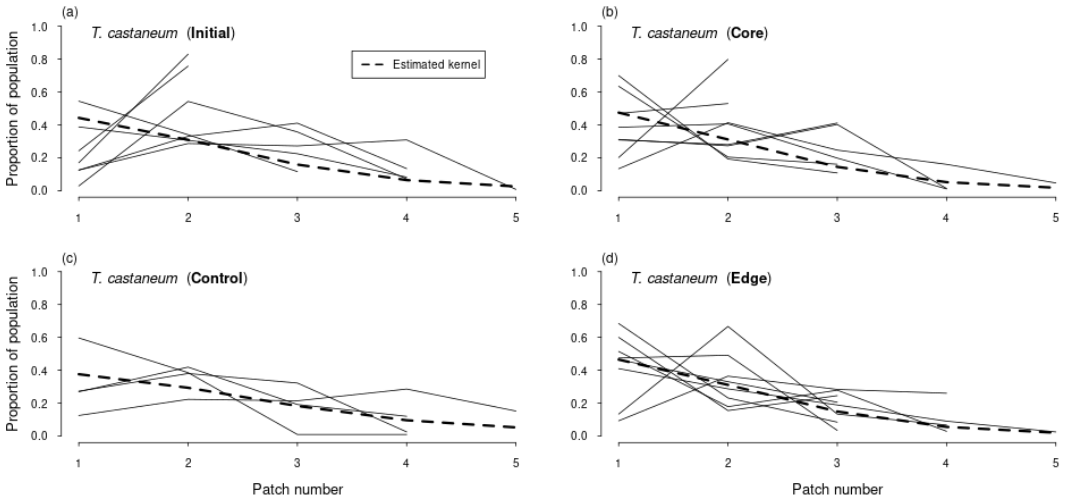

Figure C.5: Proportion of *T. confusum* beetles found in each patch of the WET experimental landscapes and the best-fit dispersal kernels for each set of populations. Lines represent the proportion of beetles (y-axis) found across patches (x-axis) for each replicate population from before range expansion (a), and following five generations of expansion for CORE, CONTROL, and EDGE populations (b, c, d, respectively). Dashed lines are the expected proportions of beetles found across patches for the fitted dispersal kernels.

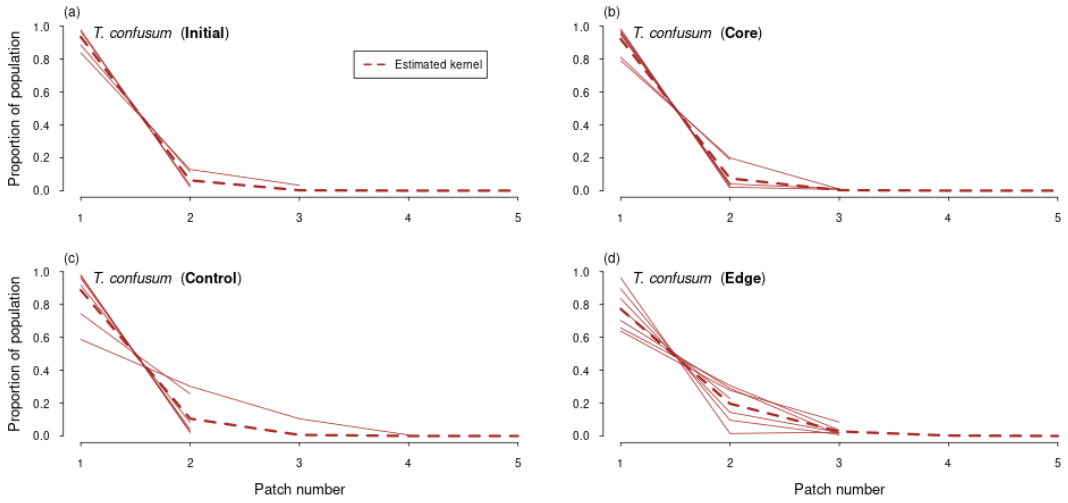

Figure C.6: Proportion of *T. confusum* beetles found in each patch of the DRY experimental landscapes and the best-fit dispersal kernels for each set of populations. Lines represent the proportion of beetles (y-axis) found across patches (x-axis) for each replicate population from before range expansion (a), and following five generations of expansion for CORE, CONTROL, and EDGE populations (b, c, d, respectively). Dashed lines are the expected proportions of beetles found across patches for the fitted dispersal kernels.

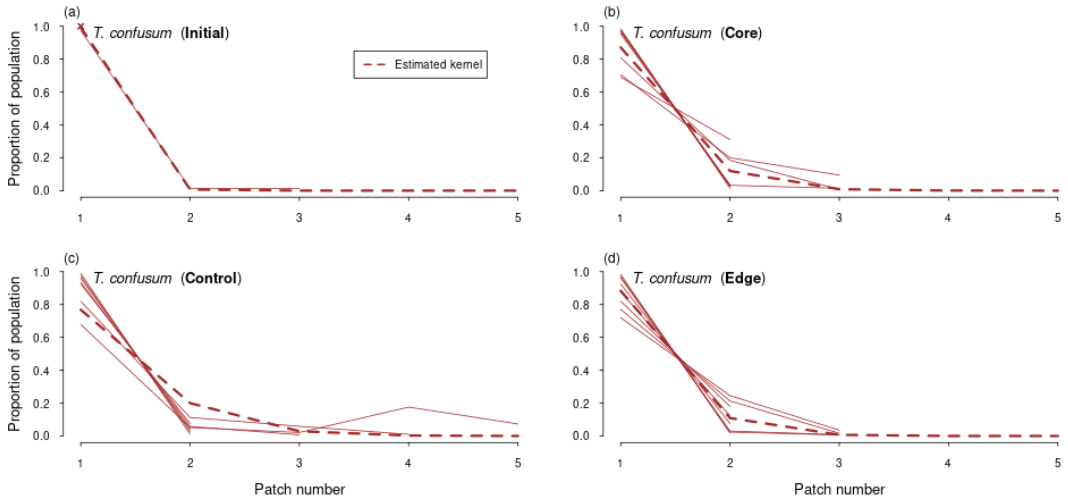

Figure C.7: The correlations between dispersal ability (i.e., diffusion coefficient) and growth rate of the F2 beetles. Diamonds represent the estimated diffusion coefficients (y-axis) and growth rates (x-axis) for replicate populations of *T. castaneum* (a, b) and *T. confusum* (c, d) that experienced range expansion in either WET (a, c) or DRY environments (b, d). Dotted lines (in a and d) are the statistically significant best-fit models to the data ($p < 0.05$; with estimates and coefficients of determination [R^2] above the lines).